INVESTIGATION OF THE SURFACE PROPERTIES OF GANGUE MINERALS IN PGM BEARING ORES

Jasmina Martinovic Bsc (Chem Eng)

A dissertation submitted to the Faculty of Engineering and the Built Environment at the University of Cape Town, in fulfilment of the requirements for the degree of Masters of Science in Engineering

Mineral Processing Research Unit
Department of Chemical Engineering
University of Cape Town

October 2004

Acknowledgements

I wish to express my gratitude to my supervisors, Dr. Dee Bradshaw and Associate Professor Peter Harris and also visiting academic Professor Janusz Laskowski for their guidance and valuable suggestions during this study.

I would like to thank the staff in the Department of Chemical Engineering at UCT, especially Dr. Lesley Parolis and Mrs Jenny Wiese for their assistance and valuable advice during the experimental work.

I thank my colleagues in the Mineral Processing Research Unit for the discussions and support during our seminars.

I am grateful to my family, especially my husband, Dragan, for all his support and encouragement throughout this study and last but not least to my daughter Jovana and friends.

Declaration

I hereby certify that this thesis is the result of my work and has not been submitted prior to this for any higher degree to any other university or institution

J.Martinovic

TABLE OF CONTENTS

LIST OF APPENDICES

TABLE OF FIGURES

LIST OF TABLES

GLOSSARY

APX4M	A commercial modified guar product manufactured by African Product Exchange
BIC	Bushveld Igneous Complex
CMC	Carboxymethyl cellulose
PGM	Platinum Group Minerals
PGE	Platinum Group Elements
SEM	Scanning Electron Microscope
SIBX	Sodium-isobutyl-xanthate supplied by Senmin
TOF-SIMS	Time of flight secondary ion mass spectroscopy
UG2	Upper Group 2
FF30	Carboxymethyl cellulose derivative from FinnFix range (Noviant group, Nijmegen)
XRD	X-ray diffraction (analysis technigue)
XRF	X-ray fluorescence
DS	Degree of substitution

GREEK LETTERS AND ABBREVIATIONS

ε	Fluid dielectric constant
κ	Debye-Huckel parameter
ζ	Zeta potential
η	Dynamic viscosity
Ek	Collection efficiency of flotation
Ec	Collision efficiency, the fraction of all particles swept out by the projected area of the bubble that actually collide with the bubble
Ea	Attachment efficiency
Ed	Fraction of particles remaining attached (detachment efficiency)

I.S	Ionic Strength
τ	Average residence (retention) time
ΔE	Hydration energy
τ_i	Position adjacent to an ion
T	Temperature
R	Reynolds constant (8.314)
PZC	Point of zero charge
IHP	Inner Helmholtz plane
OHP	Outer Helmholtz plane
ψ	Zeta potential
ψ°	Zeta potential falls exponentially with distance
z	valence
c_i	number of ions m^{-3}
F	Faraday constant
U_e	Mobility or velocity of a particle in applied electric field
Ka	Factor including double layer thickness and particle diameter (1.0 for non-polar media, 1.5 for large particles in polar media)
k	thickness of double layer
e	Electronic unit charge
IEP	Iso-electric-point

ABSTRACT

The recovery of Platinum Group Minerals (PGM) and associated sulphides by froth flotation from the Bushveld Igneous Complex is complicated by the presence of naturally floatable gangue minerals such as talc. Although talc is present in small quantities it has a disproportionate effect on concentrate grade by enhancing froth stability and increasing the entrainment of other gangue minerals. However, there is an indication that some of the other gangue minerals, which are normally considered to be hydrophilic, such as chromite and pyroxene, report to the concentrate as floatable particles. Polysaccharide depressants, such as carboxymethyl cellulose (CMC) and modified guar gums are used to reduce the floatability of naturally floatable gangue and may also be able to reduce the floatability of activated gangue.

This study examines the copper activation of a range of minerals found in the Bushveld Complex (namely pyroxene, feldspar, chromite and talc as well as the classical oxide, quartz) using zeta potential measurements, adsorption and microflotation tests. The effect on floatability is evaluated after activation and collector adsorption in the presence of a modified guar and a CMC depressant. Although quartz is not a major gangue component in PGM ores it was selected since it is a strongly negatively-charged mineral in the alkaline range and therefore likely to respond to copper activation. Steenberg and Harris, (1984) found that polymers such as guar and CMC did not appear to adsorb to a significant level on quartz.

The results obtained during the study showed that inadvertent activation by copper ions at alkaline pH values was not specific to the mineral type and could be contributing to the true flotation of these minerals. The zeta potential determinations showed that addition of copper ions increased the zeta potential on all selected minerals between pH 7-9 indicating copper adsorption and that adsorption could be attributed to the presence of $Cu(OH)^+$ species.

The presence of 10^{-3} M KNO_3 had no significant effect on the point of zero charge (PZC) which was expected and confirmed that it was a suitable indifferent electrolyte. The exception was feldspar and this was attributed to the presence of potassium ions in the mineral. The addition of 10^{-3} and 10^{-2} I.S. $Ca(NO_3)_2$ had an effect on the PZC and resulted in a decrease of the zeta potential values indicating that there was an interaction of calcium ions with the mineral surfaces. The zeta potentials of all the minerals was determined in the presence of two depressants (CMC and guar) with KNO_3 as the electrolyte showed that all minerals reacted the same way, increasing in negativity with addition of CMC and decreasing in negativity with addition of guar gum indicating that some adsorption had taken place. Although zeta potential was affected by depressant addition indicating adsorption, in the case of quartz no adsorption was measured directly which showed the limitations of zeta measurements.

Adsorption studies showed that in the presence of calcium ions at pH 9 both depressants adsorbed on all selected minerals except for quartz, with guar gum having slightly higher adsorption densities than CMC.

Microflotation tests showed that only talc was naturally floatable and the addition of copper sulphate and collector increased the floatability of all selected gangue minerals except for talc, where the floatability was actually reduced. This was attributed to the naturally hydrophobic planes of talc and the excess of $Cu(OH)_2$ adsorbing on the surface leading to lower floatability. In two cases, namely talc and quartz the floatability increased with the addition of 50ppm FF30, a carboxymethyl cellulose depressant (CMC). This was attributed to the $Cu(OH)_2$ present on the mineral surfaces being removed by CMC as a strong complex with copper is formed and enhanced floatability can be attributed to dispersion of the $Cu(OH)_2$ leaving only stable copper xanthate at the surface.

The effect of depressants on the 'inadvertent' floatability showed that adsorption of the polymers did not necessarily lead to a deactivation of the minerals but rather co-adsorbed on the surface and due to of the large size of

conclusion is speculative, as the experimental technique does not measure the amount of copper at the surface and this phenomenon should be further investigated.

The important finding was that the use of depressants could reduce the inadvertent floatability of selected gangue minerals but floatability could not be completely removed at the dosages used which suggests that relatively stable copper xanthate complexes were formed.

1. INTRODUCTION

South Africa contains the word's largest platinum group mineral (PGM) reserves and is one of the major producers of these metals. Two major platinum group mineral bearing ore bodies are exploited for their PGM content: the Merensky and Upper Group2 (UG2) reefs. Oxides and silicates are the major gangue mineral constituents in these ores and examples include pyroxene, feldspar and talc in Merensky and chromite in UG2 ore.

The recovery of platinum group minerals by flotation is complicated by the presence of naturally floatable gangue minerals. During flotation, the PGM bearing sulphide minerals are separated from the unwanted gangue. The large proportions of gangue minerals present in these ores reduce the effectiveness of the flotation process by diluting the concentrate grade and increasing the transport and smelting costs. The aim is to maximise recovery of PGM and sulphide minerals and minimise the amount of gangue minerals in concentrates.

Gangue minerals report to the concentrate from the pulp as a result of two distinct mechanisms: true flotation and entrainment. True flotation occurs as a result of attachment of particles to air bubbles and is dependent on particle surface hydrophobicity, while entrainment is dependent on properties such as size and density and is related to water recovery. Talc is a naturally hydrophobic mineral and although it is present in relatively small quantities, it has a disproportionate effect on gangue recovery as it has a strong froth stabilising effect, increasing the recovery of other gangue minerals by entrainment.

There are indications that some of the other gangue minerals, which are normally considered to be hydrophilic, such as chromite and pyroxene, report to the concentrate by flotation by various mechanisms including the presence of talc rims and inadvertent activation by reagents. In practice, polysaccharide depressants, such as carboxymethyl cellulose and modified guar gums, are

used to reduce the floatability of naturally floatable gangue and it is important to examine whether the use of these depressants can also prevent the flotation of gangue minerals that have been activated by metal ions and rendered hydrophobic by the addition of collector.

Much work has been done on the activation of sulphide minerals by metal ions (Acar and Somasundaran, 1992; Finkelstein and Allison, 1997; Laskowski, Liu and Zhan, 1997) and the mechanism of activation has been well established particularly in the acid pH range. The activation of sulphide minerals in alkaline solutions (typically found in South African PGM flotation plants) is more complex but has also been well described (Malysiak 2002). Less work has been done on the activation of oxide and silicate minerals. Fuerstenau, (1975) showed that oxide minerals could be activated with metal ions such as copper and lead ions and subsequently floated with a collector. Nagaraj, (1995) also showed that pyroxene could be activated with Cu(II) ions and addition of a collector lead to the formation of a Cu(I)-collector complex at the surface of the mineral. Wesseldijk, (1999) more recently showed that chromite could be copper activated and readily floated with xanthate in a microcell at pH 9. In addition, Malysiak and Shackelton (2003) showed that both pyroxene/pentlandite and feldspar/pentlandite systems could be copper activated. TOF-SIMS analysis showed much greater activation of the pentlandite but still showed some activation and reaction with the collector and the silicate minerals. Mailula, (2004) studied the effect of the presence and concentration of calcium ions on the activation by copper ions of pyroxene and feldspar. The microflotation tests in the presence of xanthate showed strong floatability of the activated minerals and the addition of a depressant such as guar or CMC could be used to cause some reduction in their floatability.

This project focuses on improving the flotation performance of platinum group minerals by understanding the factors affecting activation and depression behaviour of the selected gangue minerals in the flotation process.

Pyroxene, feldspar and talc are selected as they are components of the Merensky Reef, chromite as a component of UG2 and quartz as a classical probe mineral for comparison.

Techniques used include electrokinetic methods to determine zeta potential, adsorption and microflotation tests.

The objectives of this project are:

1. To use zeta potential determinations to:

    - Identify the charge on the surface of selected minerals with changing pH
    - Evaluate the effect of ion addition (K^+, Ca^{2+}, Cu^{2+}) on the surface charge of the selected minerals
    - Evaluate the effect of adding depressants on the surface charge of the selected minerals.

2. To use equilibrium adsorption techniques to evaluate the extent of adsorption of polymeric depressants (CMC and guar gum) in the presence of Ca^{2+} ions onto these minerals.

3. To use the UCT microflotation technique to:

    - Investigate the floatability of gangue minerals (pyroxene, feldspar, talc, chromite and quartz)
    - determine the extent of activation after copper and collector addition and
    - To determine the effectiveness of depressant (CMC and guar gum) addition to reduce this floatability.

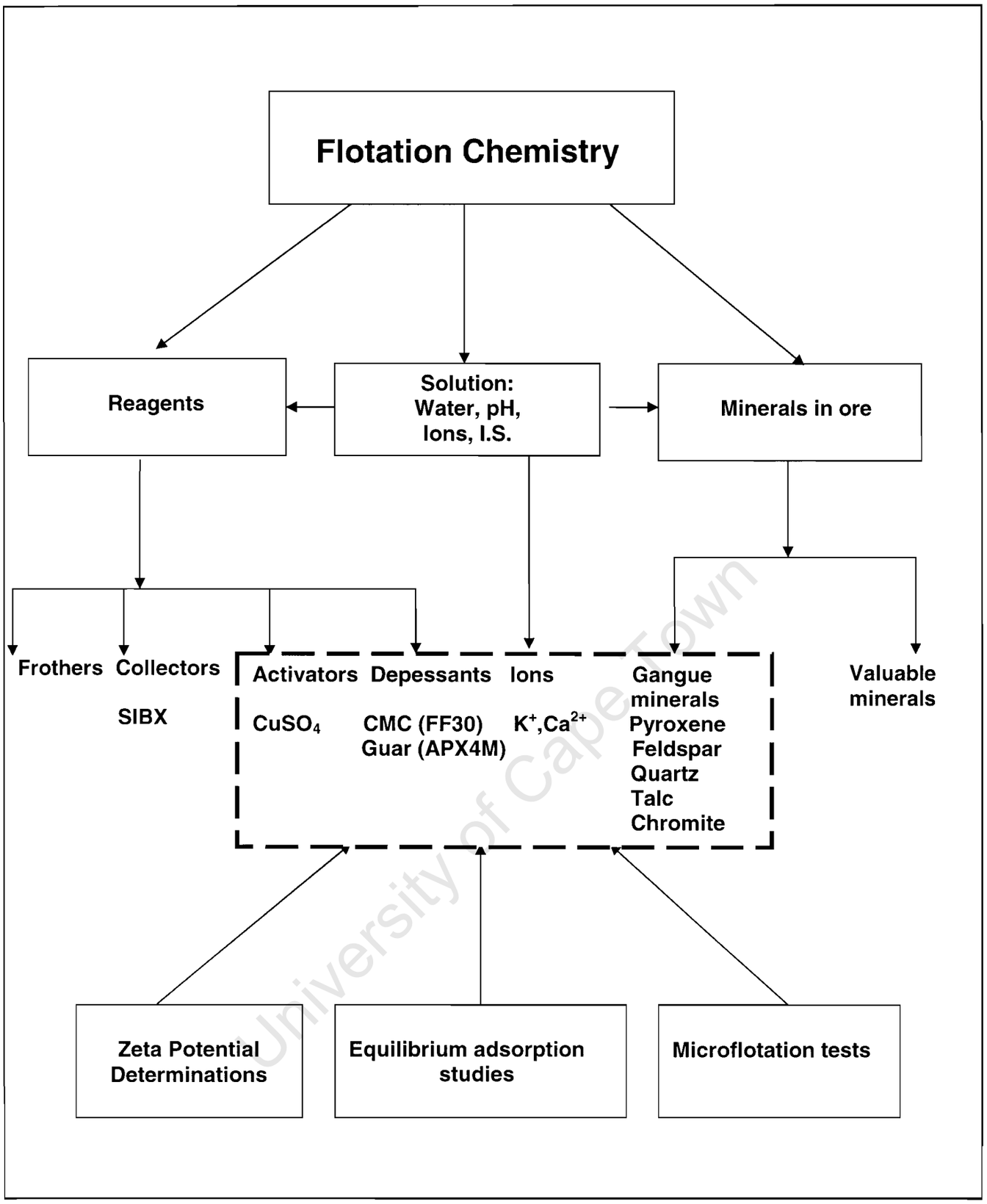

Figure 1.1: Schematic view of the scope of thesis

2. LITERATURE REVIEW

2.1. PRINCIPLES OF FLOTATION

Figure 2.1 shows a simplified schematic of the flotation process. There are two distinct zones: The pulp zone, in which the mineral recovery occurs and the froth zone, in which the concentrated mineral is separated from the bulk. Particles can either reach the froth attached to the bubbles or by entrainment in the water passing from the pulp zone to the froth zone. While the former process is selective and is responsible, in general for the collection of the hydrophobic valuables, the latter is unselective and results in the unwanted gangue reporting to the flotation concentrate. It is thus desirable to maximise the recovery by true flotation and minimise the entrainment contribution. The contribution to overall flotation of the entrained material increases linearly with increase in water recovery (Engelbrecht and Woodburn, 1975).

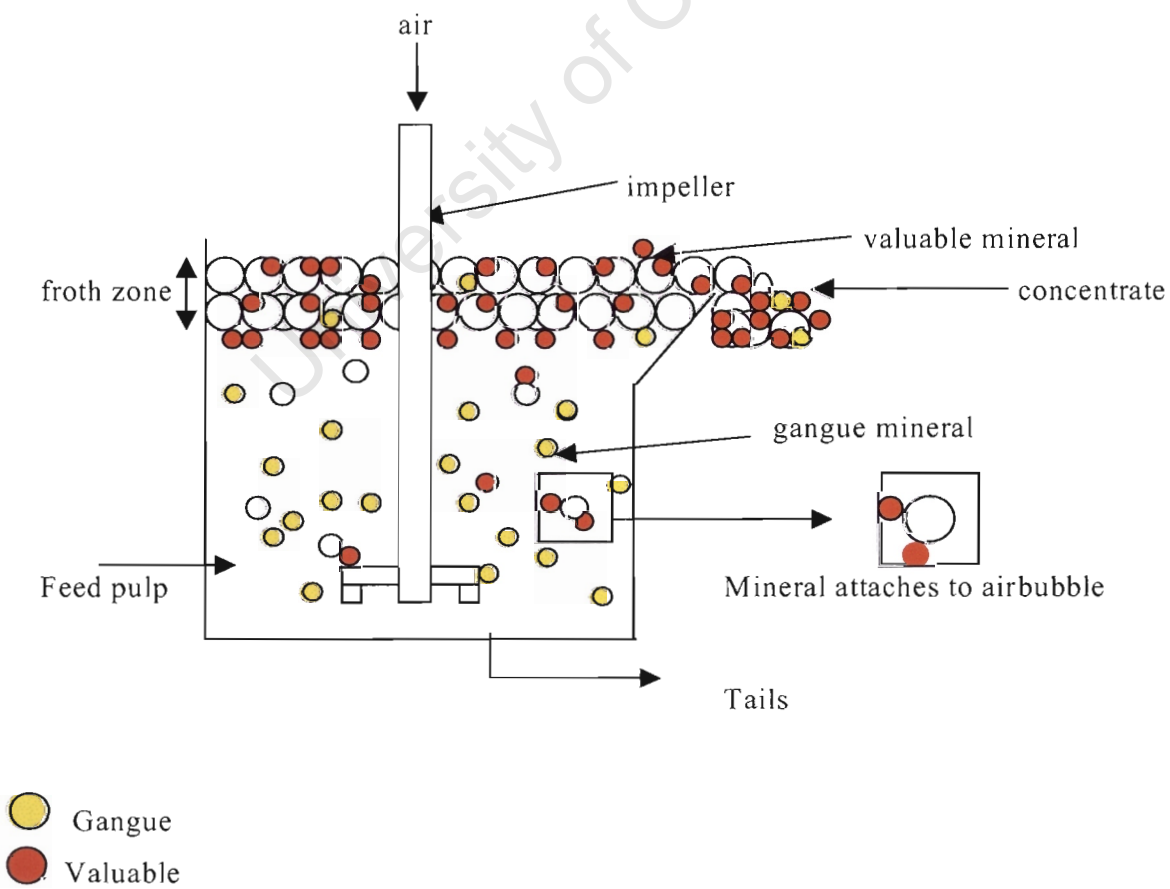

Figure 2-1: Schematic of the flotation process

The froth zone provides the environment for the separation of the valuable minerals from the gangue, allowing drainage of the entrained material back into the pulp. There is an optimum froth stability. When the froth is not stable enough the mineralised bubbles rupture before collection, when the froth is too stable, not enough drainage occurs and the water and gangue recoveries are too high. Various factors including nature and dosage of the frother as well as the nature of the particles in the froth affect its stability (Harris, 1982).

2.1.1. The sub – processes of flotation

The overall flotation process can be divided into various consecutive sub-processes which all contribute to the success of the separation of the valuable mineral from the gangue. They can be summarised by the following (Bradshaw, 1997):

1. The creation of the hydrophobic mineral particle surface, which may consist of the collector adsorption onto the surface of the mineral particles and the manipulation of the pulp environment viz. pH, agitation pulp density etc.

2. Formation of stable bubbles of a set size and distribution.

3. Mineral particle – bubble collision, resulting in possible attachment. This requires the thinning and rupture of the film between the bubble and particle and subsequent stable attachment. Detachment of the mineral from the bubble is also possible. This sub–process is also known as the particle collection.

4. The transport of the loaded bubble through the pulp phase.

5. Transfer from the pulp phase to the froth phase. There is possible elutriation of particles falling back from the froth into the pulp and entrainment of particles, not collected by bubbles, passing from the pulp into the froth.

6. The transport and collection of the loaded bubble in the froth phase.

2.1.2. Influential parameters in flotation

There are many factors that affect the flotation processes, both directly and indirectly. Crozier, (1992) has listed over 25 clearly identifiable parameters, which can be more fully described by over 100 variables, which affect the flotation performance.

Klimpel, (1984) has divided the major variables into three interactive groups: the equipment components, the operation components and the chemical components (Figure 2.2) (Heerema, 1994; Klimpel, 1984). The interactive nature of these components makes it very difficult to analyse the effect of any particular component and careful planning and analysis of experiments is necessary to interpret the effect on performance of a particular parameter.

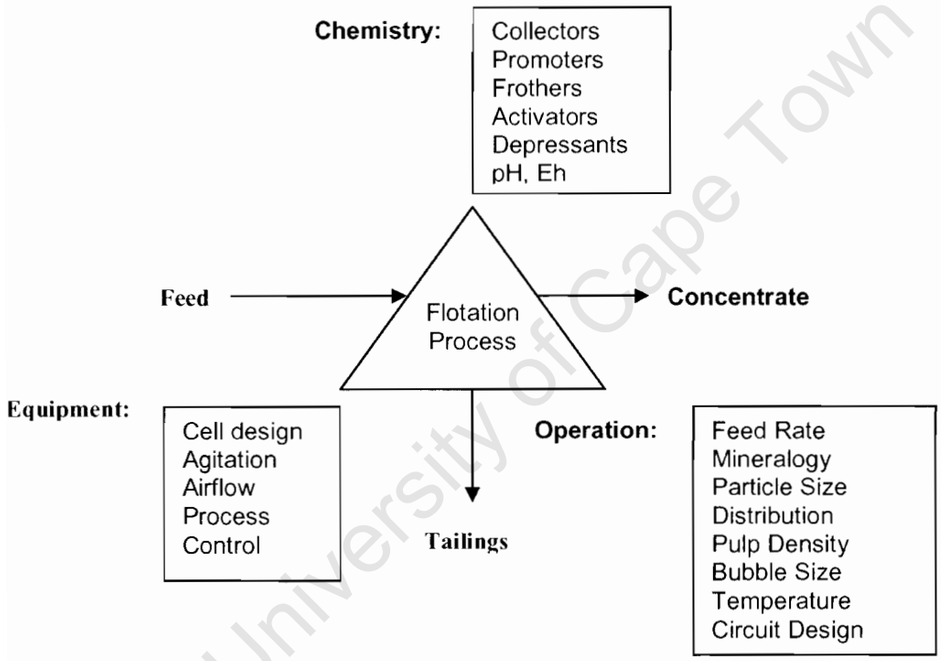

Figure 2-2: Klimpel triangular representation of flotation [Heerema, 1994; Klimpel, 1984]

2.1.3. Mathematical description of flotation

The collection efficiency (E_k) of flotation can be expressed as a function of three components (Finch and Dobby, 1990):

$$E_k = E_c E_a E_d \qquad \textbf{Equation 1}$$

where E_c = collision efficiency, the fraction of all particles swept out by the projected area of the bubble that actually collide with the bubble,

E_a = attachment efficiency, the fraction of the particles colliding with the bubble that become attached to it,

E_d = detachment efficiency, the fraction of attached particles detaching.

The collision efficiency is determined by the hydrodynamics of the system. The attachment efficiency and detachment probability are strongly affected by the hydrophobicity of the mineral particle. Upon collision between the bubble and particle, the particle can either “bounce” off the bubble surface causing it to be strongly deformed, of the particle can slide around the bubble. The particle remains in contact with the bubble for a time referred to as the sliding time, t_s. If the sliding time is sufficiently long, the film will thin to a point where rupture will occur spontaneously to form a stable three phase aggregate. The total time required for this process is known as the induction time, t_i. If the induction time, t_i is less than the sliding time, t_s, particle attachment will proceed.

2.1.4. Entrainment

Particles suspended in a flotation pulp report to the concentrate as a result of two distinct mechanisms: true flotation and entrainment. True flotation occurs a result of attachment of a particle to an air bubble and the nature of the particle surface plays important role in this mechanism. Entrainment is non-selective and occurs as a result of particle concentration in the pulp, which enters the froth phase. The major factors affecting entrainment include: particle size and shape, pulp density or % solids in the pulp, particle density, recovery of water, froth structure and froth residence time.

The ratio of the recovery of different non-floating species relative to water can be used as a measure of entrainability (Savassi, 1998). Entrainability is also known as the "degree of entrainment". The separation efficiency between the valuable mineral and fully liberated and dispersed gangue is dependent on the degree of entrainment.

The degree of entrainment has been shown to be a strong function of particle size (Smith and Warren, 1989). However, entrainment for particles larger than 50 μm was not significant and was dependent on the froth properties (i.e. structure, depth, etc.). The amount of water recovered and thus the total entrainment was affected by the froth stability, which was affected by various factors. The relationship between froth stability, particle entrainment and drainage has been reported by Subrahmanyam and Forssberg, (1988).

2.1.5. Effect of water

The molecular structure of water is unique because of the existence of the hydrogen bond and the hydrophobic forces (Israelachvili, 1992). This results in water having a high melting and boiling point compared to other substances of similar molecular structure. The characteristic of the hydrogen bond is that:

a. It is orientation dependent
b. It is stronger than a normal Van der Waal force but weaker than a covalent or ionic bond
c. It is an electrostatic interaction
d. The bond exists in varying degrees where hydrogen atoms are in contact with strongly electronegative atoms such as O, N, F and Cl
e. It can occur both intermolecularly and intramolecularly
f. The O-HO bond is generally linear but can form a bond of angle 120°. This linearity means that the preferred structure of a network of hydrogen-bonded atoms is tetrahedral, as is the case for ice and shown in Figure 2.3

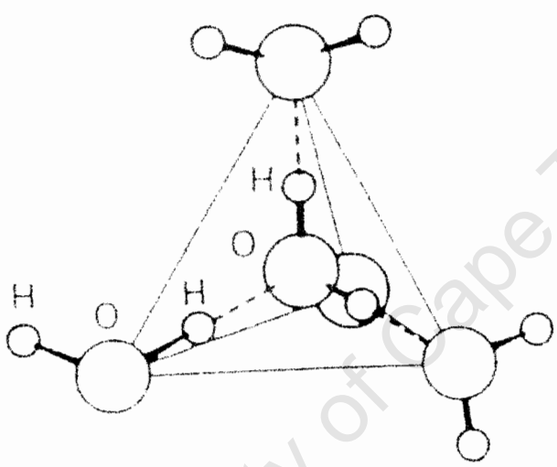

Figure 2-3: The tetrahedral structure of water molecules [Israelachvili, 1992]

These properties cause the water molecules to become associated with each other resulting in a tetrahedral coordination of water molecules. When the aqueous film on a solid is unstable, that surface is hydrophobic (Rao, 1974). Generally, hydrophobicity refers to the degree to which a molecule is repelled by water. In order to analyse particle hydrophobicity, Laskowski, (1986) compares the work of cohesion of water to the work of adhesion of the solid

particle to the water. If a particle is to be hydrophilic, its work of adhesion must exceed the work of cohesion of water. In order to minimise contact area between the water and the hydrophobic particles the force of so-called hydrophobic bonding arises. The hydrophobic effect is related to the hydrophobic interaction, which describes the unusually strong attraction between hydrophobic molecules and surfaces in water, often stronger than their attraction to air (Israelachvili, 1992). In a flotation process, hydrophobic particles attach to the gas bubbles after collision in the pulp. Hydrophilic particles do not attach and remain suspended in the system. Although many report to the concentrate through the entrainment mechanism but generally removed as tails. As a result, hydrophobic particles are floatable.

2.1.6. Effect of ions in aqueous solutions

Water molecules interact extensively with ions in solution, because of the excellent solvent properties of water with ionic compounds (viscosity, ion mobility, diffusion, etc.). Such interactions are referred to as hydration, and are characterized by the hydration energy. The interaction of ions and water molecules alters water structure (Laskowski, 1994). As shown by Samoilov, (1965), the hydration of ions in solution can be divided into two regions: close (primary) and distant (secondary) hydration. If water molecules are held permanently (e.g. complexes with some species), then $\tau_i / \tau = \infty$, and the decrease of this ratio indicates a weakening of the bonds between ions and the nearest water molecules. According to Samoilov:

$$\tau_i / \tau = \exp(\Delta E / RT) \qquad \textbf{Equation 2}$$

In the equilibrium position: τ is the average residence (retention) time, ΔE is the hydration energy, and τ_i is the position adjacent to an ion and the ratio τ_i / τ will characterize the extent of hydration in solution. Small ions and multivalent ions, such as Li^+, Na^+, H_3O^+, Ca^{2+}, Ba^{2+}, Mg^{2+}, Al^{3+}, F^-, have $\Delta E >$ O, and $\tau_i > \tau$, increasing the viscosity of aqueous solutions. Large monovalent

ions, such as K^+, NH_4^+, Rb^+, Cs^+, Cl^-, Br^-, I^-, NO_3^-, have $\Delta E < O$, and $\tau_i < \tau$ increasing water fluidity. The presence of ions affects the solubility of compounds in aqueous solutions and solubility can be determined by competition for available water between ions strongly interacting with water molecules and less strongly hydrated molecules (or ions). This "salting-out" effect is utilized to separate a hydrophilic compound from aqueous solution by precipitating it. The heavy metal ions and in particular the transition metals exist in stable form only if electron-rich ligands occupy eight octahedral orbital about the metal ion (Fuerstenau and Fuerstenau, 1982).

2.2. FLOTATION REAGENTS

Flotation reagents are added to enhance the separation, which includes imparting a hydrophobic character to the minerals to be floated and a hydrophilic character to unwanted gangue as well as creating a suitable froth phase. The classes of reagents include: collectors, frothers, depressants and modifiers including activators and pH modifiers. Reagents can have different roles according to the particular flotation system.

Although reagents are added to fulfill specific functions some interactions do occur with frothers have collecting properties and some collectors have frothing properties. Depressants and dispersants also often have interchangeable functions (Bradshaw, 1997).

2.2.1. Collectors

The role of collectors is to selectively induce hydrophobicity onto the surfaces of the desired mineral particles. In general, a collector consists of two parts: a part of the molecule that becomes attached to an air bubble (nonpolar) and the polar part which reacts with the mineral surface. Therefore collectors are concentrated at the mineral-water interface, where the non-polar groups form the hydrophobic surface in contact with water. The behaviour of the collector

is dependent on both the functional group and the alkyl chain (King, 1982). Figure 2.4 shows the structural formulas of a xanthate and a dithiophosphate (DTP) collector.

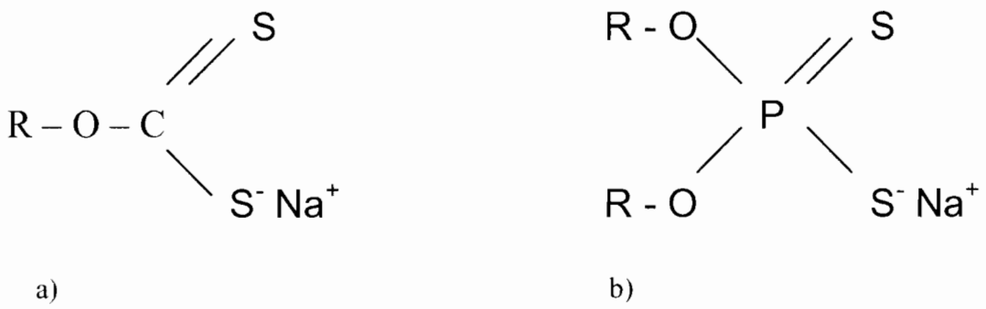

a) b)

Figure 2-4: Structure formula of xanthate a) and dithiophosphate b), [King, 1982]

The behaviour of dithiophosphates is similar to xanthates. Xanthate is known for its higher collector strength and dithiophosphate for its better selectivity.

The mechanism of mineral – collector bonding depends on the collector type, mineral surface nature and charge. The collectors SIBX (sodium-isobutyl-xanthate) and DTP, which are used for the bulk flotation of PGM containing sulphide minerals, are thiol collectors. Thiol collectors are generally used as the alkali metal salts due to their high solubility and the low effect of the cation on the behaviour of the collector (Taggart, 1945).

Xanthates are mostly used in a neutral or slightly alkaline medium. In a strong acid medium, xanthate forms xanthic acid, which decomposes to give carbon disulphide and alcohol. The tendency for a xanthate to adsorb at a mineral surface increases as the length of the alkyl chain increases. The selectivity of a xanthate collector increases as the length of the alkyl chain decreases. Xanthate collectors do not adsorb onto non-sulphide minerals and are thus not used to enhance their flotation.

2.2.2. Activators

Copper sulphate ($CuSO_4$) is a commonly used activator for sulphide minerals. The role of this reagent varies and many conflicting theories of its role have been proposed (Bradshaw, 1997). In some cases, copper sulphate has been classified as a froth modifier (pyrite flotation), while in others it is added to activate the mineral surface by the adsorption of copper ions (sphalerite flotation) (King, 1982). Whereas sphalerite activation is effective at acid pH, in the platinum industry, copper sulphate is added as an activator under alkaline conditions. Copper ions have also been shown to activate the non-sulphide gangue minerals such as quartz and other oxide minerals, making them susceptible to collector adsorption (Fuerstenau and Palmer, 1976; Wesseldijk, 1999).

2.2.3. Depressants

The role of these reagents is to reduce collection of unwanted gangue minerals typically talc or other oxide minerals. This is done by either enhancing the hydrophilic nature of the gangue surface or by preventing the formation of hydrophobic species on the mineral surface (Laskowski, 1994). Examples include polyglycol ethers, polyphenols and polysaccharides, such as carboxymetyl cellulose and guars.

Generally, organic polymers are effective depressants for talc minerals and are widely used in the platinum industry. These are natural products of high molecular weight (above 10 000) and have been used successfully with little modification to improve selectivity. The organic polymers contain numbers of strongly hydrated polar groups, which are the basis of their depressant action. Some of these depressants contain anionic (-COOH, $-OSO_3H$, $-SO_3H$) and /or cationic ($-NH_2$, -NH) groups. Generally the chosen polymers are either non-ionic or weakly anionic. Cationic polymers are unsuitable because they are unselective in most flotation systems (Mackenzie, 1986). The depressing

action of organic polymers can be altered by molecular weight variation (degree of polymerisation), or molecular form and the number of ionisable polar groups (degree of substitution). The optimum concentration of polymeric depressants varies with ore type, particle size distribution, type of depressant, molecular weight, and presence of other chemical species (Morris, 1996).

2.2.3.1. Carboxymethyl cellulose

Carboxymethyl cellulose is an anionic polymer and is prepared by steeping cellulose in a sodium hydroxide solution. The alkaline cellulose is then esterified with sodium monochloroacetate to form sodium carboxymethyl cellulose and sodium chloride (Batdorf and Rossman, 1973). The reaction is:

$$R_{cellulose}(OH) + ClCH_2COONa + NaOH \rightarrow R_{cellulose}(OH)_2(OCH_2COONa) + NaCl + H_2O$$

The monomer of the CMC is shown in Figure 2.5. The glucose units within the CMC are bonded by β-1,4 links.

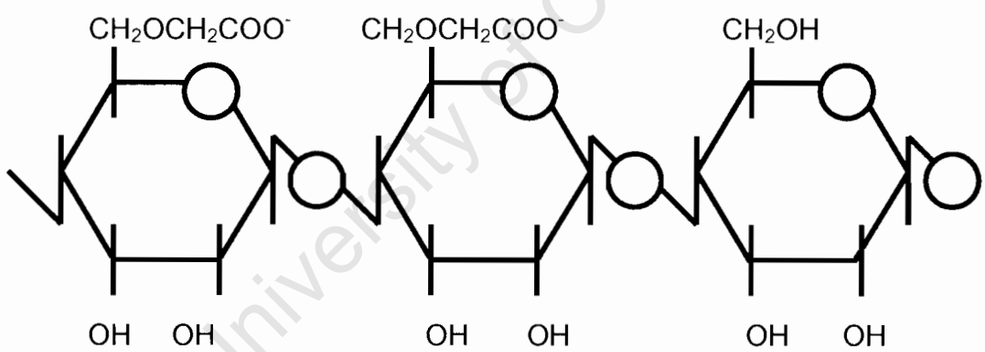

Figure 2-5: A schematic diagram of the molecular structure of carboxymethyl cellulose (CMC)

The CMC is a linear polymer with hydrophobic hydrocarbon backbone and hydrophilic pendant hydroxyl and carboxyl groups. The large number of ionic

groups that are substituted along the chain results in the molecules having a high surface charge. The extent of the carboxymethyl (-CH_2COO-) substitution is referred to as the degree of substitution (DS) and is defined as the average number of carboxymethyl groups per glucose unit. The theoretical maximum value for DS is 3, however in practice DS ranges from 0.4 to 0.8. CMC is significantly negatively charged and needs at least a degree of substitution of 0.5 for sufficient solubility.

2.2.3.2. Modified guar gum

Guar gum is a polysaccaride obtained from the seed of the guar plant (Cyamopsis tetragonolobus) and is modified by alkaline degradation. Guar gum is a galactomannan, and consists only of galactose and mannose. The unit of guar gum is showed in Figure 2.6.

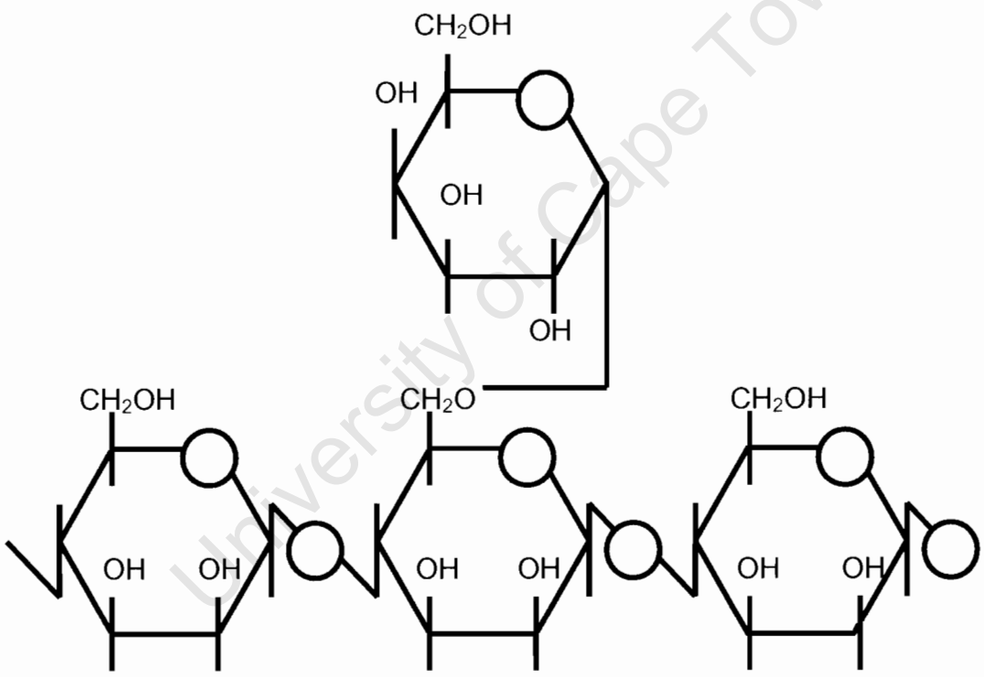

Figure 2-6: A schematic diagram of the molecular structure of guar gum

The mannose chains are attached by 1 → 4 position. The galactose units are attached by 1 → 6 linkages. There are nine hydroxyl groups per monomer unit that will be available for substitution by carboxymethyl – hydroxypropyl – and beta halogenated hydrocarbon groups (Mackenzie, 1980). The guar gum used for this study is defined as a non-ionic polysaccharide with linear chains of 1-4-β-D-mannopyranosyl units with α-D galactopyranosyl units attached by 1-6 linkages (Whistler, 1973). The modification process involves reduction of the molecular mass of the molecule and possible introduction of substituent groups into molecule. Guar gums are soluble in water even at low degrees of substitution.

2.3. MINERALOGY OF GANGUE MINERALS IN PGM BEARING ORES

2.3.1. Summary of Bushveld Igneous Complex (BIC)

The Bushveld Igneous Complex contains the world's largest known deposits of platinum, palladium, rhodium, ruthenium, iridium and osmium (Corrans et al. 1982, Buchanan, 1991). Some differentiation of the individual layers may also have taken place as different minerals crystallised out at different temperatures. The result of this was that the BIC became clearly stratified into distinct compositional units more than nine kilometres thick. In terms of Platinum Group Elements (PGEs), the most important unit in the BIC is the Critical Zone (Figure 2.7 - from Hochreiter et al., 1985). This zone is divided into the Lower Group, Middle Group and Upper Group and in each Group the chromite layers, some of which are also exploited commercially for their chromium content, are numbered from the bottom upwards. Near the top of the Critical Zone the Merensky Reef can be found. The Merensky Reef is above the Upper Group 2 (UG2) layer (Wood, 1996).

The main gangue constituent (20% to 60%) of the UG2 Reef is chromite ($FeO.Cr_2O_3$) which has a chromium-to-iron ratio of approximately 1.35. The other gangue minerals are silicates with large amounts of orthopyroxene and

plagioclase (feldspars) (Corrans et al., 1982; Liddell et al., 1986). Small amounts (<5%) of minerals such as clinopyroxene, biotite, phlogopite, talc chlorite, quartz, serpentine, ilmenite, magnetite, rutile, and calcite may also be present.

An investigation by XRD (done by Mintek) and XRF (done by Geology department at UCT) shows the typical mineralogy of Merensky reef to contain a talc abundance (%) between 0.5 and 5; feldspar between 24 and 40; pyroxene between 52 and 59; chromite between 3 and 4.5; sulphides between 0.9 and 1.11 and other between 3 and 4.5. Chalcopyrite, pyrrhotite, pyrite, pentlandite, and less frequently millerite are the major base-metal sulphide minerals, usually present in trace amounts (1%) (Dalvie, 2001).

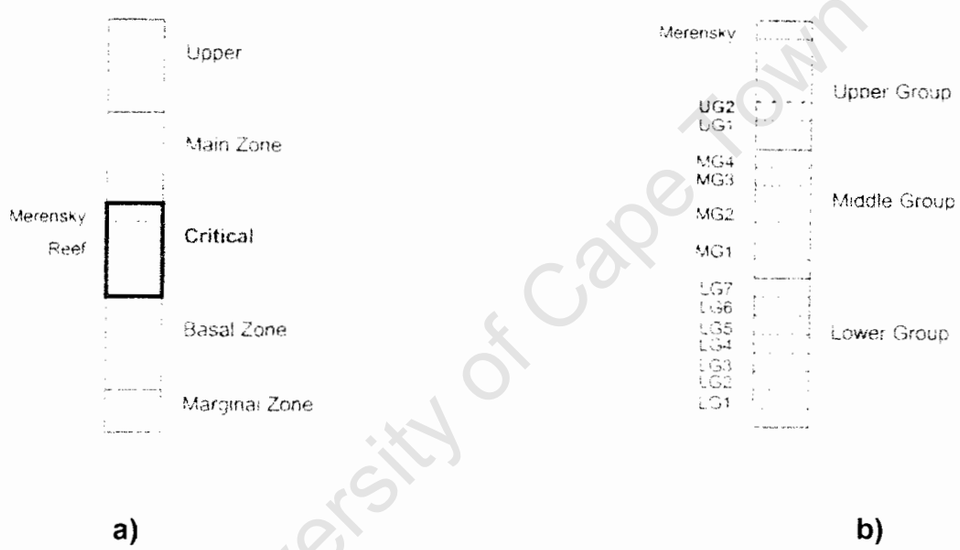

Figure 2-7: a - Generalised stratigraphy of the Bushveld Complex [Hochreiter et al., 1985]

b - Stratigraphy of the critical zone [Hochreiter et al., 1985]

2.3.2. Mineral composition of silicate minerals

The basic structural unit of the silicates is the silicon-oxygen tetrahedron in which the distance Si-O is 1.62 Å and the distance between two oxygen atoms 2.65 Å. Such discrete SiO_4 groups, possessing four negative charges, are found in the minerals commonly termed orthosilicates. The SiO_4 groups can be polymerized, giving rise to more complicated silicon-oxygen radicals and corresponding frameworks, which can be either finite or infinite. Finite groups of silicon-oxygen tetrahedra are built up in two, three, four, six, or twelve such tetrahedra and comprise a ring-wise arrangement; hence the term cyclosilicates is used to describe the corresponding minerals.

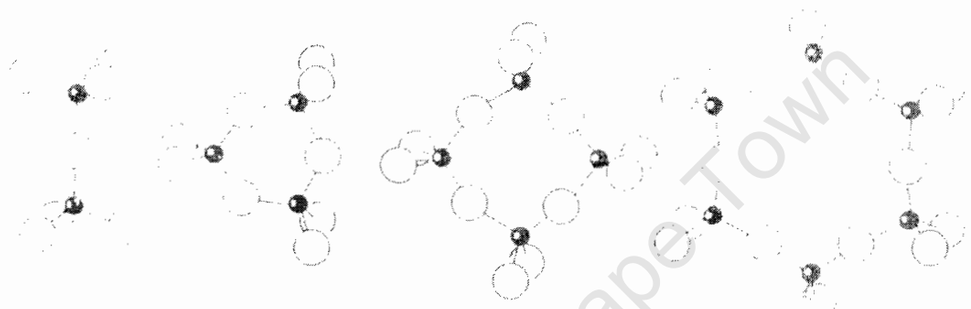

Figure 2-8: Finite groups of silicon-oxygen tetrahedral [Kostov, 1968]

Infinitely extended arrangements of silicon-oxygen tetrahedra are realized in the form of chains, in sheets (Figure 2.9), or in three-dimensional frameworks (Figure 2.10). The silicon-oxygen chains can be either single or double (ribbon-like), being termed inosilicates, in contrast with the silicates possessing sheets of silicon-oxygen terahedara, which are termed phyllosilicates. The first two (chain) types are pyroxenes, while the sheet type are the micas. Silicates with three-dimensional arrangements of silicon-oxygen tetrahedra are exemplified by quartz and feldspars.

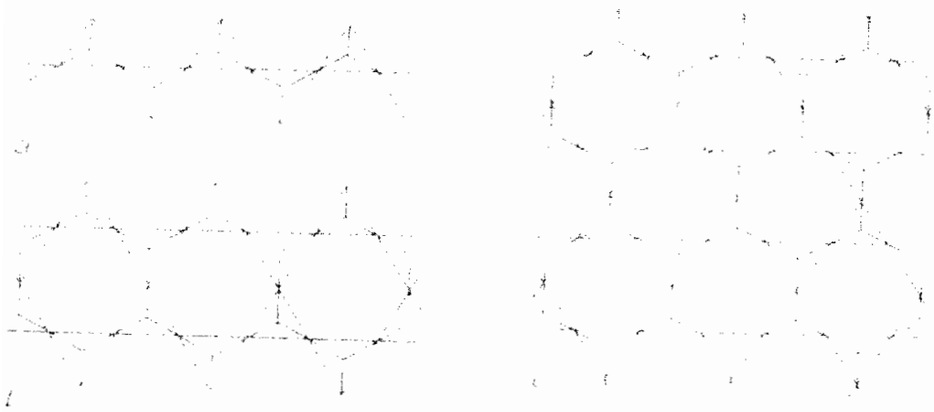

Figure 2-9: Infinite single (a), double (b) chains, sheet (c), of silicon-oxygen tetrahedra

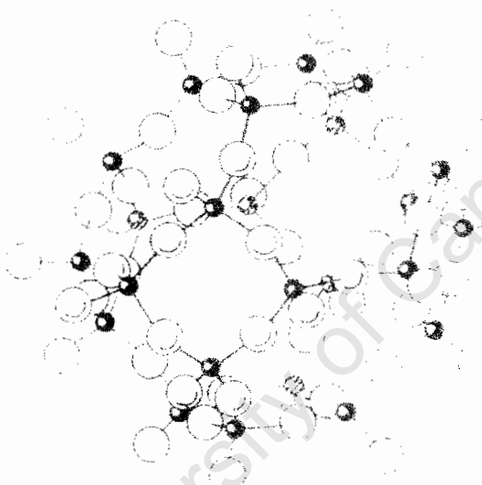

Figure 2-10: Infinite three-dimensional framework of silicon-oxygen tetrahedra

It is characteristic of the silicon-oxygen finite and infinite groups that the component tetrahedra are always linked through their corners (shared oxygens) because of the high charge of the quadrivalent silicon. There are five states discernible in the silicon-oxygen tetrahedra, and these can be denoted, according to G. A. Stepanov, as $[SiO_4]^{4-}$, $[SiO_4]^{3-}$, $[SiO_4]^{2-}$, $[SiO_4]^{1-}$,

and correspond respectively to unshared tetrahedral corners of one, two, three, or all four tetrahedral corners. In the last case the bonds are covalent; in the first they are ionic; the inter-mediate cases have a mixed ionic-covalent bonding. Of importance to the stability and properties of silicate minerals is the additional cations and, in some cases, additional anions and water molecules. The following cations commonly occur with silicate minerals, grouped according to their co-ordination number are:

co-ordination number 4: B^{3+}, Be^{2+}, Al^{3+}, Ti^{4+}, Fe^{3+}, Zn^{2+}
co-ordination number 6: Al^{3+}, Ti^{4+}, Mg^{2+}, Li^{+}, Zr^{4+}, Mn^{2+}, Ca^{2+}, Fe^{2+}, Sc^{3+}
co-ordination number 8: Zr^{4+}, Na^{+}, Ca^{2+}, Fe^{2+}, Mn^{2+}

The highest coordination number is held by K^{+} and Ba^{2+}; the odd co-ordination numbers 5 and 7 are shown by Al^{3+} and Ca^{2+}. The stability of the latter depends on the polarizing power of the silicon ion; this is relatively low in the orthoslilcate groups and high in the groups with shared oxygens. The energy released when Si-O bonds are broken down will increase with the increased number of shared oxygens around each of the silicon ions in the polymerised groups (Figure 2.11).

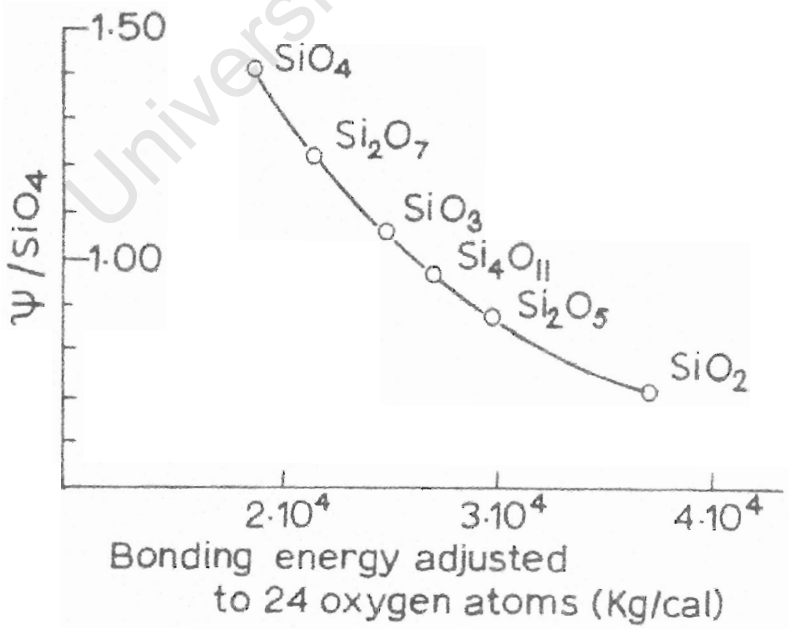

Figure 2-11: Complex anionic potential (Ψ/SiO_4) as a function of the bond energies for some silicate groups [Grasselly, from Kostov, 1968]

2.3.3. Talc

Talc is a layer silicate mineral belonging to the classic of phyllosilicates (Bragg, 1965, Morris, 1996). The basic chemical unit of the silicates is SiO_4, which is a tetrahedron shaped anionic group. The silicon to oxygen ratio is 1 : 2 : 5 as only one oxygen is bonded to the silicon with the other three being shared. The sheets are connected to each other by cations that are weakly bonded and this causes the mineral to be very soft. Figure 2.12 shows that the unit structure of talc is $Mg_3(Si_2O_5)_2(OH)_2$. The layered structure consists of two tetrahedra silica sheets with an octahedral brucite sheet sandwiched between the two silica sheets. The oxygen atoms and hydroxyl groups lie in two parallel planes with the magnesium atoms in between.

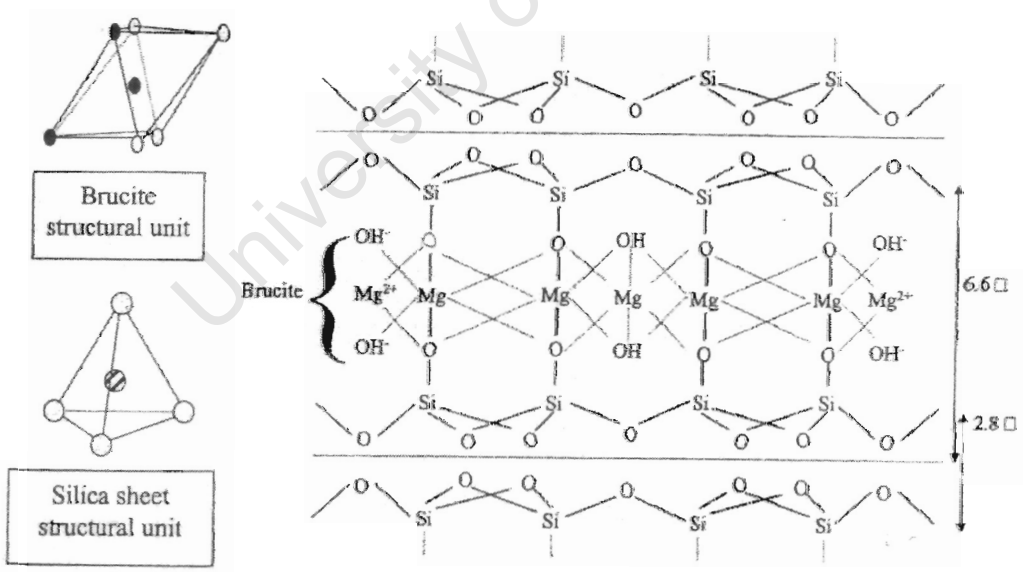

Figure 2-12: The schematic representation of the structure of talc [Morris, 1996]

The major structural characteristic of talc is that the planes are non-polar and hydrophobic and the edges are polar and hydrophilic. The physical properties

of talc are controlled by the weak van der Waals forces exiting between the talc sheets and electrostatic bonding within the layers (Fuerstenau et al., 1988; Gomes and de Oliveira, 1989, 1991). This difference in bonding mechanisms within the talc structure leads to the formation of two very distinct types of surface when talc is broken.

2.3.4. Pyroxene

The pyroxenes belong to the group of metasilicates as they contain a high proportion of silica in the form of SiO_4 tetrahedra together with a group of the elements like magnesium, calcium and sodium in varying proportions. The fundamental SiO_4 tetrahedra are linked together vertically into chains, each tetrahedron sharing two oxygens with those immediately above and below in the chain. The individual chains are joined together through the medium of the cations, Ca(II), Mg(II), Fe(II), which are linked to the free, not the shared oxygen atoms.

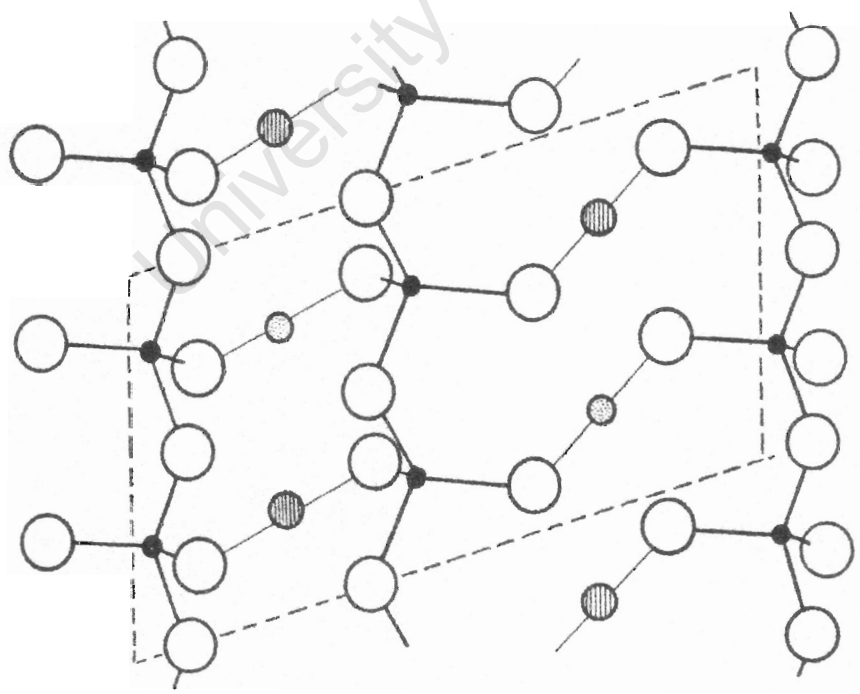

Figure 2-13: The unit cell is outlined, but only parts of its contents are shown. Si(IV) black; Mg(II) dotted; Ca(II) ruled; O(II) plain. [Hatch, 1949]

The unit chains contain Si_2O_6, or in the presence of the cations such as Mg(II), Fe(II) and Ca(II) the formula is $MgSiO_3$ for enstatite, $FeSiO_3$ for ferrosilite, and $CaSiO_3$ for wollastonite. All pyroxenes can be expressed by a simple formula with molecular percentages of these three components. The base of the triangle contains all possible proportions of enstatite to ferrosilites which is an important group of orthopyroxenes (Hatch, 1949).

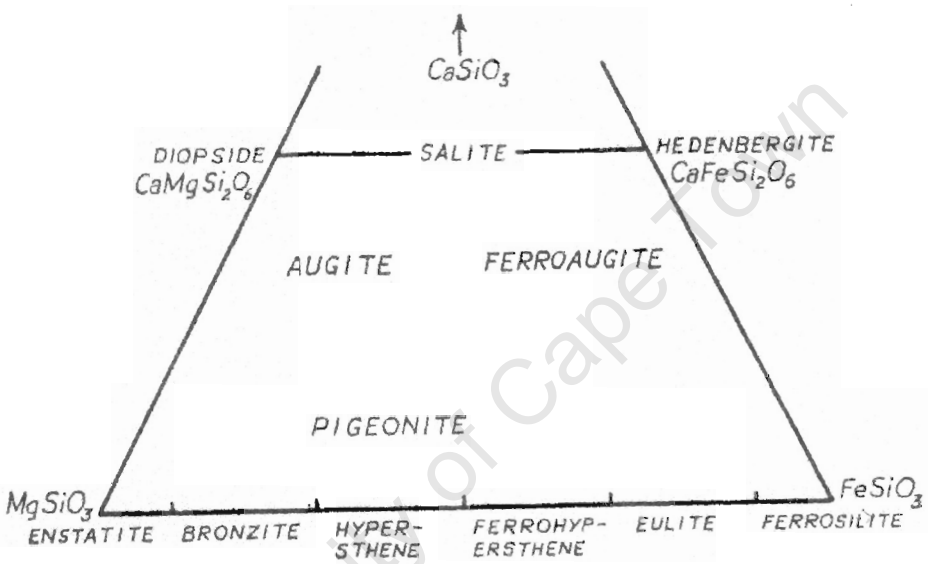

Figure 2-14: Triangular diagram showing compositional relationship between the common pyroxenes

The orthopyroxenes belong to a series called the enstatite-ferrosilite series and they can occur in two forms, one orthorhombic and the other monoclinic. Physical changes separate pyroxenes that crystallise at higher from lower temperatures, which cause the shift from magnesium-rich to iron-rich. The Merensky ore contains predominantly enstatite and the Platreef ore contains diopside.

2.3.5. Feldspar - plagioclases

Plagioclase feldspars are mixed crystals of albite and anorthite. Bowen, (1913) showed that plagioclase feldspars represent near-ideal solid solutions at high temperatures. From this it does not follow that ideality persists at lower temperatures, and plagioclases at room temperatures are extremely complicated mixed crystals. The variation exists in both high- and low-temperature forms and these have distinctive optical properties. The unit structure of feldspars consists of the positive silicon atom surrounded by four oxygen atoms in tetrahedral co-ordination. These tetrahedra are linked together by sharing corners to form interlocking oxygen-silicon chains building up a three-dimensional framework. The physical and chemical characteristics are dependent of silica framework in which form one-quarter to one-half of the tetravalent Si atoms are replaced by trivalent Al atoms (Machatschki, 1928; Barth, 1969).The ratio of substitution can be representing in two forms:

$[AlSi_3O_8]^-$ in which every fourth Si is replaced by Al

$[AlSi_2O_8]^{2-}$ in which every second Si is replaced by Al

This substitution with Al can replace maximum of 50% of the silicons Loewenstein, (1954) and distinguishing between Si and Al tetrahedral is necessary. The anorthite lattice is shown in the Figure 2.15 below:

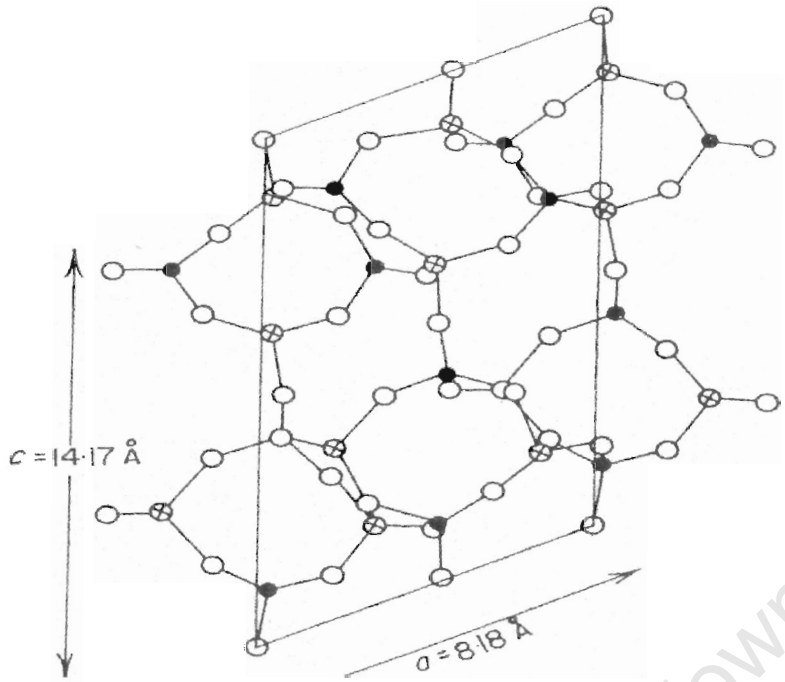

Figure 2-15: The tetrahedral framework of the anorthite lattice projected down the b axis on the plane (0 1 0). A Si-Al-oxygen chain runs parallel to an axis. The anorthite unit cell is outlined; it has the long 14-angstrom c axis.

Feldspars are electrically balanced in the presence of positive cations like Na^+, K^+ or Ca^{2+}, which are induced into the framework.

2.3.6. Chromite

Chromite belongs the spinel group of minerals (Gu and Wills, 1988), with the unit structure (Fe, Mg)O.(Cr, Al, Fe)$_2O_3$ and 45 to 55% Cr_2O_3 (Sobieraj and Laskowski, 1973; Berkman, 1976; Coertze and Coetzee, 1976). The spinels crystallize in the holosymmetric class of the Cubic System and they are double oxides of a divalent and a trivalent element respectively. The ferrous iron is usually replaced by magnesium and the chromium by aluminium and /or ferric iron. These differences in chemical composition between various chromites cause wide variations in the surface properties.

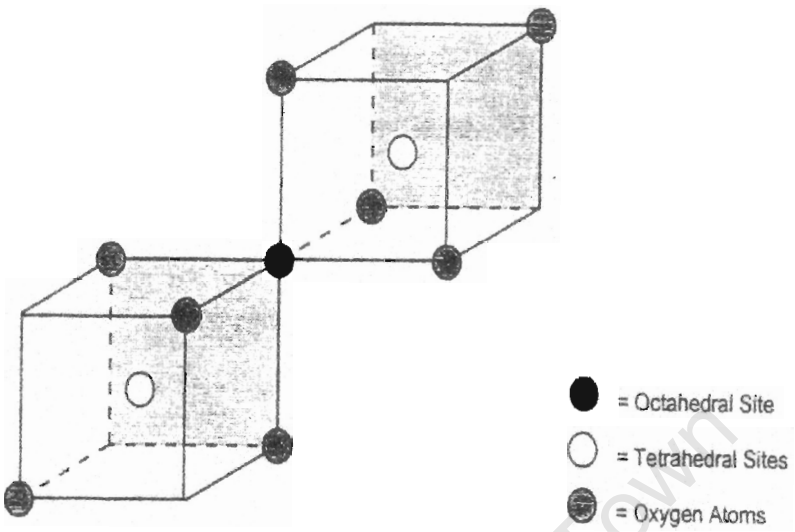

Figure 2-16: The unit crystal structure of spinel, showing the cubic arrangement of the oxygen atoms and the relative positions of the sites of tetrahedral and octahedral co-ordination [McKenzie, 1996].

Figure 2.16 shows the unit structure of chromite. The trivalent ions such as chromium and aluminium are co-ordinated octahedrally with oxygen, while the divalent ions are tetrahedrally co-ordinated (Guney et al., 1993). This characteristic makes the trivalent ions more insoluble than the divalent ions. All chromites are paramagnetic at room temperature and their susceptibilities depend on the iron content (Owada and Harada, 1985). The distribution of magnetic ions is not uniform in the crystal structure, however chromite can be separated from ferromagnetic minerals in a low intensity magnetic field (0,1T) as a non-magnetic product and in a high-intensity (about 1T) as a magnetic product from gangue minerals.

2.3.7. Quartz

Quartz is not a major gangue component in PGM ores but was selected since it is a strongly negatively charged mineral in the alkaline range and therefore likely to respond to copper activation.

Quartz belongs to the class of framework silicates and they are characterized by a three-dimensional network of tetrahedra sharing all four oxygens. The unit structure is SiO_2, with a coordination number of 4:2 The Si-O bonds have covalent character, with oxygen atoms arranged tetrahedrally around silicon Every oxygen atom is shared by two SiO_4 tetrahedra and this structure is electrically neutral. Quartz occurs as both high- and low- temperature modifications, distinguished as beta and alpha quartz. Figure 2.17 shows the structure of quartz.

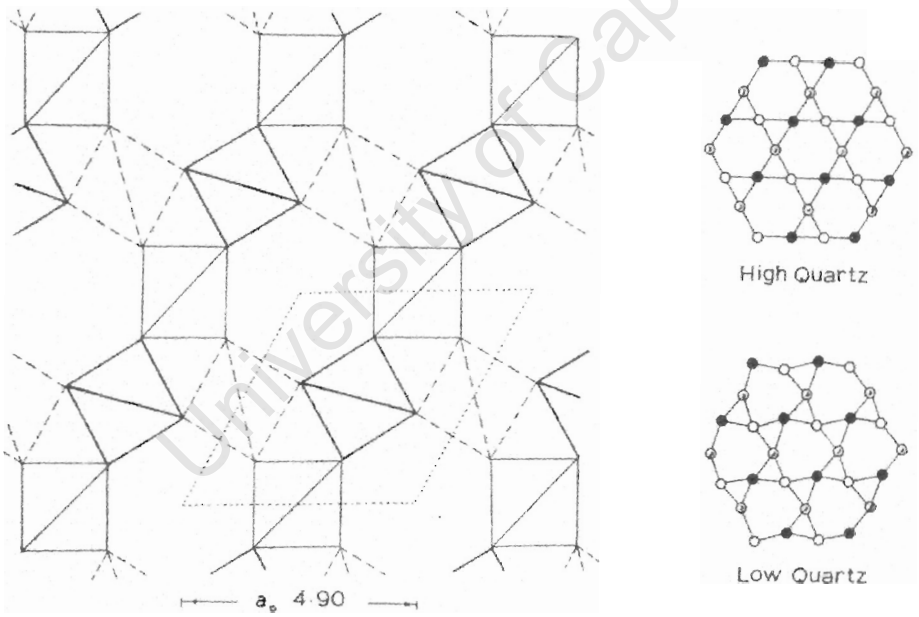

Figure 2-17: Structure of quartz (on the right is shown derivation of the low-temperature from the high-temperature modification) [Kostov, 1968]

The change from the high temperature to the low temperature modification takes place without any considerable rearrangements of the silicon tetrahedra, only slight displacement and rotation being involved. The

important fact is that for all quartz minerals SiO_4 tetrahedra are linked to one another by all their corners and the arrangement in the high (α-quartz) looks more symmetrical than in the low (β-quartz). Alpha quartz crystallizes in the holo-axial (trapezohedral) class of the Trigonal system, beta quartz belongs to the corresponding class of the Hexagonal system.

2.4. MINERAL – WATER BEHAVIOUR

2.4.1. Mineral – Water interfaces and electrical double layer

For mineral particles dispersed in water, two factors are important: (1) the interaction of water molecules with the mineral surface, and (2) the electrical double layer at the mineral surface water interface (Fuerstenau, 1982).
Water is a conductor of electricity and mineral particles in water are almost always electrically charged. The charged species will be transferred across the interface until equilibrium is established. The interface between the mineral and the solution phase can be treated as a semi-permeable membrane which allows only charged species common to both the mineral and the solution to pass through. In water, orientated water layers at the mineral surface have a significant effect on the nature of adsorption at an interface.

Figure 2.18 shows that the first layer of water at the mineral-solution interface consists of oriented water dipoles, some of them in a 'down' position with oriented hydrogen atoms towards the surface and some of them in an 'up' position with oxygen towards the mineral surface. At polar mineral interfaces hydration films show particularly strong and unusual characteristics. The first layer known as the Inner Helmholtz plane (IHP) consists of water molecules oriented by dipole-dipole interactions and the second known as the Outer Helmholtz plane (OHP) of less oriented free water molecules. Some ions will adsorb specifically within the first layer, and others with their hydration sheaths are distributed within the first and second hydration layers. In the

third layer, the bulk water consists of some flickering clusters (nuclei at the holes) at the distance of many monolayers away from the mineral surface (Leja, 1982).

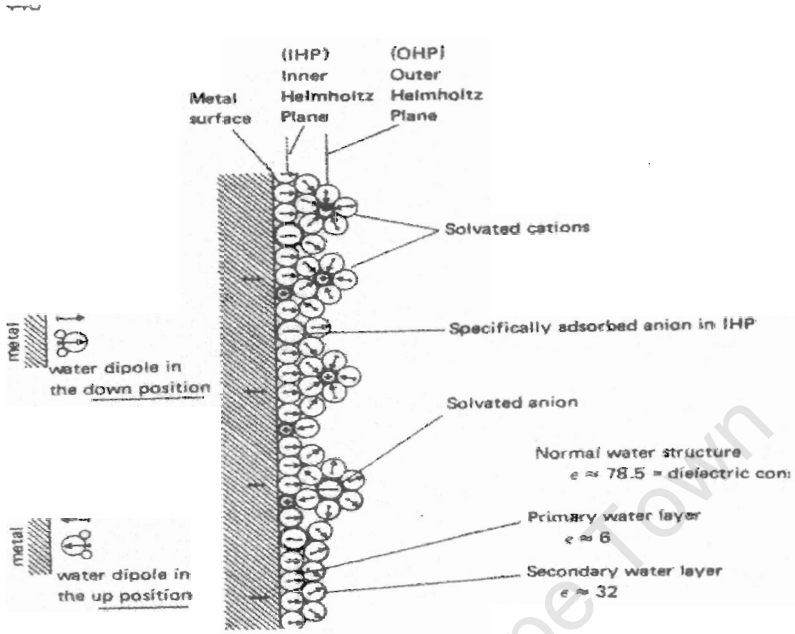

Figure 2-18: Model of a mineral/water interface [Bockris and Reddy, 1970]

Charge development on the mineral surface involves both the dissociation of surface groups and the adsorption of ions from solution. Because hydrogen and hydroxyl ions are present in the solution, the surface charge is strongly pH dependent. Water has also an important effect on the interaction between the reagents and minerals. Malysiak et al, (2003) showed that the water quality used in flotation plays an important role in the way reagents interact with mineral surface. In an investigation of pentlandite-pyroxene and pentlandite-feldspar systems he reported that flotation recoveries for all minerals were lower in synthetic process water compared to those obtained in the electrolyte solution. The lower mineral floatability was attributed to the influence of the ions present in the synthetic water, which adsorb onto the active sites of the minerals and thus interfere with the adsorption of copper (II), nickel (II) and xanthate ions.

The ions adsorbed on the mineral surfaces will be distributed according to the influence of electrical forces and thermal motion. As seen in Figure 2.18, the former form an inner region of the electrical double layer (adsorbed), the latter a diffused region. Ions of opposite change (counter ions) are attracted to the mineral surface in order to neutralise its charge, whilst ions of similar charge (co-ions) will be repelled from the surface. Those particular ions that are free to pass between both double layers are called potential determining ions and they are specific for each system. If the surface charges are zero, the electrostatic field is absent and no salt effect is observed. This point is usually called the point of zero charge (PZC) and the point at which the zeta potential of the mineral is zero is called iso electric point (IEP). The importance of the PZC is that the sign of the surface charge has a major effect on the adsorption of all other ions, particularly for those charged oppositely (counter-ions) to the surface, because their function is to maintain electroneutrality. Figure 2.19 shows a schematic view of the change in charge with distance resulting from the electrical double layer and the diffuse double layer.

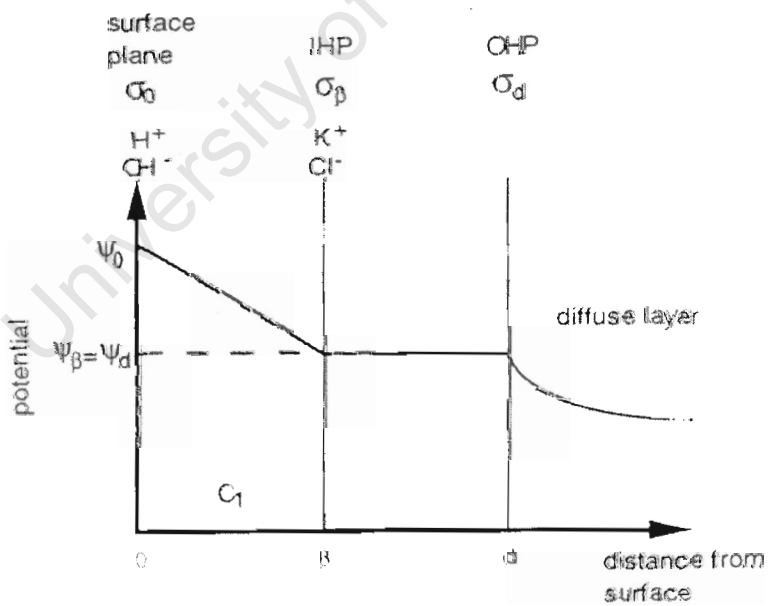

Figure 2-19: Schematic representation of an electric and diffuse double layer [Steenberg, 1982]

2.4.2. Zeta potential determinations

The zeta potential is the potential at the plane of shear. The exact location of this plane of shear is not known though there is evidence that is close to the stern plane (Inner Helmholtz plane (IHP)) which is a couple of molecular diameters from the surface (Hiemenz, 1997). The zeta potential in the solution then falls exponentially with distance from the surface (Everett, 1989):

$$\psi = \psi^{\circ} e^{(-k z)} \qquad \text{Equation 3}$$

Thus at a distance 1/k the potential has dropped by a factor of (1/e). This distance may be used as a measure of the extension of the double layer and is often called the thickness of the double layer. The e is the electronic unit charge and z is the valence. Figure 2.20 shows a schematic view of various double-layer potentials:

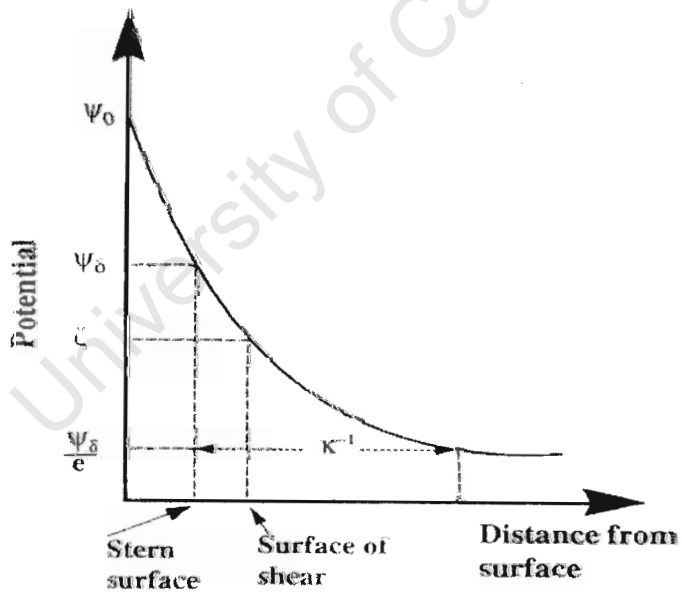

Figure 2-20: Potential distribution of the solid liquid interface [Hiemenz, 1997]

Variation of zeta potential with distance is dependent on the electrolyte concentration. $1/k = [\varepsilon RT / F^2 \Sigma c_i z_i^2]^{1/2}$, where c_i is the number of ions m^{-3}; if c_i

Variation of zeta potential with distance is dependent on the electrolyte concentration. $1/k = [\varepsilon RT / F^2 \Sigma c_i z_i^2]^{1/2}$, where c_i is the number of ions m^{-3}; if c_i is expressed in mol m^{-3} and F is the Faraday constant and ε is dielectric contant. The higher the ionic strength of the electrolyte the more compact the diffuse region becomes due to the strong inter-ionic attraction. If the concentration of electrolyte does not affect the PZC, it is known as an indifferent electrolyte. Figure 2.21 below illustrates the typical ratio of particle radius to double layer thickness.

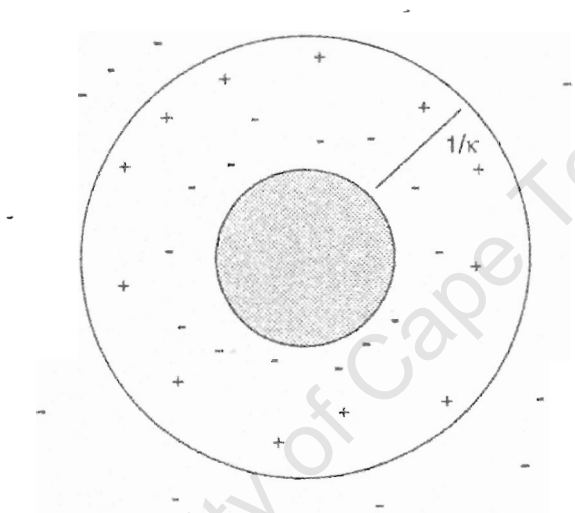

Figure 2-21: The typical ratio of particle radius to double layer thickness

Surface charge and electrical double properties in aqueous solution can be determined by electrophoretic mobility measurements. The electrophoretic mobility, U_e is the mobility or velocity of a particle in an applied electric field. Zeta potential is related to the electrophoretic mobility by the Henry equation:

$$U_e = \varepsilon \times \zeta \times f \times (Ka)/6\pi\eta \qquad \text{Equation 4}$$

Where ζ = zeta potential, U_e = mobility, ε = dielectric constant, η= viscosity, f (Ka) = factor including double layer thickness and particle diameter (1.0 for non-polar media, 1.5 for large particles in polar media).

For water at 25°C, $\eta = 8.904 \times 10^{-4}$ Pa s and $\varepsilon = 6.938 \times 10^{-10}$ F m^{-1}, the zeta potential, ζ = (mV), can be determined by

$$\zeta = 12.85\ U_e \qquad \textbf{Equation 6}$$

Zeta potential determinations are often used to investigate the behaviour of mineral surfaces in an aqueous system. The electrical double layer controls the adsorption of ions and zeta potential determinations can indicate adsorption by taking the sign of the zeta coefficient into account. The determination of positive zeta coefficients will indicate cationic adsorption, while negative determination indicates anionic adsorption. Thus determining the sign of the change of charge of the mineral surface is necessary in order to ascertain the response of a mineral to flotation with anionic or cationic collectors. The formation of an electrical double layer at the interface between oxide and silicate minerals in aqueous medium can be controlled by broken –Si-O and –M-O bonds at the surface of mineral (Fuerstenau, 1982). In the case of these minerals the potential-determining ions will be H^+ and OH^- ions, from which the surface charge can be calculated as a function of pH and electrolyte concentration. Figure 2.22 shows breaking Al-O and Si-O sites at the mineral surface:

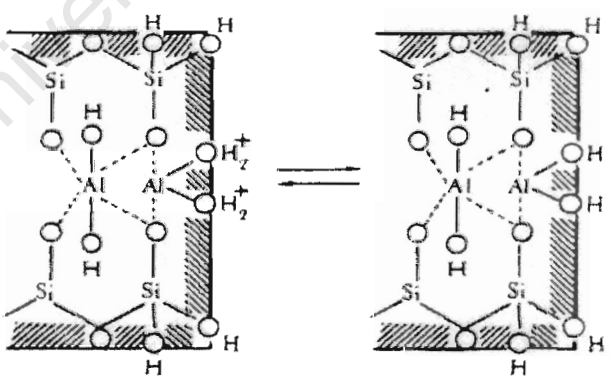

Figure 2-22: Schematic illustration of aluminium- silicate particle [Everett, 1989]

It is characteristic for all oxide minerals that their surfaces after hydroxylation show a positive charge at low pH and negative charge at high pH with point of

zero charge somewhere between and following the simple reactions that can take place (Laskowski, 1996):

$-MOH + H^+ = MOH_2^+$	**at low pH values**	**Equation 7**
$-MOH + OH^- = -MO^- + H_2O$	**at high pH values**	**Equation 8**
At the p.z.c: $[-MOH_2^+] = [-MO^-]$		**Equation 9**

The nature of the surface of silicate minerals depends on their crystal chemistry, which in turn determines the nature and the extent of broken bonds at the surface. The PZC for different crystals in silicate group minerals will vary. Deju and Bhappu, (1966) reported that the point of zero charge of silicate minerals increases as the oxygen-silicon ratio increases as is shown in Figure 2.11 but also depends on the purity of minerals.

2.5. ADSORPTION ONTO MINERAL SURFACES

Adsorption may, in general, be either physical or chemical in nature. The charge transfer (or sharing of electrons) is used to differentiate between the physical and the chemical adsorption process. Physical adsorption is usually (but not always) fast and reversible, while chemical adsorption is generally slow and irreversible and requires an appreciable energy of activation (Leja, 1982). In many cases adsorption is intermediate. For the zeta potential sign to reverse, the charge in the Stern plane should change during adsorption. Fuerstenau, (1976) suggests three mechanisms of adsorption of copper ions onto quartz surfaces:

a. Water formation by combination of the hydroxyl ion of the hydroxy complex and adsorbed hydrogen ion,
b. Hydrogen bonding of the hydroxy complex with the surface

a. Water formation by combination of the hydroxyl ion of the hydroxy complex and adsorbed hydrogen ion,
b. Hydrogen bonding of the hydroxy complex with the surface
c. Formation and adsorption of the metal hydroxide on the solid surface

For example, Ca^{2+} ions are surface active and they can reverse zeta potential but only around the PZC (James and Healy, 1972). James and Healy have also another explanation of zeta potential reversal in the presence of hydrolysed metal ions. They postulated that zeta potential reversal is due to the onset of nucleation of a coating of the metal hydroxide. In the case of hydrolysing metal ions for anionic solids such as oxides and silicates, there exists two zeta potential reversals and it is now well established that pH and concentration control the range where the surface becomes coated with a uniform monolayer of hydrous oxide. This specific adsorption is also called surface complexation as complexes are formed between the charged surface sites and the electrolyte ions.

2.5.1. Effect of ions on the surface of gangue (oxide) minerals

Ions have a strong effect on both the surface charge and floatability of talc (Fuerstenau, 1988). The nature and degree of hydrolysis of ionic species is strongly dependent on the pH (critical pH of solubility), which is the solubility limit for concentration (Cs) of the hydrated species in solution. This hydrated species precipitates in the form of metal hydroxides and can precipitate into or out of solution. The general electrophoretic mobility behaviour of oxide minerals in the presence and absence of hydrolysable ions is given by (James and Healy, 1972). Figure 2.23 shows the effect of heavy metal ions on zeta potentials.

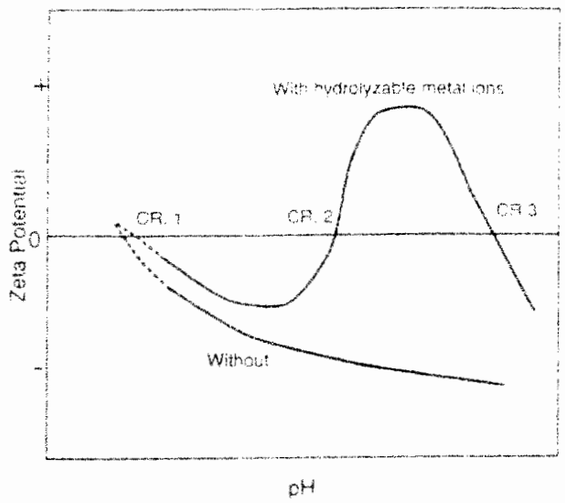

Figure 2-23: Schematic illustration of the general electrophoretic mobility [after James and Healy, 1972]

The pH values of the electrokinetic potential are listed as CR.1, CR.2 and CR.3 in order of increasing pH. According to James and Healy, CR.1 was the iso-electric-point for the solid, CR.2 is the pH of surface precipitation and between CR2 and CR3 bulk precipitation occurs, and CR.3 was the iso-electric-point of the metal hydroxide. Although it was not possible to identify the forms in which hydrolysable ions adsorb, electrokinetic experiments were able to give an indication of the adsorption of metal ions species on mineral surfaces for the interpretation of flotation results.

Laskowski, Liu and Zhan, (1997) conclude that electrokinetic and flotation tests can be used to study the mechanism of sphalerite activation and activation of sulphide minerals with metal ions which is a well known phenomenon (Somasundaran, 1986).

2.5.1.1. Effect of copper ions on gangue minerals

The presence of metal ions in the flotation pulp can have a major influence on the flotation behaviour. Their inadvertent activation can seriously impact selectivity and the flotation separation as inorganic or multivalent metal ions charged oppositely to the surface can function as a link between the collector and the mineral surface (Fuerstenau and Fuerstenau, 1982).

The activation of sulphide minerals by metal ions has been reviewed (Acar and Somasundaran, 1992; Finkelstein and Allison, 1997; Laskowski, Liu and Zhan, 1997) but less work has been done on the activation of oxide and silicate minerals. Fuerstenau, (1975) showed that oxide minerals could be activated with metal ions such as copper and lead and subsequently floated with a collector and later Nagaraj and Brinen, (1996) also showed using SIMS and XPS analysis that the addition of collector changed the form to Cu^{2+} to Cu^{+} on the surface of pyroxene and pyrite.

Wesseldijk, (1999) investigated the possible activation of chromite surfaces after the addition of copper sulphate at a range of pH values. Zeta potential results showed that Cu^{2+} was adsorbed on the chromite surface at pH values where $CuOH^{+}$ was formed, charge reversal was also observed and maximum flotation recovery was achieved at pH 6 supporting copper activation. The excess of copper present in $Cu(OH)_2$ would be precipitated at higher pH (about 9) reducing the hydrophobicity of chromite. The zeta potential was determined on the chromite surface in the presence of $1*10^{-4}$ mol/l of copper sulphate. The logarithmic concentration of copper species (King, 1982) is shown in Figure 2.24.

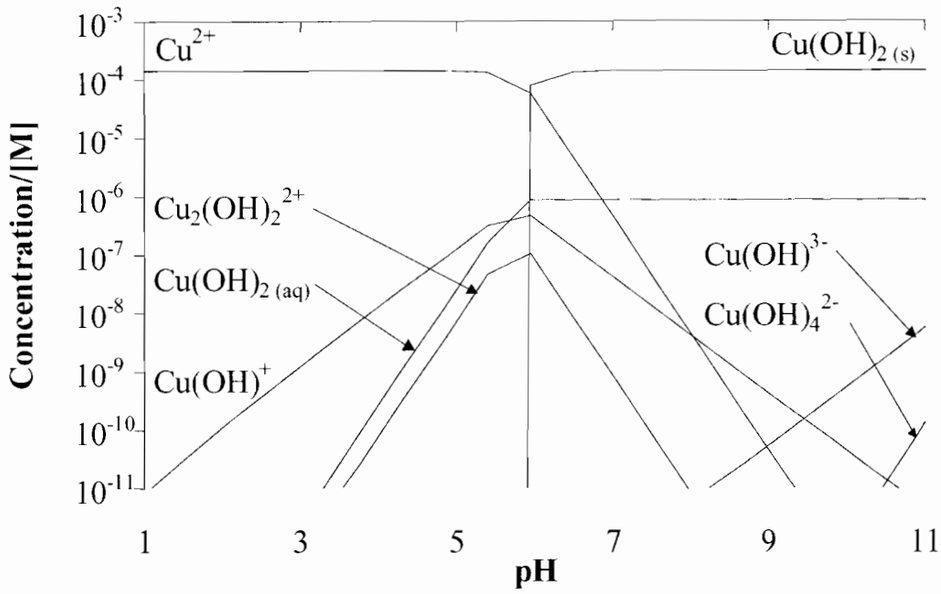

Figure 2-24: Logarithmic concentration of copper species for $1*10^{-4}$ mol/l Cu^{2+} [King, 1982]

More recently Malysiak and Shackelton, (2003) showed with TOF-SIMS analysis that the possibility for activation of the pentlandite was greater although some activation and reaction with the collector was obtained with the pyroxene and feldspar. Mailula, (2004) reported low floatability in the absence of copper and xanthate but strong floatability of activated pyroxene and feldspar in the presence of the copper and xanthate.

2.5.2. Adsorption of polymers onto minerals

Adsorption of polymer segments will take place if the interaction energy (adsorption energy) of the segments is larger than the interaction between solvent molecules and the surface. In solution, the segments have many degrees of freedom, which are (strongly) diminished when they adsorb. Thus, the energy of adsorption has to overcome the loss of conformational entropy (Fleer, Stuart, Scheutjens, 1993). When polymers adsorb, conformational entropy is maintained through sections of the chain, which are not attached to the surface (loop and tails). Figure 2.25 shows the schematic representation

of adsorbed polymer molecule at the solid-liquid interface (train-loop-tail conformation).

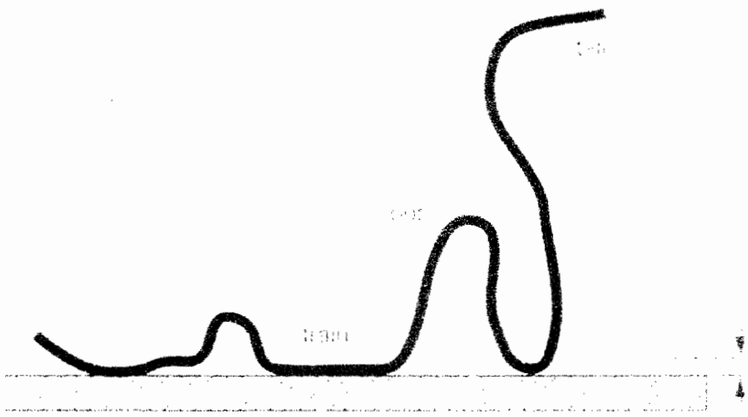

Figure 2-25: Schematic representation of an adsorbed polymer molecule

The sequence of segments which is attached to the surface, is called a train. Loops are sections between two trains while tails consist of segments at the end of the chain dangling in the solution. Parameters that affect the conformation of the adsorbed polymer layer (i.e. the contribution of trains, loops, and tails) are the adsorption energy, the adsorbed amount of polymer, and molar mass of polymer (i.e. the length of the chain), (Hoogendam, 1998).

In general for uncharged polymers, the size of the loops and tails increases with the length of the chain. Polyelectrolytes are charged polymers and can be distinguished by their fixed charges (strong) and with their charges dependent on pH and salt concentration (weak). Both electrostatic interactions and the charge of the mineral surface affect adsorption. When the polyelectrolyte and the mineral have the same sign, electrostatics work against the adsorption. Adsorption can only take place if the non-electrostatic interaction is high enough to overcome the electrostatic repulsion between segments and mineral and the mutual repulsion between segments. Salt has this ability and can increase the adsorbed amount, as well for uncharged

mineral surfaces. In the case when the polyelectrolyte and the mineral have the opposite charge, electrostatics favours the adsorption and the presence of salt can have effect of increasing or decreasing the adsorption. The presence of metal cations for adsorption of anionic polyelectrolytes onto negatively charged mineral surfaces can overcame the electrostatic repulsion and allow cation binding or complexation of the anionic groups of the polymer (Laskowski, and Liu, 1989).

2.5.3. Adsorption of CMC and guar gum onto gangue minerals

The adsorption onto a variety of minerals with selections of polysaccharide depressants was investigated by Steenberg and Harris (1984). In order to determine whether specific interactions occurred on certain minerals and to study the adsorption mechanisms, the study covered a range of minerals from the layer-silicates, oxides, as well as sulphides with polymers such as CMCs, guar gums and a starch depressant. It was established for all polymers that adsorption onto talc occurred first on the basal plane and then on the talc edge, while for oxide type minerals, because of their hydrophilic nature, adsorption could be compared to that on the hydrophilic talc edge.

Shortridge (1999) investigated the difference in the depressant behaviour of guars and CMCs with varying molecular weights, ionic strength and dosage on the flotation of talc. Microflotation tests showed that ionic conditions (ionic strength, type of cations) played an important role in the performance of the CMC depressants in reducing the flotation of talc. Ca^{2+} ions were more effective than Mg^{2+} and K^{+} ions in enhancing the depressant action of the CMCs. It was also established that guar gum adsorbed more strongly than CMC and the adsorption of guar gum was independent of water quality. Dalvie (2001) showed that recovery of talc could be effectively reduced with addition of polymeric depressants in conjunction with an inorganic dispersant, sodium hexa-meta-phosphate. The investigation by Mailula, (2004) showed

the ability of polymeric depressants to counteract activation by a typical reagent suite onto pyroxene and feldspar surface using microflotation. The recent investigation by Parolis et al (2003) on two types of talc (New York and Barberton talc) showed that in the presence of divalent cations (Ca^{2+} and Mg^{2+}) the adsorption density of three different CMCs increased in comparison to the adsorption with K^{+}.

Both Malysiak and Shackelton (2003) and Mailula, (2004) studied the effect of the presence of calcium on copper activation and showed that there appeared to be competitive adsorption in that calcium reduced the effect of the activation. Figure 2.26 and 2.27 shows the effect of ionic strength of $Ca(NO_3)_2$ on the recovery of pyroxene and feldspar in the presence of $CuSO_4$ and SIBX

.

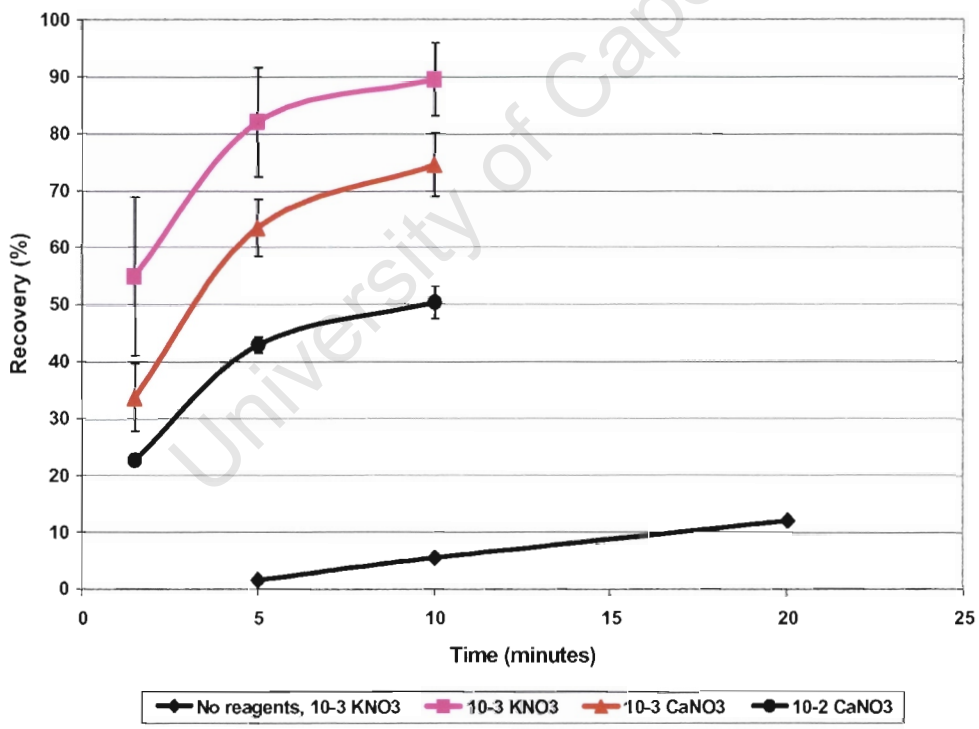

Figure 2-26: The effect of ionic strength on the recovery of pyroxene in the presence of 5 10^{-5} M copper sulphate and 5 10^{-5} M SIBX at pH 9 [Mailula, 2004]

Figures 2.26 and 2.27 showed that the presence of 10^{-2} I.S. $Ca(NO_3)_2$ has reduced the extent of activation on both pyroxene and feldspar. This also indicates that this effect was not mineral specific.

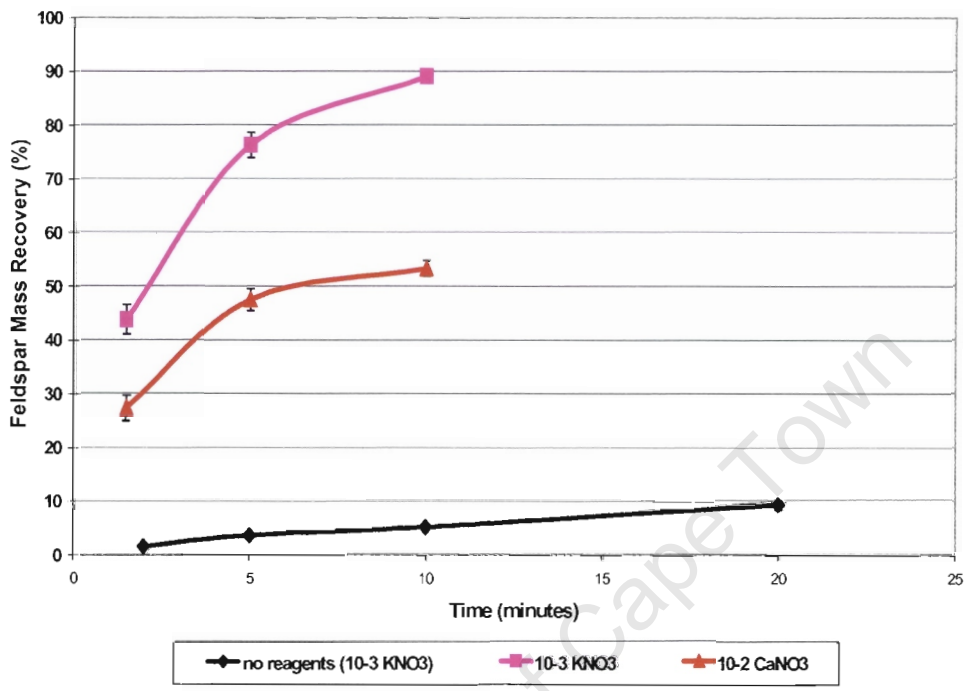

Figure 2-27: The effect of ionic strength on the recovery of feldspar in the presence of 1 10^{-5} M copper sulphate and 1 10^{-5} M SIBX at pH 9 [Mailula, 2004]

2.6. SUMMARY OF LITERATURE REVIEW

There are indications from the previous work that gangue minerals from PGM ores could be rendered hydrophobic by inadvertent activation by metal ions and subsequent reaction with the collector. The activation by copper ions of these sulphide minerals in alkaline solutions and the use of complexing agents to deactivate siliceous minerals has been described by previous researchers (Malysiak and Shackelton, 2003). In their studies the effect of the presence of calcium ions on copper activation has shown that calcium reduced the effect of the activation. Another investigation of these silicate

minerals showed that they are strongly floatable after activation by copper ions and addition of collector but the addition of polymeric depressants was found to cause a slight reduction in their floatability (Mailula, 2004). However, there is not much information available in the literature about silicate minerals in terms of inadvertent activation by copper ions and subsequent flotation due to the adsorption of xanthate ions and the reduction of floatability by the addition of polymeric depressants.

2.7. SCOPE AND KEY QUESTIONS

In this study the surface properties and interactions with copper ions of a range of gangue minerals; talc, pyroxene, feldspar, chromite and quartz were examined using zeta potential, adsorption and microflotation data. Quartz is not a major gangue mineral in PGM ores but was selected because of the strongly negatively charged mineral surface and therefore it is expected to respond easily to copper activation. With copper sulphate addition, copper ions are expected to interact with the silicate mineral surface and make it amenable for collector adsorption and thus change its surface properties and floatability. The use of polymeric depressants, CMC and guar gum in practice is mainly to reduce the recovery of naturally floatable minerals such as talc.

This study also investigates the influence of these depressants on the floatability of these copper-activated gangue minerals and the overall objectives are to:

To investigate whether inadvertent copper activation is mineral specific and to evaluate whether the floatability of copper activated minerals can be reduced by addition of polymeric depressants

The following key questions address the objectives:

- How do selected ions (K^+, Ca^{2+}, Cu^{2+}) in solution influence the surface charge of gangue minerals during the zeta potential determinations?

- Do they respond differently and what is effect of ionic strength?

- Is the effect of Cu^{2+} ions specific to mineral type?

- How does the presence of K^{+} ions affect the mineral surface charge when adding of CMC or Guar gum?

- Can polymeric depressants adsorb onto all selected mineral surfaces in the presence of Ca^{2+} ions and which one has higher adsorption densities?

- Are selected gangue minerals naturally floatable?

- Can selected gangue minerals be activated by copper sulphate and collector?

- Can polymeric depressants reduce floatability of all activated gangue minerals?

- What is the difference in behaviour between guar and CMC and how is this affected by dosage?

- Can the zeta potential and adsorption be used to interpret flotation response?

3. EXPERIMENTAL DETAILS

3.1. MATERIALS

3.1.1. Minerals

Talc from Scotia Mine, chromite from the Ntuane Chrome Mine, part of the Bushveld Complex, feldspar and orthopyroxenes from Merensky Reef and quartz from Delmas was used. The –38 µm size fraction was used for the adsorption tests and was further ground using a mortar and pestle for the zeta potential measurements to obtain sub 15µm particles. This was confirmed using the Malvern Particle Size Analyser. The surface area was determined using BET techniques and these are shown in Table 3.1. For microflotation tests the -106 + 75 µm size fraction was used and prepared by dry-milling in a rod mill and then dry-screened.

Table 3.1: Surface area (-38 µm) of the minerals used for adsorption tests

Mineral	Source	Surface area (m^2/g)
Chromite	Ntuane Chrome Mine	2.14
Feldspar	Merensky Reef	3.50
Pyroxene	Merensky Reef	3.10
Quartz	Delmas	2.81
Talc	Scotia Mine	2.08

The chemical composition of the minerals used for study was determined by Inductively Coupled Plasma (ICP) Spectrometry by the Department of Geology, UCT and these are shown in Table 3-2.

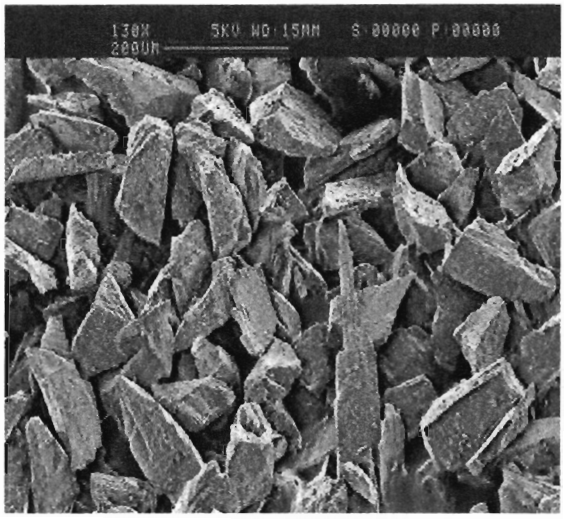

Figure 3-2 b: SEM images of the pyroxene sample used for the microflotaiton tests

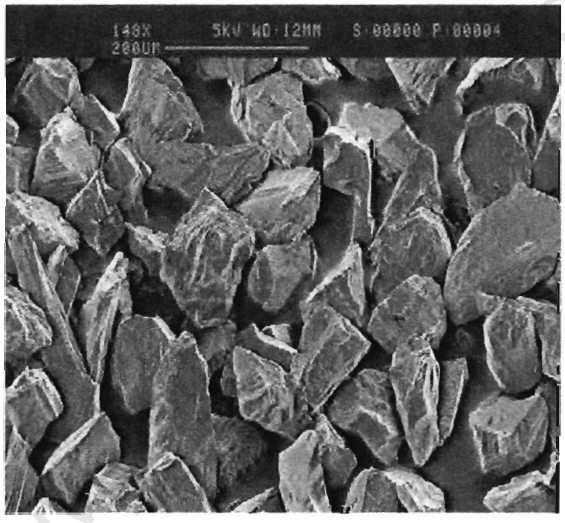

Figure 3-3c: SEM images of the feldspar used for the microflotation tests

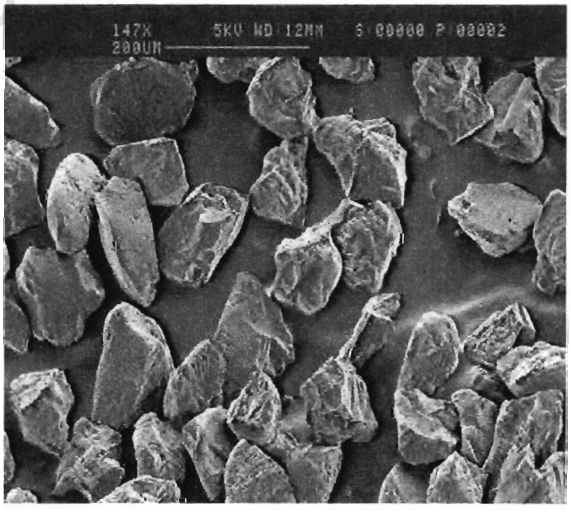

Figure 3-4 d: SEM images of the quartz sample used for the microflotation tests

Table 3-2 : Chemical composition (wt. %) of the mineral

Mineral	Element Wt.%						
	Mg	Al	Si	Ca	Cr	Fe	K
Chromite	0	6.4	0.79	0.06	38.5	20.9	0.009
Feldspar	0.65	9.57	15.4	9.87	0.029	0.45	0.114
Pyroxene	11.0	0.74	18.7	0.87	0.106	15.9	0.022
Talc	15.92	0.06	13.6	0	0.045	8.7	0.004

Figure 3-1 a, b, c, d, e show the SEM images scanned at 200µm of all five minerals selected for investigation and used for microflotation tests with a size distribution of (+75 -106µm).

SEM images for all five minerals clearly demonstrate uniformity of the sample and shape that is characteristic for each type of mineral. It is noted that Scotia talc is much more textured than the other minerals and the pyroxene more plate like.

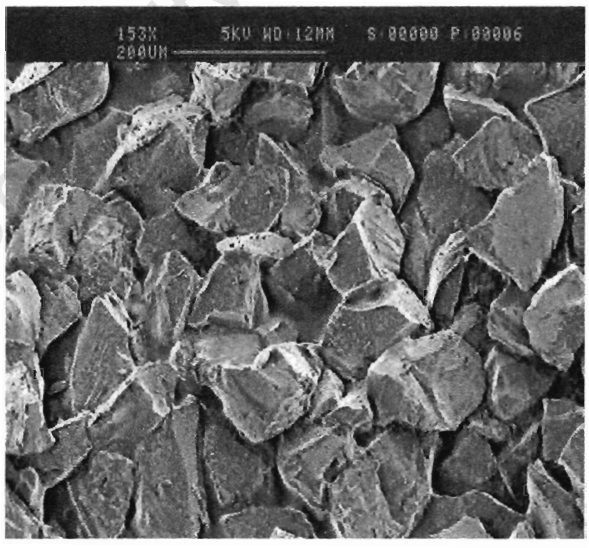

Figure 3-1 a: SEM images of the chromite sample used for the microflotation tests

Figure 3-5 e: SEM images of the talc sample used for the microflotation tests

3.1.2. Mineral preparation for pyroxene and feldspar

A selected ore sample used for the experiments was obtained from Anglo Platinum Research centre. A 20-kg product was separated into 2-kg bags, which were to be magnetically separated using the Frantz Separator and separated at the Department of Geology, UCT. The Frantz separator separates different minerals depending on their magnetic susceptibility. The following magnetic susceptibilities were obtained:

- Chromite - 0.35 – 0.45 amp
- Pyroxene - 0.8 – 1.20 amp
- Feldspar - 1.4 – 1.75 amp

Chromite was separated first because of high magnetic susceptibility and then the current was increased to 0.8 to separate pyroxene (magnetic) from the feldspar (non-magnetic). The side tilt on the Franz was kept at 15^0 and the front tilt at 25^0. It was agreed that the samples were pure enough to perform microflotation tests.

3.2. REAGENTS

3.2.1. Inorganic

The sources of the desired metallic cations used in the experiments were, $CuSO_4$, KNO_3 and $Ca(NO_3)_2.4H_2$. $CuSO_4$ was used at a concentration of $1*10^{-4}$ M. The ionic strength of solution was set according to the following formula:

$$u = \frac{1}{2} \sum c_i . z_i^2 \qquad \textbf{Equation 10}$$

Were is: u = ionic strength, c_i = concentration of ion *i* and z_i = valency

Table 3-3 reports the concentrations of salts used to set the ionic strength of solution:

Salt	Molar Concentration	Concentration of metallic ion in mg/l (ppm)	Ionic Strength
KNO_3	10^{-3} mol/dm^3 10^{-2} mol/dm^3	39 K^+ 390 K^+	10^{-3} 10^{-2}
$Ca(NO_3)_2.4H_2O$	3.33 x 10^{-4} mol/dm^3 3.33 x 10^{-3}mol/dm^3	13.3 Ca^{2+} 133.3 Ca^{2+}	10^{-3} 10^{-2}

For all experiments KNO_3 at 10^{-3} ionic strength was used as the indifferent electrolyte and for adsorption studies $Ca(NO_3)_2$ was used at 10^{-2} ionic strength.

The microflotation tests used purified sodium isobutyl xanthate (SIBX) obtained from SENMIN as the collector. Experiments were performed using $1*10^{-4}$ $CuSO_4$ and $1*10^{-4}$ M SIBX, and based on the reaction stochiometry there would always be an excess of copper ions (50%) available in solution according to the following reaction:

$$Cu^{++} + 2\,X^- \Leftrightarrow CuX_2 \qquad \textbf{Equation 11}$$

3.2.2. Depressants

The carboxymethylcellulose (FF30) from Noviant and modified guar (APX4M) from Agricultural Product Exchange were used. The depressants were made up as 1% solutions. The depressant was added at a slow rate to a stirred beaker containing the de-ionised water. The solution was then made up to a 100ml and allowed to equilibrate overnight. The depressants were used for a maximum of four days and then fresh solution was made up.

3.2.2.1. Characterisation of depressants

The characterisation of the depressants was performed by the Depressant Research Facility at the University of Cape Town.

Table 3-4: Characterisation of the depressants used in the testwork

	FF30	APX4M
Purity	98 %	88.8 %
pH (1%)	6.72	4.04
Moisture	5.7 %	10.8 %
Viscosity(1.5%) **(1.0%)** **(0.5%)**	14.32 7.80 4.09	7.25 3.88 1.98
% Insolubles	2.8 %	14.6%
Mw	250 000	311 300
Mn	63 000	89 900
PD	4.0	3.5
DS	0.76	/

3.3. ZETA POTENTIAL DETERMINATIONS

Zeta potential determinations can provide the guidelines for establishing the charge of the mineral surface. The effect of dissolved mineral species and their hydroxy species on the electrokinetic properties of various oxide minerals was obtained by conducting zeta potential experiments in selected inorganic electrolyte solutions as a function of pH. The effect of the adsorption of selected ions and polymeric depressants was also investigated. Zeta potential determinations were carried out on dilute dispersions of the minerals using a Malvern Zetasizer 4. The instrument gives the electrophoretic mobility from which the zeta potential was calculated using the Smoluchowski equation, since $k_a << 1$ (Hunter, 1993).

3.3.1. Experimental procedure

The electrolyte used for the zeta potential test was potassium nitrate (KNO_3) at a concentration of 10^{-3} M (10^{-3} I.S.). A stock solution of acid (10^{-2} M HNO_3) and base (10^{-2} M KOH) was prepared and used as pH modifiers. These reagents were all analytical grades and prepared in deionised water.

The selected mineral was ground with a ceramic pestle and mortar to obtain very fine particles, which were suspended in a 100 ml 10^{-3} M KNO_3 solution to maintain the ionic strength. The calculated amounts of electrolyte and inorganic reagents and/or depressant were added to a beaker containing de-ionised water. This solution was stirred and made up as a 0.1% solution. This mixture was then stirred and sonicated. The pH modifiers were then added to obtain the desired pH. The mineral zeta potential measurements were made at pH 10 and pH adjusted down to pH 3 to prevent immediate leaching out of ions which could influence the results. In the presence of copper sulphate, measurements had to be started at low pH, since the precipitation of $Cu(OH)_2$ at high alkaline pHs was expected to interfere with the measurements.

3.4. EQUILIBRIUM ADSORPTION STUDIES

Equilibrium adsorption studies were performed on the five minerals (talc, pyroxene, feldspar, quartz and chromite) with two polymer depressants FF30 and APX4M in the presence of $Ca(NO_3)_2$ to ascertain the differences in behaviour of the selected minerals. The concentration of polymer before and after adsorption was determined by measuring the total organic carbon in solution using a SGE ANATOC II TOC analyser.

3.4.1. Adsorption procedure

2g of the -35µm size fraction for each mineral was conditioned in 100ml of 10^{-2} ionic strength of $Ca(NO_3)_2$ and known concentration of polymer solution, including a blank. The pH was adjusted to pH 9 which was the same as for the microflotation tests. KOH and HNO_3 were used as the pH modifiers. The suspension was stirred at room temperature and the timer was started at the time of addition of the mineral and stopped after 30 minutes. A 20ml aliquot was taken and filtered through a Millipore 0.45µm filter to remove mineral particles. The solution was analysed for organic carbon content before and after adsorption and each adsorption was done in duplicate. The obtained readings were converted to concentration from the calibration curve and the amount of polymer adsorbed per unit surface area of each mineral was calculated and results averaged. Two different concentrations of polymer were used: 50 and100mg/l.

3.5. MICROFLOTATION TESTS

Microflotation experiments were carried out using the U.C.T. flow-through microflotation cell (Bradshaw and O'Connor, 1996). The flow-through microflotation cell was developed to measure the success of the mineral collection sub-process in the flotation system and is useful for the investigation of the floatability of pure minerals. The mechanisms occurring between the reagents and a specific mineral can be investigated, since the influences of froth characteristics, cell dynamics and competition of other minerals in the pulp are not present. A microflotation cell in this work was used to investigate the recovery of gangue minerals as well as to determine the flotation response of selected copper activated minerals and to elucidate the factors influencing the behaviour of polymeric depressants. The pH was set at 9 for all the tests. Blank experiments without any reagent additions were also performed to determine natural floatability. The microflotation apparatus is shown in Figure 3.6.

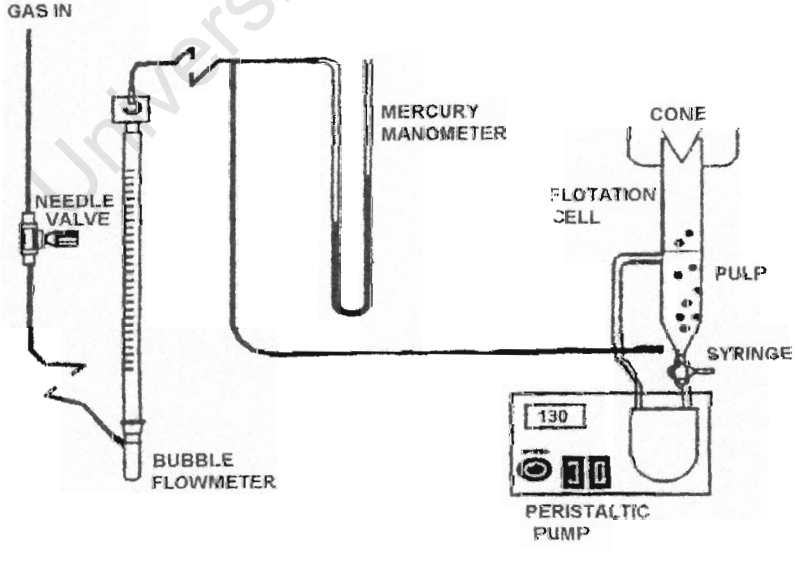

Figure 3-6: A schematic diagram of a UCT flow-through microflotation cell

3.5.1. Microflotation procedure

The following conditioning procedure was used for all microflotation tests:
2 g of +75-106µm size fraction for each mineral sample was chosen and sonicated for 30 seconds in 50 ml deionised water, after which the ultrafines were decanted with the supernatant liquid.
Reagent conditioning was in the 100ml beaker with electrolyte solution and pH adjusted accordingly.

For the activation experiments copper sulphate was added and conditioned for 5 minutes followed by the addition of SIBX and conditioned for 2 minutes. Where specified, depressant was added and conditioned for 2 minutes. An overhead stirrer was used for conditioning since magnetic bars will tend to grind the particles to a finer size. The pulp was transferred to the microflotation cell and the cell filled. Air was introduced into the cell as the flotation gas via a syringe needle. Air flowrate was adjusted with the needle valve and was measured with the bubble flowmeter. Air pressure was measured with a water manometer. The gas bubbles rose through the cell, passing through the pulp where collision between bubbles and mineral particles occurred. The cone into the launder area deflected the rising bubbles, where they burst and any attached mineral was collected. After a set time the needle was removed and the particles in the launder were recovered as the flotation product. The concentrate was collected, filtered, dried and weighed. The operating conditions were set an air flowrate of 10 cm^3/min and the peristaltic pump at 100 rpm.
Concentrates were collected at time intervals of 1.5, 5 and 10 minutes in the concentrate launder, after which they were dried and weighed.

3.5.2. Experimental programme

Table 3.5 shows the experimental programme conducted to investigate the effect of collector (SIBX), activator ($CuSO_4$), calcium ions, ionic strength and two different depressant dosages.

Table 3-5: Microflotation experimental programme

Minerals	$CuSO_4$ moles/l	SIBX moles/l	Depressant Type	Depressant Dosage (ppm)
Pyroxene	-	-	-	-
	$1*10^{-4}$	$1*10^{-4}$	-	
	$1*10^{-4}$	$1*10^{-4}$	APX4M	50,100
	$1*10^{-4}$	$1*10^{-4}$	FF30	50,100
Feldspar	-	-	-	-
	$1*10^{-4}$	$1*10^{-4}$	-	-
	$1*10^{-4}$	$1*10^{-4}$	APX4M	50,100
	$1*10^{-4}$	$1*10^{-4}$	FF30	50,100
Quartz	-	-	-	-
	$1*10^{-4}$	$1*10^{-4}$	-	-
	$1*10^{-4}$	$1*10^{-4}$	APX4M	50,100
	$1*10^{-4}$	$1*10^{-4}$	FF30	50,100
Chromite	-	-	-	-
	$1*10^{-4}$	$1*10^{-4}$	-	-
	$1*10^{-4}$	$1*10^{-4}$	APX4M	50,100
	$1*10^{-4}$	$1*10^{-4}$	FF30	50,100
Talc	-	-	-	-
	-	-	APX4M	50,100
	-	-	FF30	50,100
	$1*10^{-4}$	$1*10^{-4}$	-	-
	$1*10^{-4}$	$1*10^{-4}$	APX4M	50,100
	$1*10^{-4}$	$1*10^{-4}$	FF30	50,100

All experiments were performed in electrolyte $Ca(NO_3)_2$ at 10^{-2} ionic strength and the first test was a blank test without any reagent addition.

4. RESULTS OF ZETA POTENTIAL DETERMINATIONS

Zeta potential determinations were used to investigate the possible effect of copper and calcium ions on the selected gangue minerals and to specifically evaluate whether the adsorption was mineral or pH specific.

KNO_3 was selected as the indifferent electrolyte in solution for the zeta potential determinations.

4.1. REPRODUCIBILITY

In order to establish the reliability of the zeta potential determination procedure, determinations were carried out on a sample of quartz without any reagent addition in five repeats. The zeta potential determinations and standard deviations for each pH are show in Table 4.1.

Table 4-1 : Zeta potential determinations and standard deviations for quartz from pH 3 - 10

pH	Zeta potential determinations [mV]					Std Dev	Std Error
	Test 1	Test 2	Test 3	Test 4	Test 5		
3	-21.5	-22.2	-22.0	-21.8	-21.8	0.5	0.223
4	-36.2	-33.7	-33.4	-33.5	-33.1	0.9	0.402
5	-37.1	-39.8	-35.7	-38.7	-39.7	1.2	0.536
6	-44.4	-41.3	-41.0	-40.4	-42.1	1.1	0.492
7	-47.2	-44.7	-48.0	-47.9	-46.6	1.0	0.447
8	-46.1	-46.4	-48.2	-46.1	-46.8	0.8	0.357
9	-48.4	-47.8	-48.2	-44.1	-45.8	1.2	0.536
10	-47.9	-43.5	-45.1	-43.3	-42.4	1.3	0.581

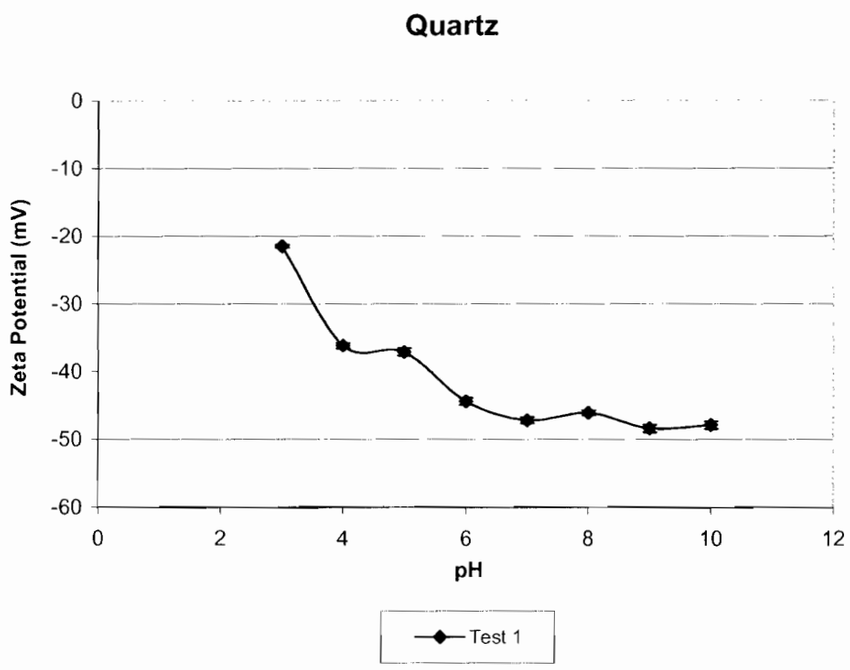

Figure 4-1: Zeta potential determination reproducibility of quartz in 10^{-3} M KNO_3

Figure 4.1 shows the zeta potential-pH curve of quartz and the low standard deviation obtained for each pH measured, shows that the technique and the procedure used gave reproducible results. The results and details of all experiments can be found in Appendix 2.

4.2. EFFECT OF IONS ON THE SURFACE PROPERTIES OF GANGUE MINERALS

Firstly the zeta potential of the selected minerals was determined in 10^{-3} M KNO_3 as the electrolyte without any reagent addition and thereafter in the additional presence of 1x 10^{-4} mol/l copper sulphate.

4.3. THE EFFECT OF COPPER IONS AND pH

The results obtained for pyroxene, feldspar, talc, chromite and quartz are presented in the following Figures 4.2 - 4.6:

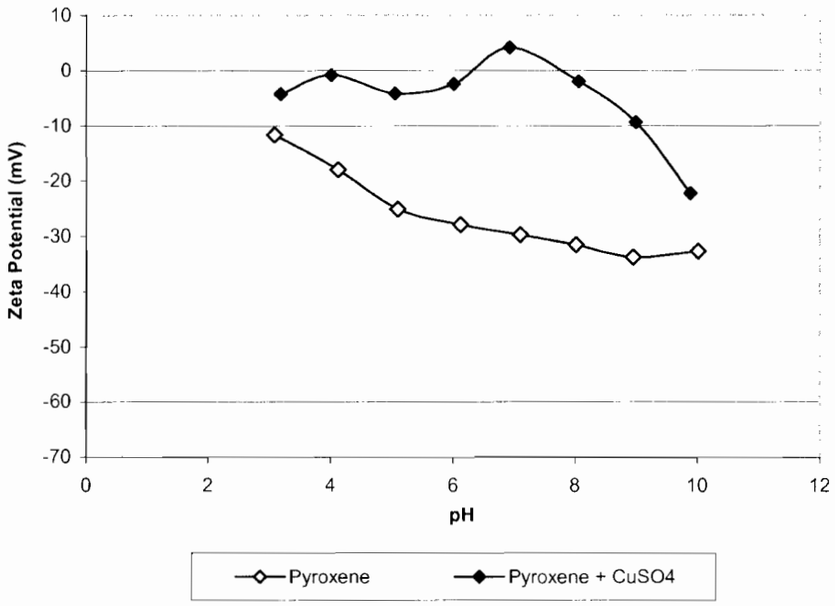

Figure 4-2: The effect of 10^{-4} M $CuSO_4$ addition on the zeta potential values of pyroxene with 10^{-3} M KNO_3 as the electrolyte from pH 3 to 10

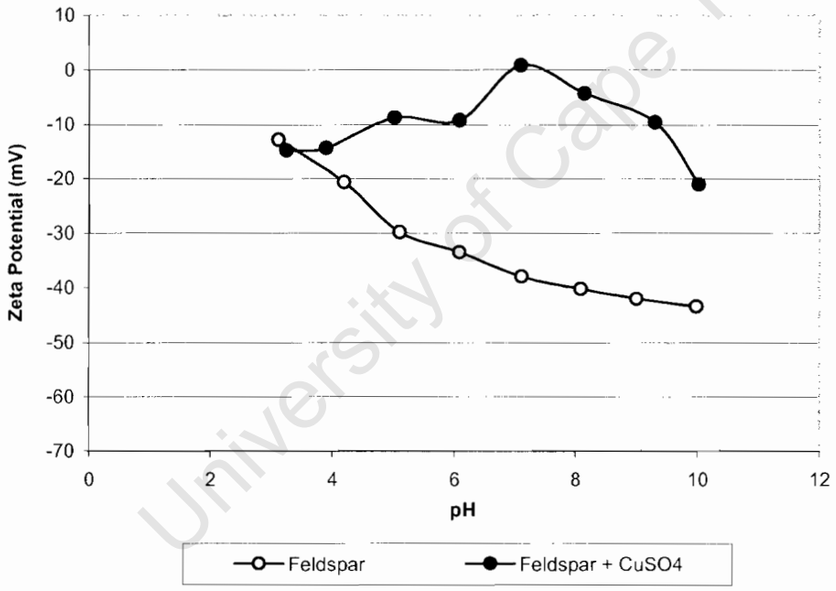

Figure 4-3: The effect of 10^{-4} M $CuSO_4$ addition on the zeta potential values of feldspar with 10^{-3} M KNO_3 as the electrolyte from pH 3 to 10

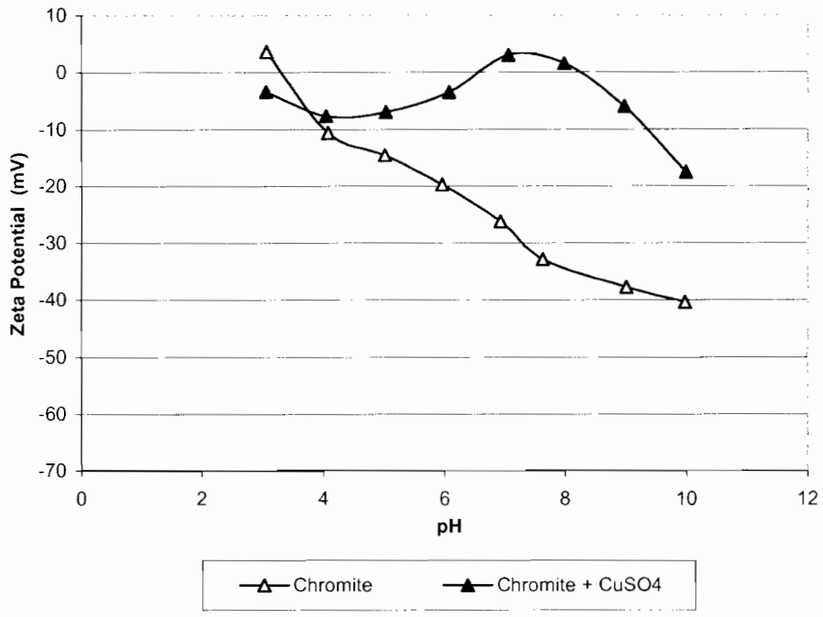

Figure 4-4: The effect of 10^{-4} M $CuSO_4$ addition on the zeta potential values of chromite with 10^{-3} M KNO_3 as the electrolyte from pH 3 to 10

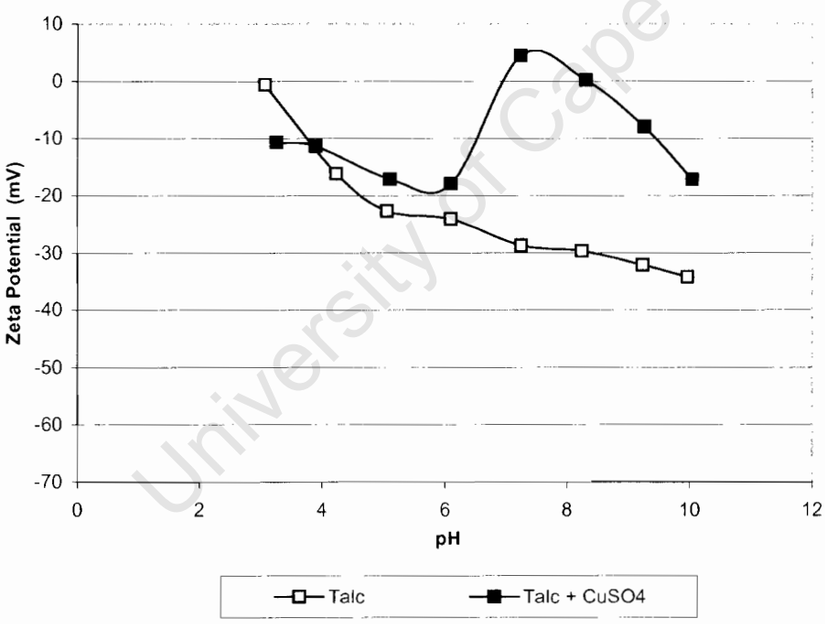

Figure 4-5: The effect of 10^{-4} M $CuSO_4$ addition on the zeta potential values of talc with 10^{-3} M KNO_3 as the electrolyte from pH 3 to 10

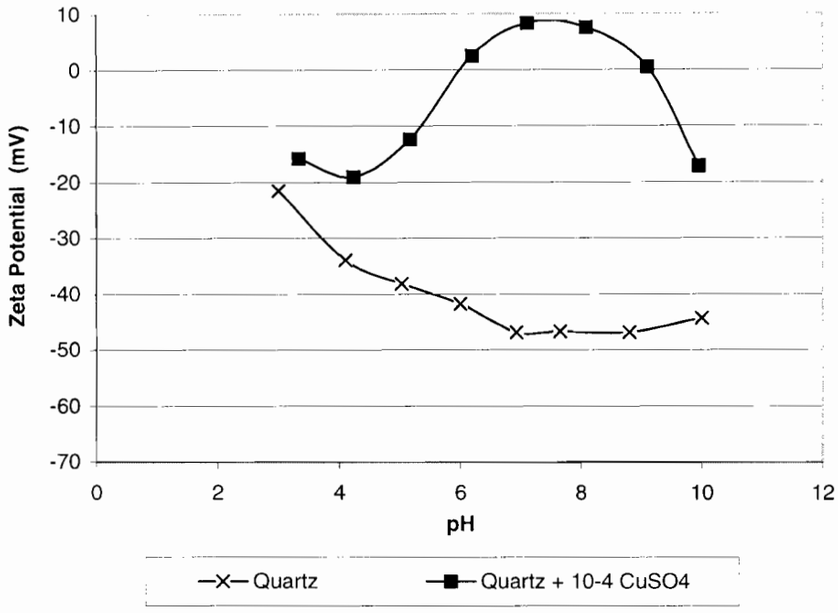

Figure 4-6: The effect of 10^{-4} M $CuSO_4$ addition on the zeta potential values of quartz with 10^{-3} M KNO_3 as the electrolyte from pH 3 to 10

Figure 4.2 shows the zeta potential for pyroxene at various pH values. The estimated IEP would be less than two which is consistent with the value of pH 3.8 reported by (Fuerstenau and Fuerstenau, 1982).

In the presence of Cu (II) ions, the zeta potential values were significantly changed, shifting to more positive values compared to those obtained without Cu (II) ions indicating that positively charged copper species adsorb onto the surface of pyroxene. The interactions between copper species and the mineral surface will be discussed more in Chapter 7.

Figure 4.3 show the zeta potential for feldspar at various pH values and that the estimated IEP would be less than two. This is not consistent with the values (between pH 2 and pH 3.6) reported in the literature (Fuerstenau and Fuerstenau, 1982). Malysiak, (2003), reported the IEP at pH 4 for feldspar and the differences can be attributed to the presence of ions originating from the mineral itself.

In the presence of Cu (II) ions, the zeta potential values show a similar trend, to that observed with pyroxene. This indicates that the adsorption of copper (II) ions is not selective, which is also observed by Malysiak and Shackleton, (2003).

Figure 4.4 shows the zeta potential for chromite at various pH values and indicates that chromite has a IEP of about pH 3.8, which corresponds to that reported by Wesseldijk, (1998) and which is expected as the chromite was from the same source as was used for this investigation.

Figure 4.5 shows the zeta potential for talc at various pH values, indicating that talc has IEP at about pH 3.0. This is consistent with the IEP reported by Fuerstenau and Fuerstenau, (1982) as well as for previous minerals. For all minerals investigated a similar trend was found with addition of $CuSO_4$, indicating non-selectivity of copper (II) ions adsorption and subsequent activation of the mineral.

Figure 4.6 shows the zeta potential for quartz at various pH values and indicates that quartz has a IEP at about pH 2.2 which corresponds to that reported in the literature (Fuerstenau and Fuerstenau, 1982). A similar trend was found for quartz as for all other minerals indicating non-selectivity of the adsorption of positively charged copper species. Figure 4.6: shows that the extent of Cu (II) activation onto the quartz surface was higher than that obtained with the other minerals and the surface became more positively charged between the pH ranges of 6-9 when charge reversal was observed. Figure 4.6 shows that quartz was strongly negatively charged (about –50mV) which would have resulted in greater adsorption of positively charged copper species onto the quartz surface.

It can be seen from the results that the addition of copper ions can activate all minerals and that the charge reversal and maximum positive zeta potential occurs between pH 7-9. At these values the gangue mineral surface becomes hydrated with OH^- ions and then interacts with metal ions, which would react with collector and resulting in the formation of surface active copper hydroxyl

species (James and Healy, 1972). The relationship is similar to that obtained by previous researchers in terms of activation by metal ions. Copper activation is shown to be unselective because copper hydroxyl complexes adsorbed on all minerals evaluated.

4.4. THE EFFECT OF POTASSIUM AND CALCIUM IONS AND IONIC STRENGTH

The effect of ionic strength and type of electrolyte on selected minerals was evaluated. Experiments were performed with KNO_3 and $Ca(NO_3)_2$ at an ionic strength of 10^{-3} and 10^{-2}.

Figures 4.7- 5.1: show the effect of ionic strength of KNO_3 and $Ca(NO_3)_2$ on the selected gangue minerals.

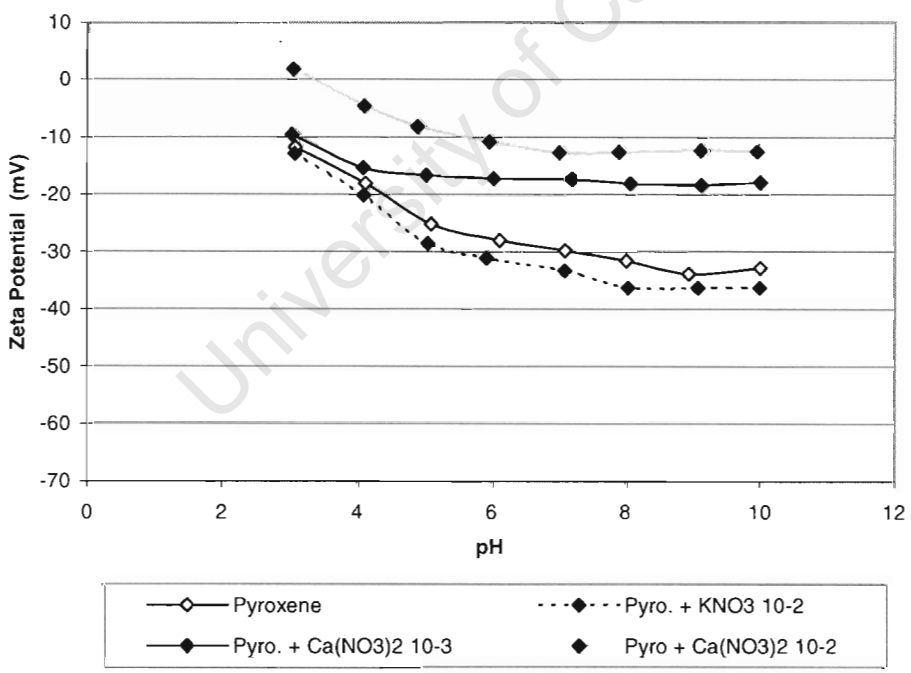

Figure 4-7: The effect of pH and potassium and calcium ions at different ionic strength on the zeta potential values of pyroxene (std.10^{-3} KNO_3)

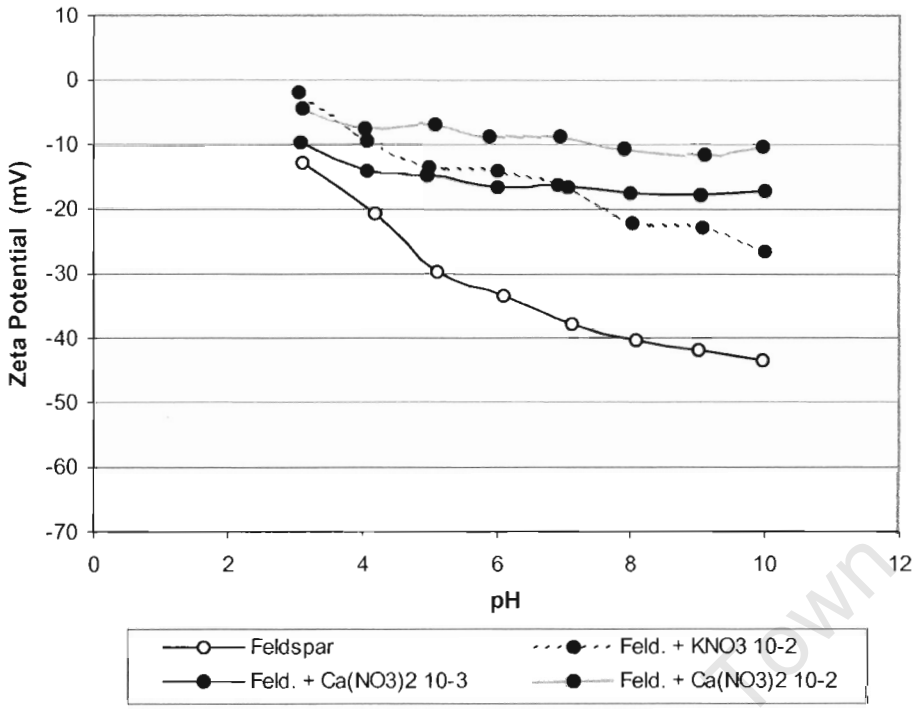

Figure 4-8: The effect of potassium and calcium ions at different ionic strength on the zeta potential values of feldspar (std.10^{-3} KNO_3)

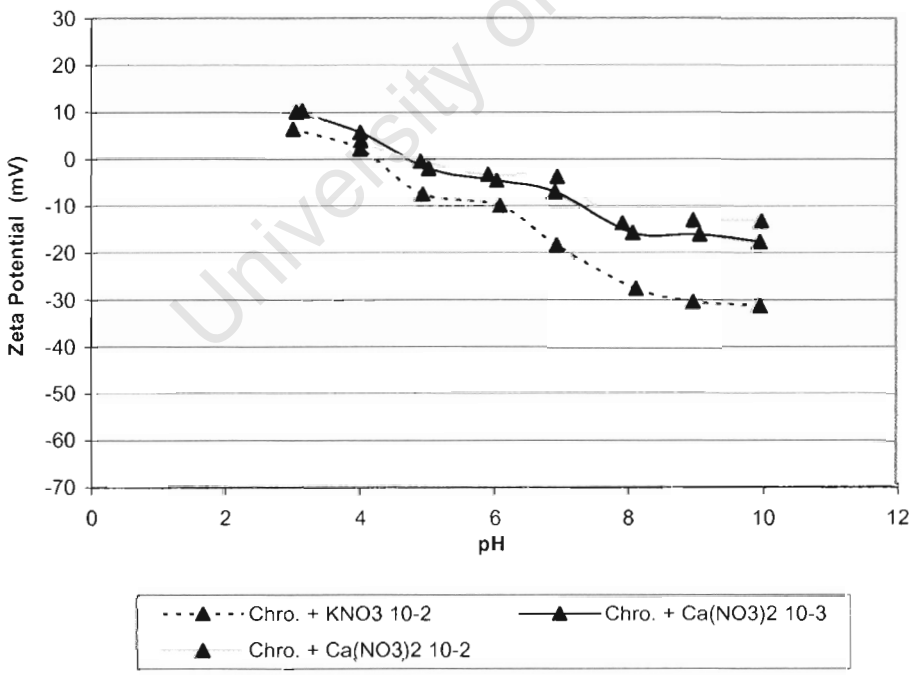

Figure 4-9: The effect of potassium and calcium ions at different ionic strength on the zeta potential values of chromite (std.10^{-3} KNO_3)

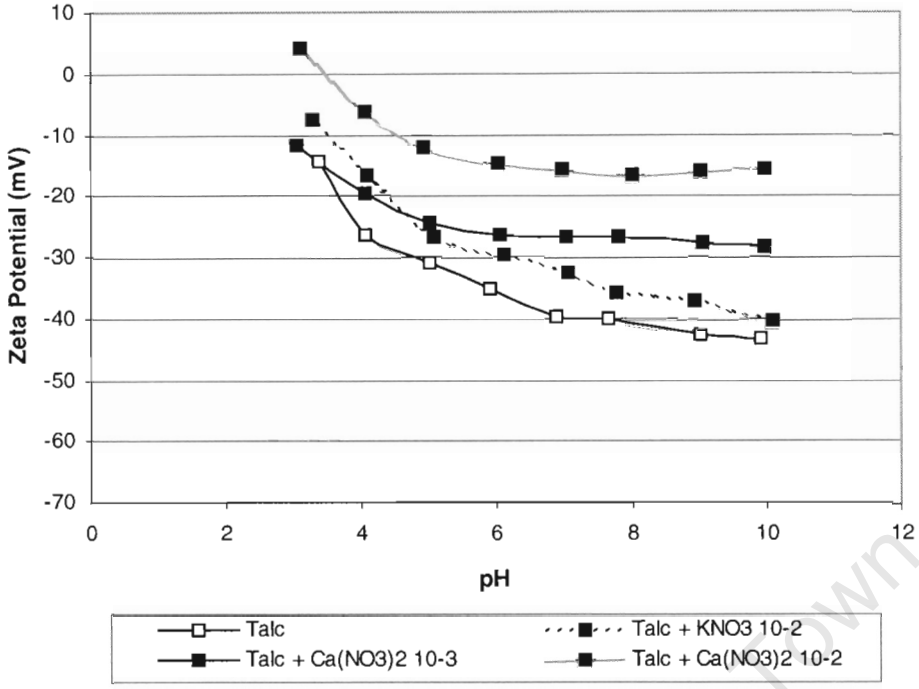

Figure 4-10: The effect of pH and potassium and calcium ions at different ionic strength on the zeta potential values of talc (std.10^{-3} KNO_3)

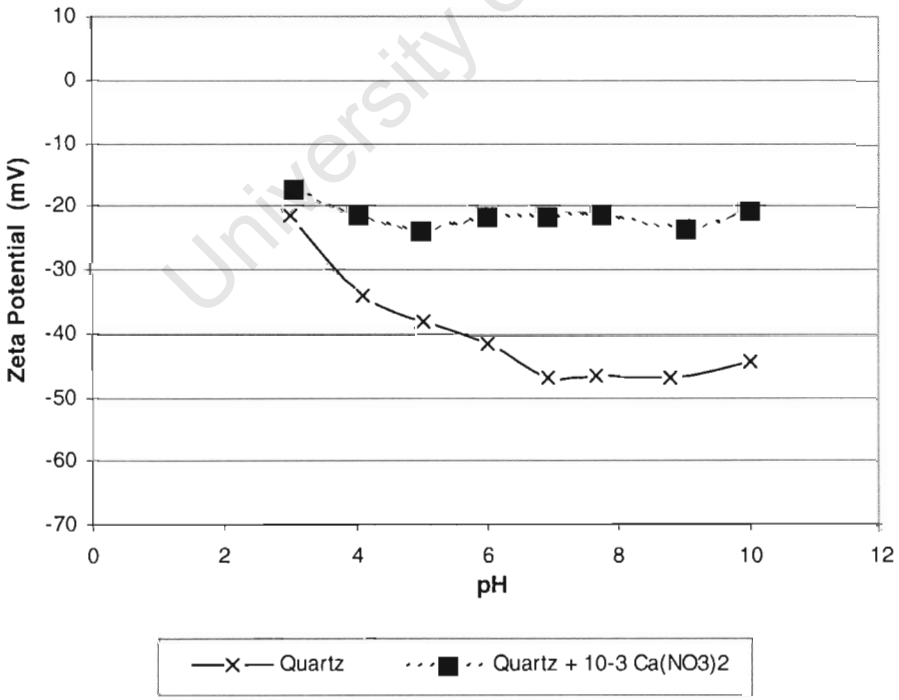

Figure 4-11: The effect of pH and potassium and calcium ions at different ionic strength on the zeta potential values of quartz (std.10^{-3} KNO_3)

KNO_3 was selected as an indifferent electrolyte and was not expected to affect the PZC. The results show that increasing the ionic strength of KNO_3 from 10^{-3} to 10^{-2} had no significant effect on the PZC for all minerals except feldspar. Increasing the ionic strength compressed the thickness of the double layer, which was caused by a decrease in negativity of zeta potential values. A decrease in negativity can be caused by the shifting of the plane of shear away from mineral surface or by the influence of the adsorption characteristics of the presence ions. This new distance from the surface is actually the thickness of the double layer. In the presence of calcium ions increasing the ionic strength from 10^{-3} to 10^{-2}, caused a significant move of the point of zero charge, compressing the double layer and shifting the curve positively over the whole pH range.

It can be seen clearly from the comparison of $Ca(NO_3)_2$ as the electrolyte to the KNO_3 as the indifferent electrolyte for all selected minerals, except for feldspar that the calcium ions increased the IEP indicating strong adsorption on all gangue minerals, particularly at alkaline pH values. Malysiak and Shackelton, (2003) in an investigation of the effect of water quality on floatability with an emphasis on the Ca^{2+} ions also used zeta potential determinations to show that the calcium ions adsorbed onto the pyroxene surface and the zeta potential increased with alkalinity of the synthetic water.

4.5. THE EFFECT OF POLYMERIC DEPRESSANTS

The effect of CMC, a charged depressant and guar, an uncharged depressant were evaluated. Figure 4.12 shows the effect of two polymeric depressants, guar gum (APX4M) and carboxymethyl cellulose (FF30) at a concentration of 100 mg/l on pyroxene, feldspar, chromite, talc and quartz.

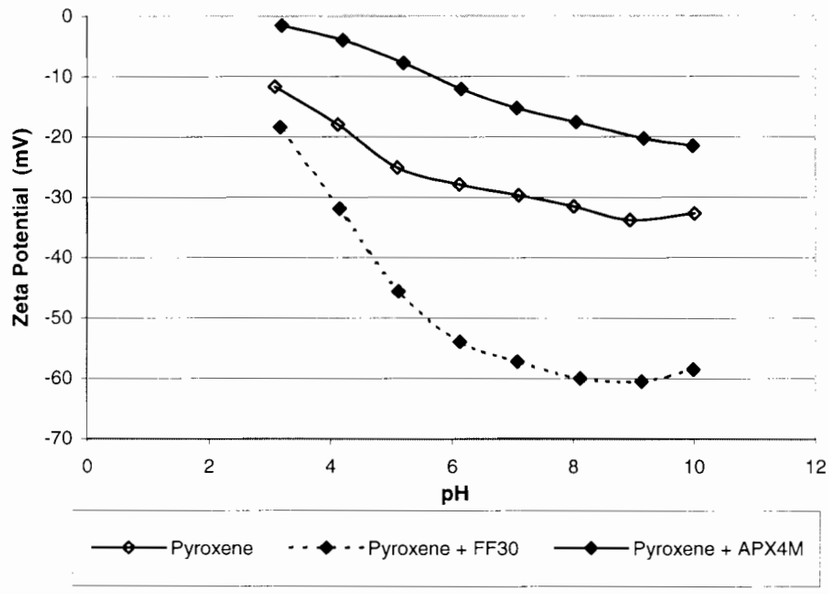

Figure 4-12: The effect of pH and polymeric depressants on the zeta potential values for pyroxene with 10^{-3} KNO_3 as the indifferent electrolyte

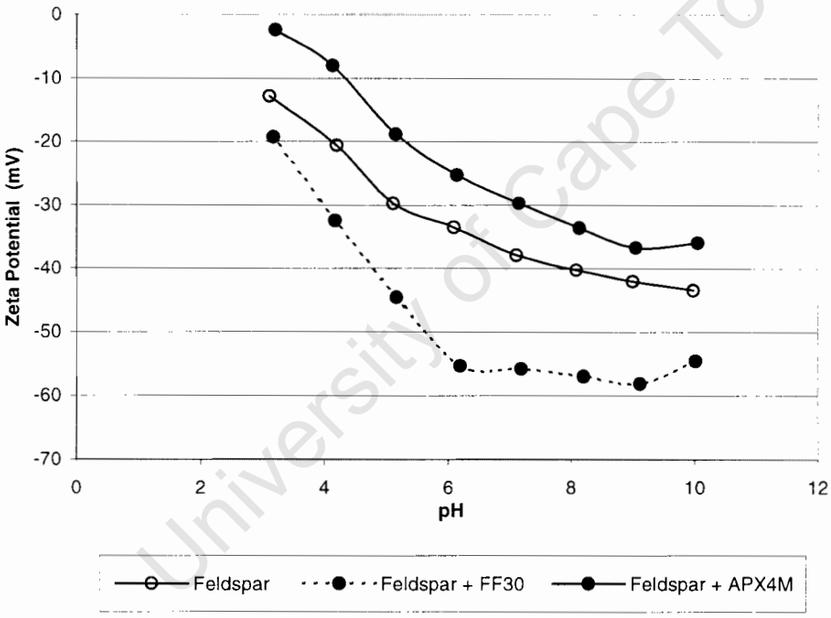

Figure 4-13: The effect of polymeric depressants on the zeta potential values for feldspar with 10^{-3} KNO_3 as the indifferent electrolyte

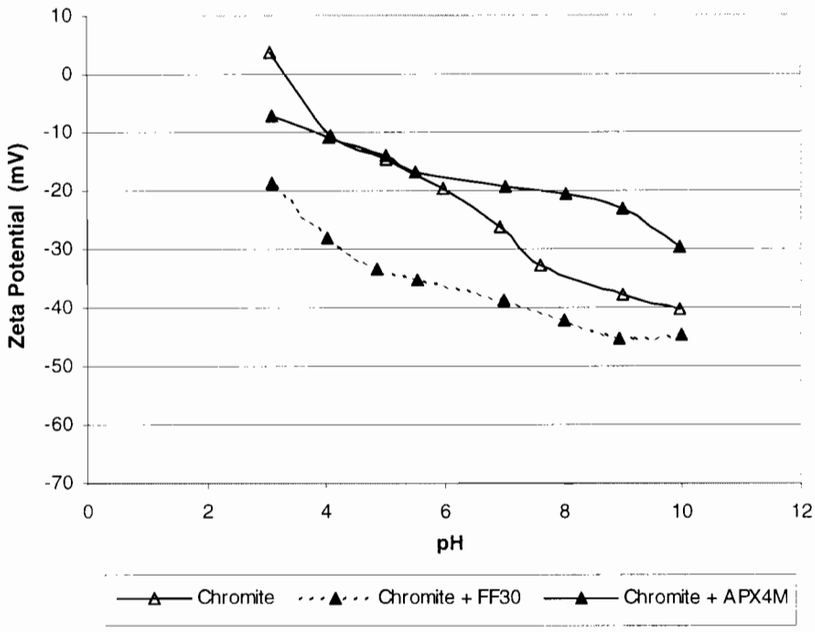

Figure 4-14: The effect of pH and polymeric depressants on the zeta potential values for chromite with 10^{-3} KNO_3 as the indifferent electrolyte

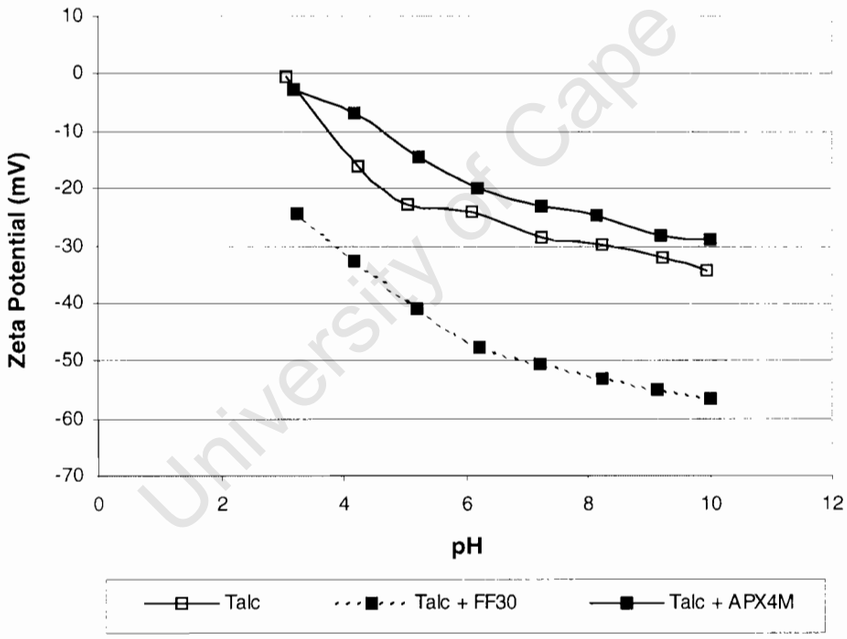

Figure 4-15: The effect of pH and polymeric depressants on the zeta potential values for talc with 10^{-3} KNO_3 as the indifferent electrolyte

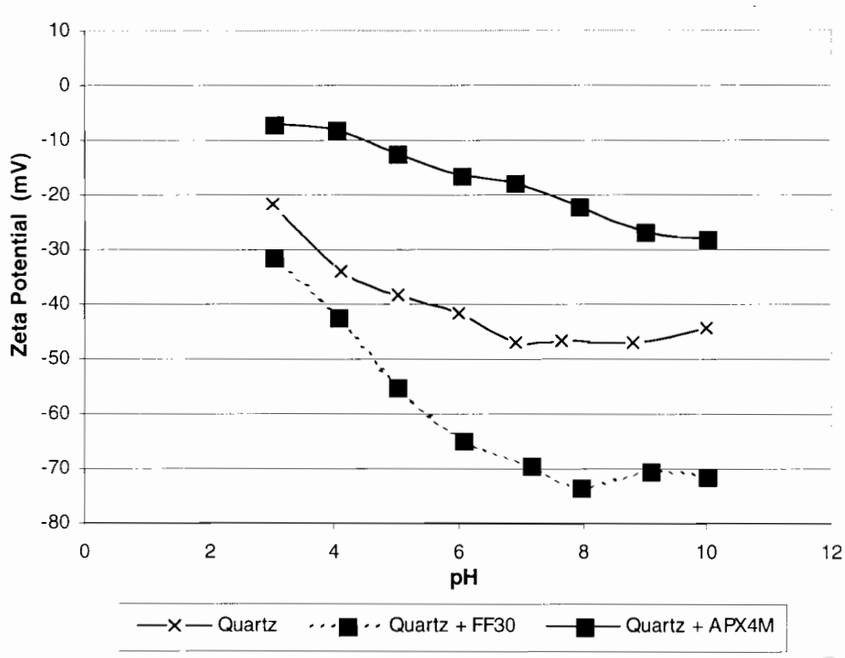

Figure 4-16: The effect of pH and polymeric depressants on the zeta potential values for quartz with 10^{-3} KNO_3 as the indifferent electrolyte

The zeta potential results show that both depressants adsorbed on all gangue minerals increasing the negativity with CMC and decreasing the negativity with guar gum. The greatest negativity was observed for quartz and high negative zeta potentials in the region of -70 mV in the presence of FF30 were obtained indicating strongly negative surface charge. This was expected as guar gum is an uncharged polymer and is expected to cause decreasing negativity while CMC is a strongly negatively charged polymer and is expected to increase the negative zeta potential.

Steenberg and Harris, (1984) found the same in an investigation of talc and observed that these big molecules expanded double layer. The presence of substituent groups for CMC influences the conformation of the polymer rather than the bonding to the surface. Zeta potential determinations do not measure the extent of adsorption but indicate that adsorption has occurred. The results

also indicate that depressants adsorb unselectively because of their similar behaviour on all selected minerals.

4.6. KEY FINDINGS

- The copper ions adsorbed onto all selected gangue minerals and charge reversal of positively charged copper species occurred between pH 7-9, indicating that copper adsorbed unselectively.

- The extent of Cu (II) adsorption onto the quartz surface was greater than that obtained with other minerals as shown by the increased positive charge in the range of charge reversal pH 6-9.

- Calcium ions adsorbed strongly on pyroxene, chromite, talc and quartz compared to the potassium ions causing a change in the zeta potential, particularly at alkaline values.

- Indications were that both depressants adsorbed on all selected gangue minerals with increased negativity of zeta potential values obtained with CMC and decreased negativity obtained with guar gum.

- Although zeta potential determinations do not give the extent of adsorption, for both depressants the changes in zeta potential indicated that some adsorption had taken place.

5. RESULTS OF ADSORPTION STUDIES

5.1. ADSORPTION ISOTHERMS: INFLUENCE OF pH, IONIC STRENGTH AND POLYMER DEPRESSANTS

The effect of pH and ionic strength in the presence of calcium ions on the adsorption of carboxymethyl cellulose and guar gum on talc, pyroxene, feldspar, quartz and chromite has been investigated. Adsorption isotherms at room temperature were compiled by measurement of the difference in the polymer concentration in solution before and after contacting with the mineral, by measuring the total organic carbon.

Adsorption studies were conducted on FF30 and APX4M in an ionic strength of 10^{-2} $Ca(NO_3)_2$ at pH 9. Those values were chosen to simulate water conditions of a typical concentrator in a plant. Malysiak and Shackleton, (2003) also noted the importance of carrying out tests in water of a similar composition to that existing on typical concentrator.

It was established that the ion type and ionic strength are predominant factors affecting adsorption density. In the recent work performed on New York talc with different CMCs by Parolis et al, 2003, results indicated that higher adsorption densities were obtained as the degree of substitution of the polymers was decreased although the difference was not as significant with Ca^{2+} compared to Mg^{2+} and K^{+} ions. The polymers showed the same behaviour with respect to the type of ions present but higher adsorption densities were obtained with Ca^{2+} ions than with Mg^{2+} ions followed by K^{+} ions.

The adsorption isotherms generated in the presence of Ca^{2+} ions and CMC and guar gum on the pyroxene, feldspar, talc, chromite and quartz are shown in the Figure 5.1.

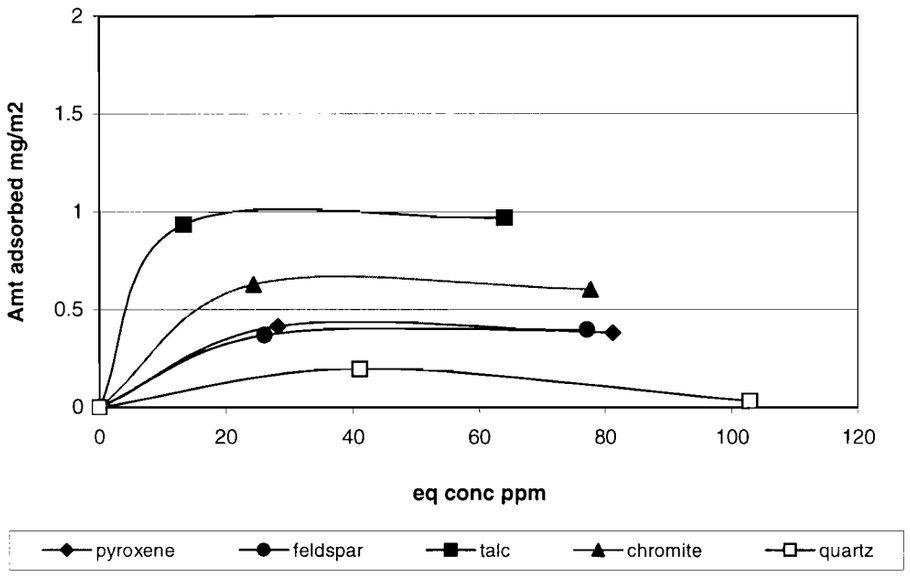

Figure 5-1: The adsorption density of FF30 on talc, pyroxene, feldspar, quartz and chromite at 10^{-2} $Ca(NO_3)_2$ ionic strength

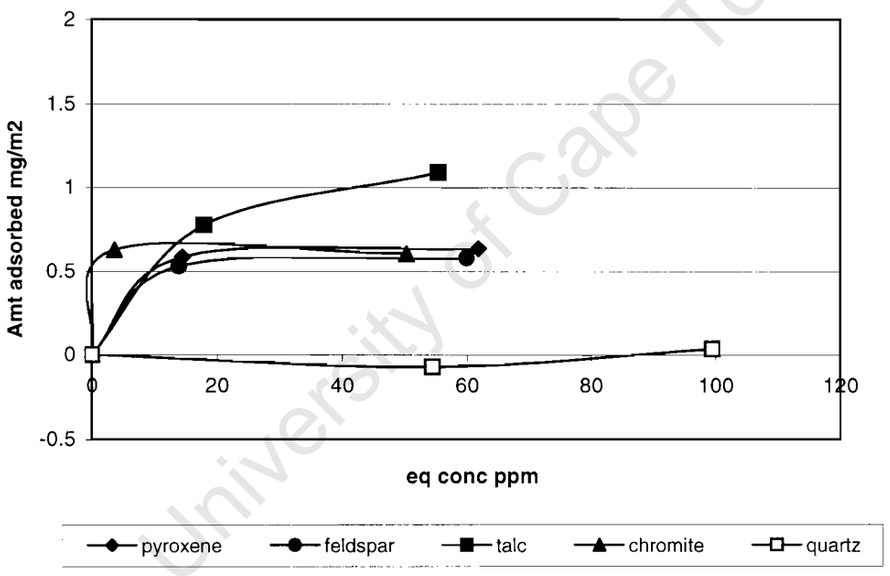

Figure 5-2: The adsorption density of APX4M on talc, pyroxene, feldspar, quartz and chromite at 10^{-2} $Ca(NO_3)_2$ ionic strength

In the presence of CMC (Figure 5.1) adsorption isotherms indicate that a higher adsorption density was obtained with talc, than with chromite, followed by pyroxene and feldspar and the lowest (close zero) with quartz. The low adsorption density for quartz indicated that adsorption was not observed contrary to indications from results obtained for zeta potential determinations. The high negative zeta potential of quartz, coupled with the negative charge of the CMC, was expected to prevent adsorption from taking place (Steenberg and Harris, 1984).

The results obtained with guar gum showed that higher adsorption densities were obtained for all minerals compared to those obtained with CMC and that little adsorption was obtained for quartz. Talc had the highest adsorption density while pyroxene, feldspar and chromite almost the same followed by approximately zero with quartz. This can be related to the different charge of polymers, as well as to differences in the crystal structure of minerals. In the case of quartz the Si-O bond is covalent and that is related to its high stability compared to the other minerals (see figure 2.11) and this also contributed to low adsorption. The CMC (FF30) is a highly charged polymer with DS of (0,76) while guar gum is non-ionic.

The results obtained with talc by Steenberg and Harris, (1984) established that, for all polymers, adsorption occurs first on the basal plane and then on the talc edge. The area occupied per molecule of the polymer can be calculated if the relative areas of basal plane and edges are taken into account. In the case of hydrophilic minerals such as pyroxene, feldspar, quartz and chromite, adsorption of the polymers can be compared to that on the hydrophilic talc edge.

5.2. KEY FINDINGS

- The adsorption study indicated that both depressants (APX4M and FF30) adsorbed onto all selected minerals except on the quartz.

- In comparison to the extent of adsorption obtained with CMC, higher adsorption densities were obtained with guar.

- Despite zeta potential determinations indicating that there was adsorption of polymers onto quartz – none was measured in the adsorption tests.

6. RESULTS OF MICROFLOTATION TESTS

The effect of xanthate ions on copper activated mineral surfaces and the possibility of depressant to counteract activation was investigated in terms of flotation response. Microflotation tests were performed at pH 9 for all minerals.

6.1. REPRODUCIBILITY

The aim of the reproducibility tests was to establish the reliability of the microflotation apparatus and the flotation procedure. For all tests, xanthate was added at a concentration of $1*10^{-4}$ M. Concentrates were collected at time interval 1.5, 5 and 10 minutes. The talc recovery-time curves obtained in triplicate are plotted in Figure 6.1. The recoveries and standard deviation for the total concentrate collected over period of 10 minutes are given in Table 6-1.

Table 6-1 : Talc recovery and standard deviation

Run	Ionic Strength	pH	Total mass (g)	Time (min)	Recovery (%)	Mean recovery (%)	Std Dev
1	10^{-2} $Ca(NO_3)_2$	9	2.15	1.5	18.60		
				5	41.86		
				10	63.25	20.44	2.13
2	10^{-2} $Ca(NO_3)_2$	9	2.17	1.5	21.66	38.50	3.87
				5	37.33	59.57	4.24
				10	58.52		
3	10^{-2} $Ca(NO_3)_2$	9	2.2	1.5	21.07		
				5	36.32		
				10	56.95		

The examples of reproducible results and details of all experiments can be found in Appendix 4.

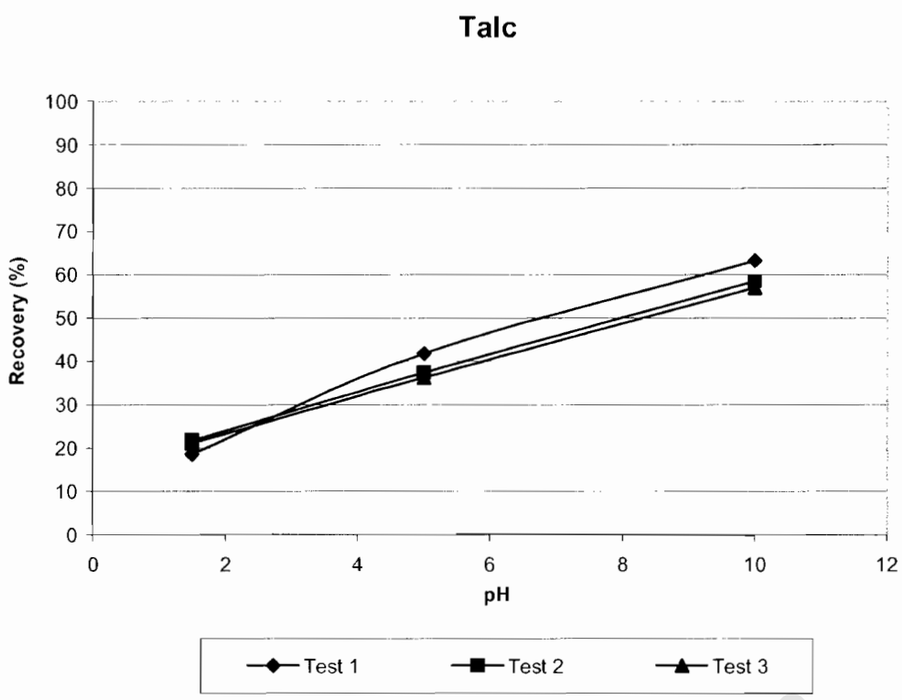

Figure 6-1: Microflotation reproducibility for talc in $Ca(NO_3)_2$ at 10^{-2} ionic strength

The talc recovery-time curves and the low standard deviation confirmed that reproducible results could be obtained using the microflotation apparatus and the flotation procedure.

6.2. NATURAL FLOATABILITY OF GANGUE MINERALS

Figure 6.2 shows the results of the microflotation of gangue minerals at 10^{-2} $Ca(NO_3)_2$ ionic strength to evaluate the natural floatability of these minerals. No other reagents were added.

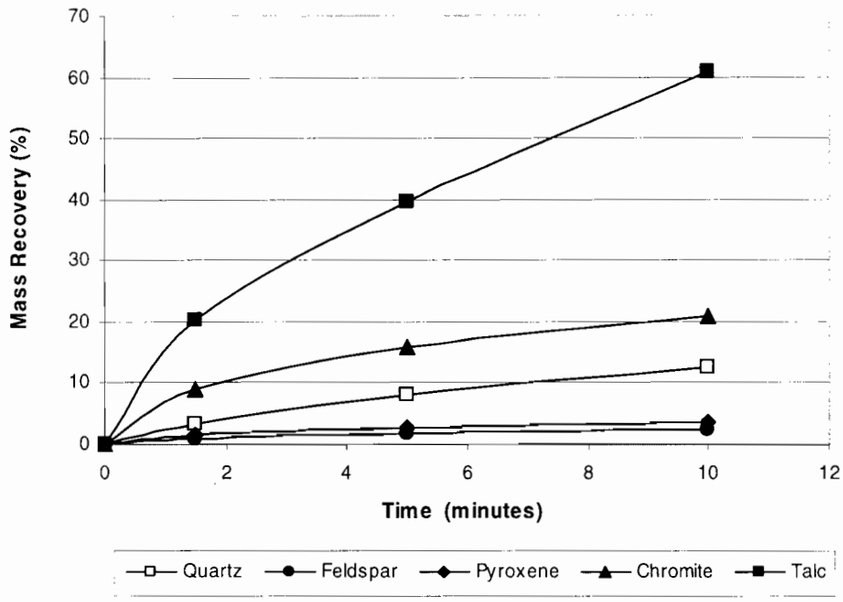

Figure 6-2: Natural floatability of gangue minerals under 10^{-2} $Ca(NO_3)_2$ ionic strength

It can be seen that only talc is naturally floatable with a mass recovery of about 60%, while chromite, quartz, pyroxene, and feldspar are not naturally floatable with mass recoveries less than 20% obtained after 10 minutes. The slight natural floatability of the chromite (about 20%) was unexpected but it was insufficient to interfere with the copper activation studies.

6.3. EFFECT OF REAGENT ADDITION ON THE GANGUE MINERALS

In order to observe the effect of depressants on the recovery of all gangue minerals 10^{-4} M $CuSO_4$ and SIBX (sodium iso-butyl xanthate), and depressants guar gum (APX4M) or CMC (FF30), at dosages of 50 or 100 mg/l were added in the presence of 10^{-2} ionic strength $Ca(NO_3)_2$. Previous studies showed that the extent of activation was strongly dependent on the amount of copper present and for this investigation the copper concentration was specified to be greater than the concentration of SIBX so that an excess of copper ions (50%) was available in solution. In all experiments, copper

sulphate was added before the SIBX. Figure 6-4 shows the results of these experiments for each mineral compared to those obtained when no reagents were added.

6.4. EFFECT OF REAGENT ADDITION ON THE RECOVERY OF TALC

The effect of depressant type and concentration on the recovery of talc in the absence of activation was evaluated.

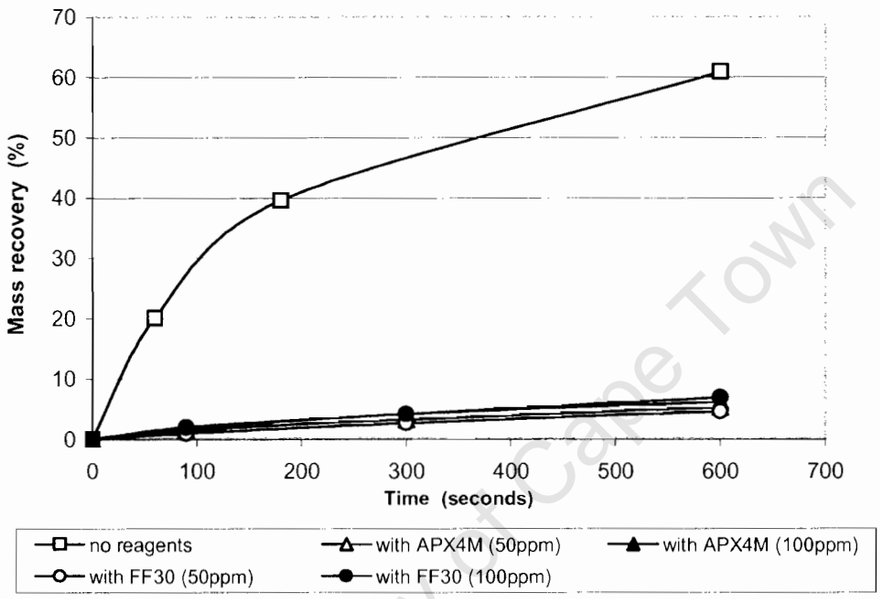

Figure 6-3: The effect of adding APX4M and FF30 on the flotation response of talc under 10^{-2} $Ca(NO_3)_2$ ionic strength

Figure 6-3 shows that addition of both APX4M and FF30 can reduce floatability of talc from 60 to less than 10%. The dosage of 50ppm is adequate for both polymers to reduce talc floatability and no further change was obtained with 100ppm.

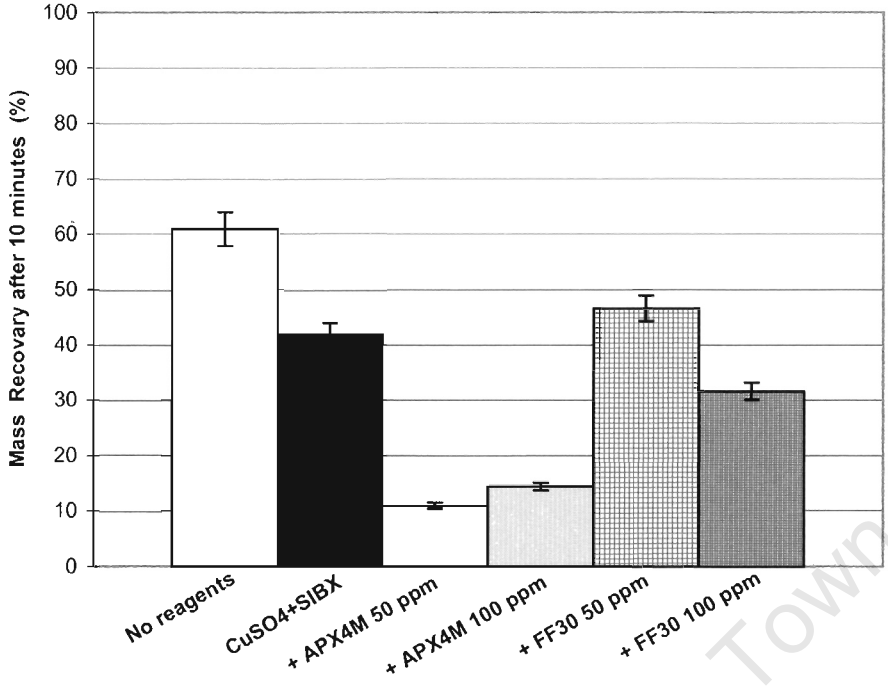

Figure 6-4: The effect of adding reagents on the floatability of talc under 10^{-2} $Ca(NO_3)_2$ ionic strength.

It can be seen that after adding $CuSO_4$ and SIBX the floatability of talc was reduced from 60 to 40% showing that activation was not occurring. It is possible that a copper xanthate complex was formed, which was not adsorbed on the hydrophobic plane of talc surface. The excess of $Cu(OH)_2$ was also expected to adsorb at the surface leading to lower floatability. After the addition of APX4M floatability was reduced from 60 to 10 % (50ppm) and slightly less from 60 to 15% (100ppm). FF30 also reduced the floatability of activated material but only with dosage of 100ppm while with the dosage of 50ppm showed a slight increase in floatability.

6.5. EFFECT OF REAGENT ADDITION ON THE RECOVERY OF PYROXENE

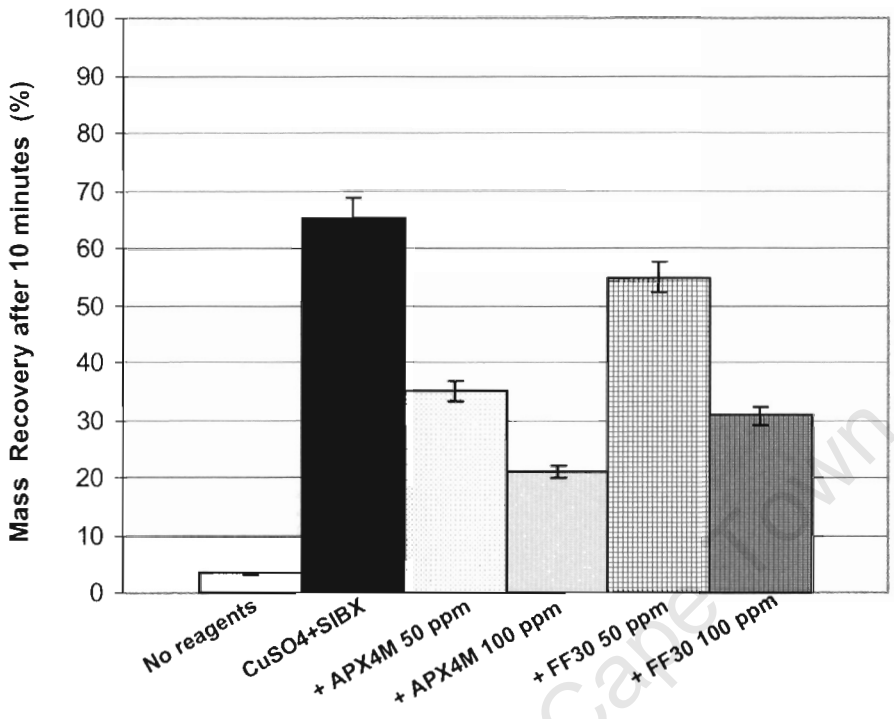

Figure 6-5: The effect of adding reagents on the floatability of pyroxene under 10^{-2} $Ca(NO_3)_2$ ionic strength.

The results showed that pyroxene was not naturally floatable however, after adding $CuSO_4$ and SIBX pyroxene could be activated and floatability was increased up to 65 %. After the addition of APX4M floatability was significantly reduced compared to that obtained with CMC and also showed that guar was much more effective depressant than CMC depressant.

6.6. EFFECT OF REAGENT ADDITION ON THE RECOVERY OF FELDSPAR

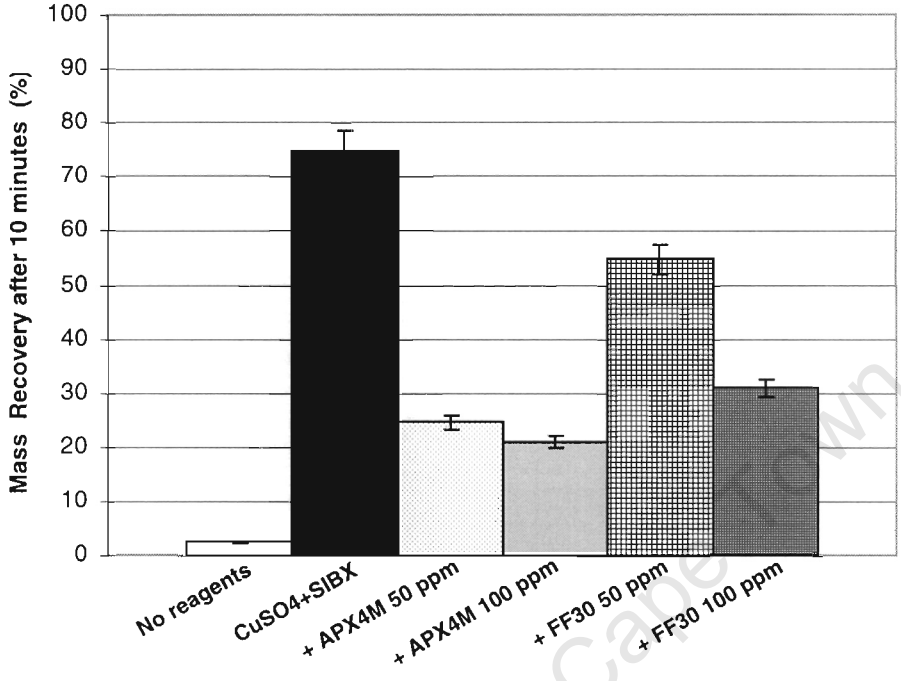

Figure 6-6: The effect of adding reagents on the floatability of feldspar at 10^{-2} $Ca(NO_3)_2$ ionic strength.

Figure 6.6 shows that a similar effect was observed with feldspar. It can be seen that feldspar was not naturally floatable but after the addition of $CuSO_4$ and SIBX it has activated and floatability increased up to 75%. The addition of APX4M reduced the floatability of activated material as did the addition of FF30 but to a much less extent than guar. Increasing the concentration from 50 to 100 ppm increased the degree of depression, however the difference between the two dosages was more marked with CMC than with guar.

6.7. EFFECT OF REAGENT ADDITION ON THE RECOVERY OF CHROMITE

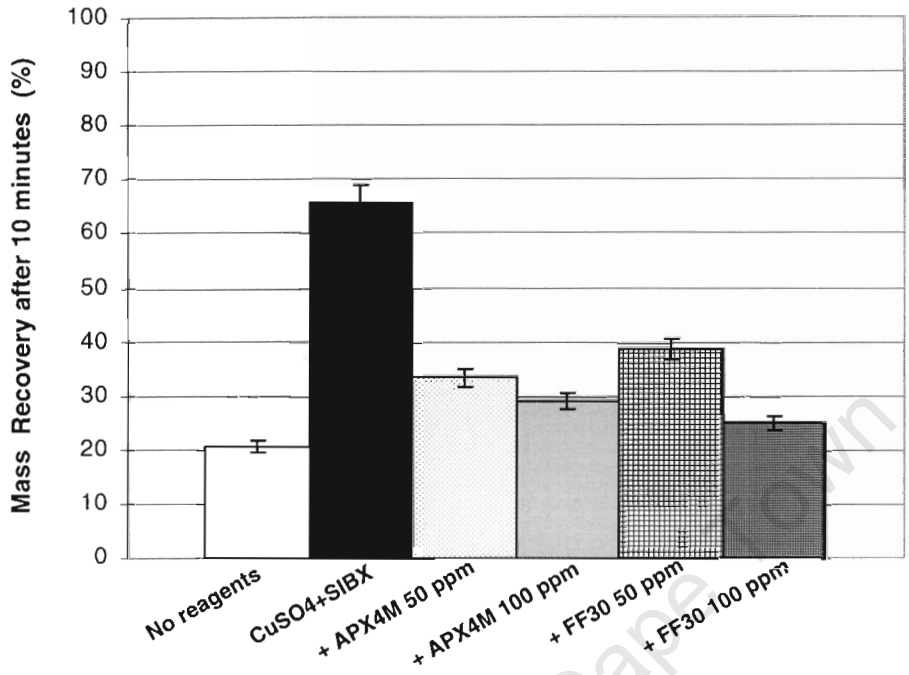

Figure 6-7: The effect of adding reagents on the floatability of chromite under 10^{-2} $Ca(NO_3)_2$ ionic strength.

Figure 6.7 shows that a similar effect was observed with chromite and that chromite is not naturally floatable. However, after addition of $CuSO_4$ and SIBX chromite was also activated and floatability increased up to 65%. Results obtained with chromite indicated that the effectiveness for both depressants to reduce floatability was very similar. Increasing the concentration from 50 to 100 ppm reduced the recoveries but not to any great extent.

6.8. EFFECT OF REAGENT ADDITION ON THE RECOVERY OF QUARTZ

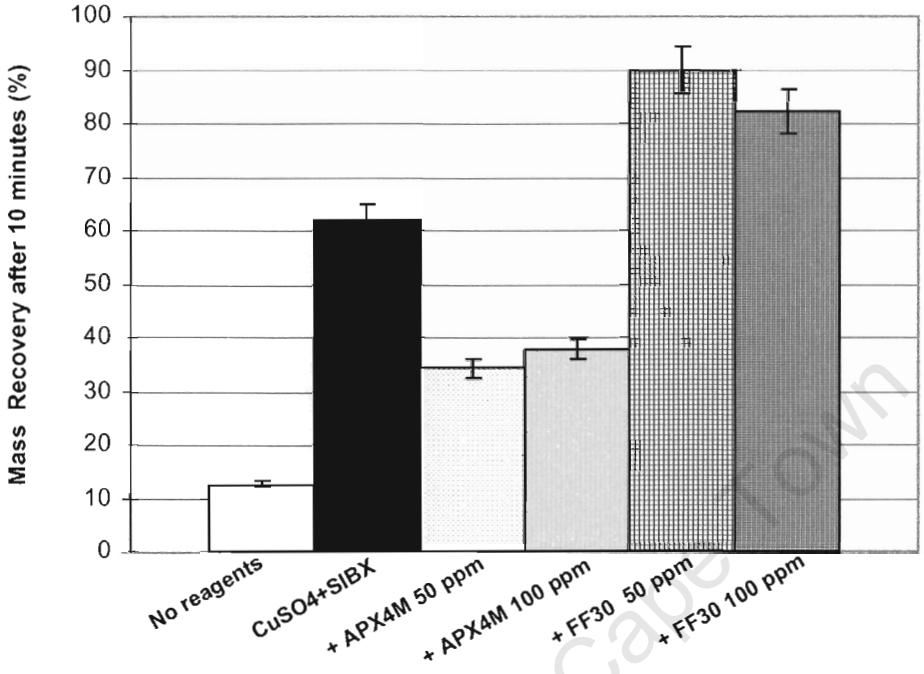

Figure 6-8: The effect of adding reagents on the floatability of quartz under 10^{-2} $Ca(NO_3)_2$ ionic strength

It can be seen that quartz was not naturally floatable however after addition of $CuSO_4$ and SIBX it was also activated and floatability increased up to 60%. The addition of APX4M resulted in a significant decrease in the floatability while with FF30 the opposite effect was observed and the floatability of activated material increased from 60 to 90% at a dosage of 50ppm and from 60 to 80% at a dosage of 100ppm.

Zeta potential results with copper addition showed very strong adsorption compared to other minerals however this is not reflected in the microflotation results. It could be expected to increase more than 60%. CMC forms a strong complex with copper and the precipitation of CMC by copper ions is used as quantitative method for the determination of degree of substitution. The enhanced floatability can be attributed to the dispersion of the $Cu(OH)_2$ leaving only the stable copper xanthate at the surface.

6.9. KEY FINDINGS

- Microflotation tests with all selected gangue minerals in the presence of $Ca(NO_3)_2$ at 10^{-2} ionic strength showed that only talc was naturally floatable.

- The addition of copper sulphate and subsequent collector addition activated all selected gangue minerals except talc, which was slightly depressed.

- The addition of both FF30 and APX4M reduced the natural floatability of talc at a dosage of 50ppm which was not improved by increasing the dosage.

- Microflotation tests showed that guar gum could reduce the floatability of all activated gangue minerals including talc, while CMC can reduce all except quartz. Guar was more effective than CMC in reducing floatability at lower dosage.

7. DISCUSSION

Zeta potential determinations obtained during the study of all five minerals over the pH range from 3 to 10, with the exception of chromite at pH 3, displayed a negative zeta potential with the zeta potential increasing negatively as the pH is raised. As expected the quartz sample displayed the highest negative zeta potential. The addition of copper sulphate (10^{-4} M) caused a significant change in the zeta potential of all minerals in the alkaline range indicating a strong interaction of the copper with all minerals.

In all cases at around pH 7 the zeta potential becomes positive. This charge reversal is indicative of a specific adsorption occurring at which the maximum concentration in solution of the hydrated copper species $CuOH^+$ occurs (Wesseldijk, 1999). The fact that all minerals behave the same shows that the copper adsorption was not specific for any of the minerals examined. It is of interest to note that the largest charge reversal occurred with quartz where the zeta potential stayed positive from pH 6 to pH 9 indicating strong adsorption on the mineral which also possessed the most negative natural zeta potential. At acidic pH values (pH 4) the copper would be expected to be present in the form of free Cu^{2+} ions and not to adsorb. At pH 7 the amount of $CuOH^+$ present becomes significant while at pH 9 the majority of the copper would be present as $Cu(OH)_2$ with a small quantity of $CuOH^+$ based on the following equilibria (Figure 2.24 , Wesseldijk, 1999):

$$Cu^{2+} + H_2O \rightarrow CuOH^+ + H^+ \qquad \textbf{Equation 12}$$

and

$$CuOH^+ + H_2O \rightarrow Cu(OH)_{2(s)} + H^+ \qquad \textbf{Equation 13}$$

Consequently it would also be expected that a significant quantity of $Cu(OH)_2$ is likely to be co-adsorbed on the surface of the mineral via hydrogen bonding to the specifically adsorbed $CuOH^+$. The presence of the neutral $Cu(OH)_2$ species would not be observed by zeta potential measurements.

Malysiak and Shackelton, (2003) found that calcium competed with the copper ions in adsorption on pyroxene and feldspar and Mailula (2004) found that the presence of calcium reduced the floatability of activated pyroxene and feldspar. This is only possible if the calcium ion shows a strong interaction with the mineral surface. A change in the I.S. of the indifferent electrolyte resulted in very little change in zeta potential over the whole pH range. The presence of even a low concentration (10^{-3} I.S.) of calcium caused a significant move in the zeta potential in the positive direction particularly at alkaline pH values. At the higher concentration (10^{-2} I.S.) the curve was shifted positively over the whole pH range implying a strong interaction of calcium ions with the mineral surface.

Zeta potential measurements were not done in the presence of both copper and calcium ions since they are both positively charged ions and therefore the adsorption of one cannot be distinguished from the other. The zeta potentials of all minerals in the presence of CMC (FF30) and guar (APX4M) would be expected to cause a change in the zeta potential if adsorption was occurring. The change in zeta potential would not give an indication of the extent of adsorption but indicate that some adsorption had taken place. Results showed that all minerals reacted in the same way, which was the typical behaviour also observed by Steenberg and Harris, (1984) with similar types of polymers adsorbed on talc and some sulphide and oxide minerals.

A significant increase in the negative zeta potential on the addition of FF30 showed that adsorption of the CMC was occurring under these conditions and the high negative charge on the polymer overcame any reduction in zeta potential that would be expected by the expansion of the double layer to accommodate the large molecules. On the other hand, the decrease in the negative zeta potential in the presence of guar again indicated adsorption but, since this polymer has almost no charge, the expansion of the double layer leads to lower zeta potential values.

Adsorption studies obtained on the all minerals in presence of Ca^{2+} (10^{-2} I.S.) at pH 9 and two depressants guar and CMC indicated that adsorption did not

take place on the quartz which was in accordance to work reported by Steenberg and Harris, (1984). However, both adsorption and zeta potential determinations results indicated that adsorption in the presence of CMC as a high negatively charged polymer (DS-O.76) will not take place for quartz. Higher adsorption densities onto talc, pyroxene, feldspar and chromite are exhibited by guar gum compared to CMC. This can be attributed to higher molecular weight of guar and maybe more favourable cis-configuration of hydroxyl group onto talc surface reported by Subramain and Laskowski, (1997). However, differences in the crystal structure of minerals with respect to ions present (Ca^{2+}) can also influence the extent of polymer adsorption as indicated from zeta potential and adsorption results.

Microflotation tests were also performed at pH 9 in the presence of calcium at a concentration of 10^{-2} I.S. Both Malysiak and Shackelton, (2003) and Mailula, (2004) reported that there was the effect of competitive adsorption of calcium and that calcium reduced the effect of copper activation.
As discussed previously the copper at this pH value would be present as $CuOH^+$ and $Cu(OH)_2$. Both copper species should then be available for reaction with the xanthate collector through the following mechanisms (Fornasiero and Ralston, 1992):

$$Cu(OH)_2 + 2X^- \Leftrightarrow Cu(OH)X + OH^- + X^- \Leftrightarrow CuX_2 + 2OH^- \qquad \textbf{Equation 14}$$

$$CuOH^+ + 2X^- \Rightarrow CuX_2 + OH^- \qquad \textbf{Equation 15}$$

$$CuX_2 \Rightarrow CuX + \tfrac{1}{2}X_2 \qquad \textbf{Equation 16}$$

The stoichiometry of these reactions implies that one molecule of copper reacts with two molecules of xanthate to form a Cu(II) xanthate which decomposes rapidly to form Cu(I) xanthate and dixanthogen. Consequently, since the copper sulphate and xanthate are added in equimolar concentrations, only 50 per cent of the copper would be present as Cu (I) xanthate and 50 per cent remain in the form of $Cu(OH)_2$. However this

assumes that the presence of species such as Cu(OH)X at the surface is very small.

The decrease in floatability in the presence of a polymer does not imply that the hydrophobic copper xanthate has actually been removed from the surface (i.e. deactivation). The polymer may simply be co-adsorbing at the surface and, because of the large size of the polymer, simply prevent particle-bubble attachment. However the adsorption of the polymer may, in fact, lead to deactivation but confirmation of this is beyond the scope of the present project and should be further investigated. The important finding is that copper activated minerals can be depressed in the presence of a polymer.

Zeta potential results for talc indicated that, activation must have occurred from zeta potential data and the reaction with collector most probably lead to the formation of a copper xanthate complex away from the talc surface implying that the hydrophobic xanthate complex was not stably adsorbed. This phenomenon appears to be specific for talc and may result from the naturally hydrophobic planes. The excess $Cu(OH)_2$ would still remain adsorbed at the surface leading to a lower floatability.

For all the other minerals, the floatability after copper activation and collector addition was significantly enhanced indicating the formation of a reasonably stable hydrophobic copper xanthate attached to the surface. The addition of the modified guar gum, APX4M, (Figure 7.1) resulted in a significant decrease in the floatability of the copper-activated mineral.

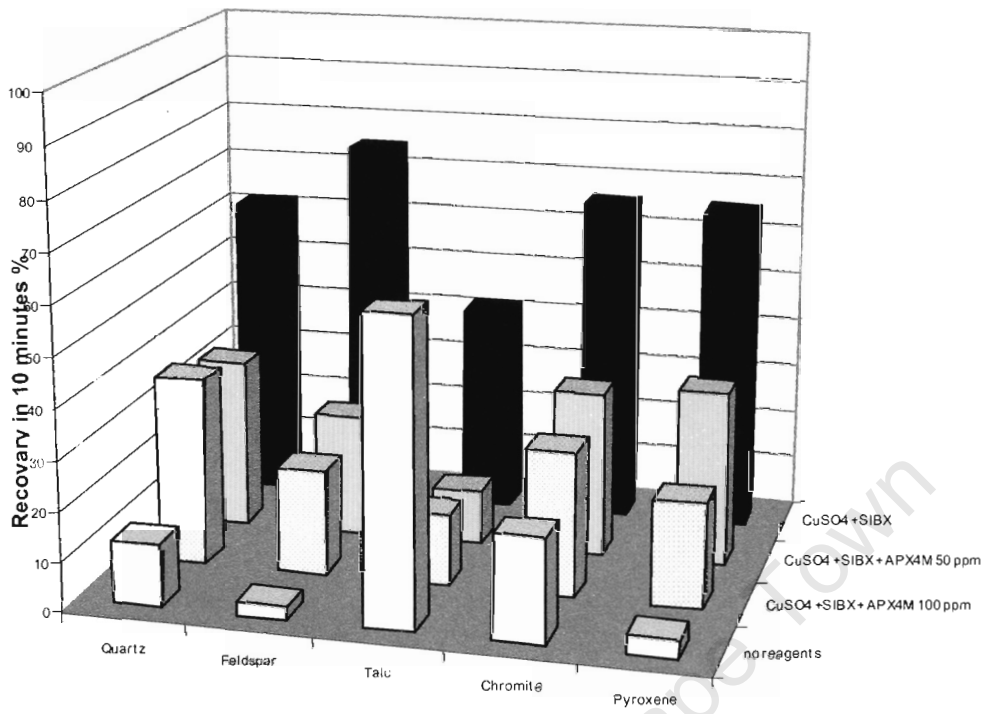

Figure 7-1: The effect of adding reagents with guar gum (APX4M) as a depressant on the floatability of quartz, feldspar, talc, chromite and pyroxene (as mass recovery percentage)

The recovery of talc in particular was significantly reduced to between 10 and 15 per cent. For all the other minerals the floatability caused by the activation could be significantly reduced but could not be completely removed in the presence of APX4M. Increasing the concentration from 50 to 100 ppm did not, apart from pyroxene, increase the degree of depression. The effect of the CMC, (FF30) on the copper activated floatability was much less than that found for the guar as shown in Figure 7.2.

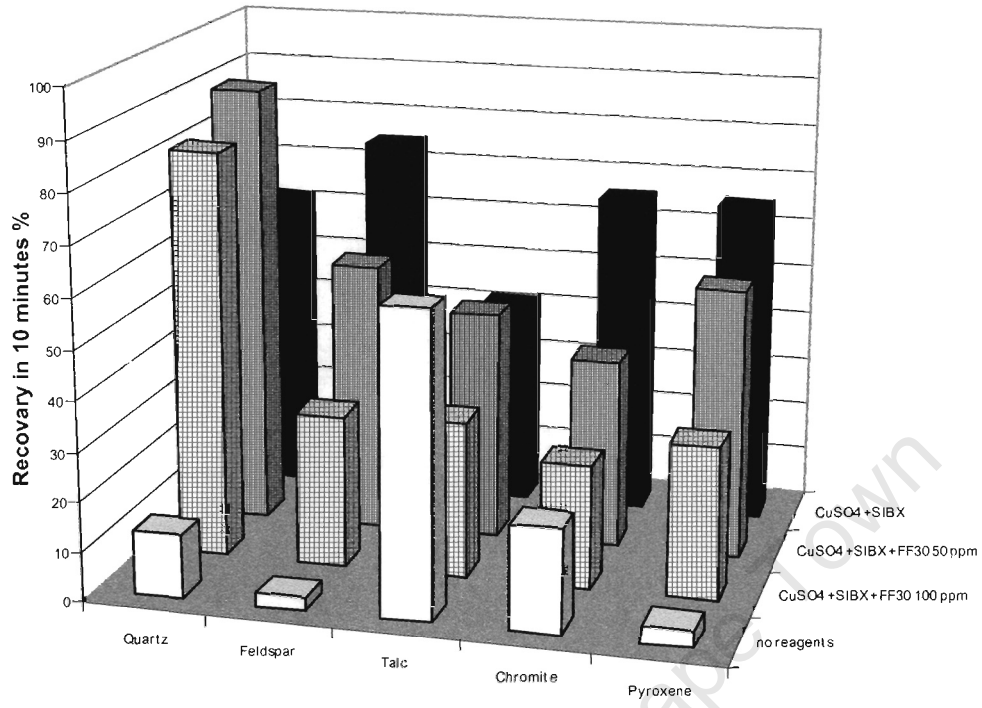

Figure 7-2: The effect of adding reagents with CMC (FF30) as a depressant on the floatability of quartz, feldspar, talc, chromite and pyroxene (as mass recovery percentage)

In fact in two cases, talc and quartz the floatability increased on the addition of 50 ppm FF30. Increasing the concentration of the CMC to 100 ppm always lead to a decrease in recovery. However, recoveries of more than 30 per cent of all the minerals could still be obtained, which implies that the depressant did not lead to a deactivation of the mineral but rather a co-adsorption of the depressant on the mineral. However, this conclusion is speculative, as the experimental technique does not measure the amount of copper at the surface.

It would be expected that the presence of a copper xanthate at the surface would create a more negative surface due to its hydrophobic nature and the adsorption of the strongly negatively charged CMC would therefore be more difficult due to the charge repulsion. This repulsion would not affect the low-

charged guar to the same extent. The increase in the floatability of talc and quartz in the presence of 50 ppm CMC suggests that $Cu(OH)_2$ was present on the mineral surfaces since CMC forms a strong complex with copper. The enhanced floatability of talc and quartz can be attributed to the complexation and dispersion of the $Cu(OH)_2$ leaving only the stable copper xanthate at the surface. The high floatability of quartz would be expected since the zeta potential data indicated that the adsorption of the copper was greater on quartz than on the other minerals.

8. CONCLUSIONS

1. For all selected gangue minerals, the zeta potential increased in negativity as the pH was raised, although positive values were only obtained with chromite below pH 3.

2. Increasing the ionic strength of KNO_3, an indifferent electrolyte, had no significant effect on the iso electric point and resulted in a very little change in zeta potential over the whole pH range for all minerals except feldspar, which was attributed to presence of potassium in mineral.

3. Increasing the ionic strength of $Ca(NO_3)_2$ had an effect on the iso electric point and resulted in decreasing zeta potential values indicating that this was an interaction of calcium with the mineral surfaces of pyroxene, chromite, talc and quartz.

4. The addition of copper ions increased the zeta potential of all selected gangue minerals between pH 7-9 indicating the copper adsorption was not mineral specific and could be attributed to $Cu(OH)^+$ species. This caused charge reversal obtained particularly at alkaline pH values.

5. Addition of both depressants led to a change in zeta potential with CMC showing an increase in negativity with CMC and guar gum a decrease in negativity on all gangue minerals. The increase in negativity obtained with CMC (FF30) was expected due to its high negative charge. Whereas the guar gum (APX4M) with almost no charge resulted in inclusion of counter ions in the double layer, which leads to lower zeta potential.

6. Adsorption studies showed that in the presence of Ca^{2+} ions at pH 9, CMC (FF30) and guar gum (APX4M) adsorbed on all selected gangue

minerals except quartz, which was not consistent with results from zeta potential measurements.

7. Slightly higher adsorption densities were obtained with guar gum than with CMC for all minerals except for chromite, which was similar.

8. Microflotation tests on all selected gangue minerals showed that only talc is naturally floatable (about 61%) with values below 10% obtained for talc, pyroxene, feldspar, chromite and quartz.

9. Microflotation tests showed that the addition of copper sulphate and collector increased floatability of all selected gangue minerals between 62 to 75% except for talc, where the floatability was actually reduced from 61 to 42 per cent. This was attributed to naturally hydrophobic planes of talc and excess of $Cu(OH)_2$ adsorbed at the surface leading to lower floatability.

10. In two cases, talc and quartz, the floatability increased with the addition of 50ppm FF30 which was attributed to $Cu(OH)_2$ present on the mineral surfaces since CMC forms a strong complex with copper and enhanced floatability can be attributed to dispersion of the $Cu(OH)_2$ leaving only stable copper xanthate at the surface.

11. The use of depressants can reduce inadvertent floatability of gangue minerals with guar gum being much stronger than CMC. Guar gum could reduce floatability of all activated gangue minerals, while CMC could reduce floatability of all except quartz. However, the floatability could not be completely removed at the dosages used. The results suggest that, apart from talc, relatively stable copper xanthate complexes are formed on these gangue minerals.

9. LIST OF REFERENCES

Acar, S. and Somasundaran, P., 1992, "Effect of dissolved mineral species on the electrokinetic behaviour of sulphides", Mineral Engineering, Vol. 5 no. 1, pp 27-40

Barth, T.F.W., 1969, *Feldspars*, Chapter 3, pp 88-146, London

Batdorf, J.B. and Rossan, J.M., 1973, in *Industrial Gums*, ed. R. L. Whistler, Academic Press New York

Bowen, N.L., 1913, Amer. Journ. Sci., Vol. 35, p 583

Bradshaw, D.J. and O'Connor, 1996, C.T., "Measurement of the sub – process of bubble loading in flotation", Mineral Engineering, 9 (4), pp 443-448

Bradshaw, D.J., 1997. "Synergistic effects between thiol collectors used in the flotation of pyrite", PhD Thesis, University of Cape Town

Berkman, D.A., 1976, "Field Geologists", Manual. Parkville: Australian Inst. Of Mining and Metallurgy, pp 68

Bockris, J.O'M., and Reddy, A.K.N., 1970, *Modern Electrochemistry*, Vol. I and II Plenum, New York; Chapters 7-10

Bragg, L. and Claringbull, G.F., 1965, "Crystal Structures of Minerals", Vol. 4, G. Bell and Sons Ltd., London

Buchanan, D.L., 1991," Platinum Group Metals, The Bushveld Complex: Geology, Mines, Prospects, Revenues and Costs, Engineering and Mining Journal, pp 23-26

Coertze, F.J. and Coetzee, C.B., 1976, Chromium. in : Minerals Resources of the Republic of South Africa, ed. C.B. Coetzee. Pretoria : Government Printer, 5th ed., pp 117-122

Corrans, I.J., Brugnman, C.F., Overbeek, P.W. and McRae, L.B., 1982, "The recovery of platinum-group metals from ore of the UG2 Reef in the Bushveld Complex, Proc. 12th CMMI Congress Johannesburg, ed. H.W. Glen, pp 629-634

Crozier, R.D., 1992, *Flotation:Theory, Reagents and Ore Testing,* Pergamon Press. New York.

Dalvie, M.A., 2001, "The Effect of Polysaccharides and Inorganic Dispersants on the Effect on the Flotation Performance of a Merensky ore", MSc Thesis, Faculty of Engineering and the Built Environment, University of Cape Town, Cape Town, South Africa

Deja, R.A. and Bhappu, R.B., 1966, "A chemical interpretation of surface phenomena in silicate minerals", Society of Mining Engineers, pp. 329-332

Engelbrecht, J.A. and Woodburn, E.T., 1975, "The effects of froth height, aeration rate and gas precipitation on flotation", J.S Afr. Inst.Min. Metall., Oct. pp 125-132

Everett, D.H., 1989, *Basic Principles of Colloid Science,* Department of Physical Chemistry, University of Bristol, Chapter 3, pp 37-45

Finch, J.A. and Dobby, G.S., 1990, *Column Flotation*. Pergamon Press, Oxford

Fornasiero, D. and Ralston, J., 1992, "Iron hydroxide complexes and their influence on the interaction between ethyl xanthate and pyrite", J. Colloid Interfacial Sc., Vol. 151, pp 225-235

Finkelstein, N.P., and Allison, S.A., 1997, "The activation of sulphide minerals for flotation": a review, International Journal of Mineral Processing, Vol. 52, pp 81-120

Fleer, G.J., Cohen Stuart, M.A., Scheutjens, J.M.H.M., Cosgrove, T. and Vincent, B., 1993, *Polymers at interfaces*, Chapman and Hall, London

Fuerstenau, D.W., and Palmer, B.R., 1976, "Anionic flotation of oxides and silicates ", in *Flotation*: A. M. Gaudin memorial Volume ed. M.C. Fuerstenau., AIME, New York, pp 148-196

Fuerstenau, D.W., and Fuerstenau M.C., 1982, "The flotation of oxide and silicate minerals," Principles of Flotation," King, R. P., ed. S.A.M.M., Johannesburg, pp 109-158

Fuerstenau, M.C., Lopez-Valdivieso, A. and Fuerstenau, D.W., 1988, "Role of hydrolysed cations in the natural floatability of talc, Int. J. Miner. Process., Vol. 23, pp 161-170

Gomes, L.M.B. and Oliveira, J.F., 1989, "Floatability control of talc by the use of carboxymethyl cellulose, Metalurgia-abm, 45 (382), 908-913

Gomes, L.M.B. and Oliveira, J.F., 1991, "The control of natural floatability of talc with carboxymethyl cellulose and aluminium chloride, Fine Particles Processing Flotation, Vol. 2, 17th Int. Miner. Process. Congress, pp 353-364

Gu, F. and Wills, B.A., 1988, "Chromite - Mineralogy and Processing", Minerals Engineering, Vol. 1, no. 3, pp 235-240

Guney, A., Onal, G., Dogan, M.Z. and Celik, M.S., 1993, "Mechanism of anionic collector adsorption in chromite flotation", Proc. XVIII Int. Min. Proc. Congress Sydney, pp 937-940

Harris, P.J. 1982, "Frothing phenomena and froths", in *Principles of Flotation*, ed. R. P. King., S. Afr. Inst. Min. Metall. Jonannesburg

Hatch, F.H., Wells, A.K. and Wells, M.K., 1949, "The petrology of the Igneous Rocks, Vol. 1, Great Britain, pp 50-55

Heerema, R., 1994, Flotatie: Praktische Aspecten, deel II. Delf: Delf University of Technology, mp 3290

Hiemenz, P.C. and Rajagopalan, R., 1997, "Principles of Colloid and Surface Chemistry", Marcel Dekker Inc.;New York, pp 541-546

Hochreiter, R.C., Kennedy, D.C., Muir, W. and Wood, A.I., 1985,"Platinum in South Africa (Metal Review Series no. 3), J.S. Afr. Inst. Mining and Metallurgy, pp 165-185

Hoogendam, C.W., de Keizer, A., Cohen Stuart, M.A., Bijsterbosh, B.H., Batelaan, J.G. and van der Horst, P.M., 1998, "Adsorption Mechanisms of carboxymethyl cellulose on mineral surfaces", Langumir 8: 3825-3831

Hunter, R.J., 1993, Introduction to modern colloid science, Oxford University Press

Israelachvili, J.N., 1992. "Intermolecular and surface forces", 2nd ed. Academic Press. London. pp 122-141

James, R.O. and Healy, T.W., 1972, "Adsorption of Hydrolyzable Metal Ions at the Oxide-Water Interface", Journal of Colloid and Interface Science, Vol. 40, no.1

Kostov, I., 1968, *Minerology*, University of Sofia, Bulgaria

King, R.P., 1982, *Principles of flotation*, S. Afr. Inst. Min. Metall. Jonannesburg

Klimpel, R.R., 1984. Froth flotation: The kinetic approach. Proceedings of Mintek 50, Johannesburg, South Africa

Laskowski, J.S., 1986, "The relationship between floatability and hydrophobicity", in *Advances in Minerals Processing*, ed. P. Somarsundaran, SME, Littleton, Colorado. pp 189-208

Laskowski, J.S., 1994,"Flotation of potash ores", in *Reagents for Better Metallurgy*, ed. P.S. Mulukutla., SME, Littleton, Colorado. pp 225-228

Laskowski, J.S., 1996, "Surface processes course manual", University of Cape Town

Laskowski, J.S., Liu and Zhan Y., 1997, Sphalerite Activation: Flotation and Electrokinetic studies, Minerals Engineernig, Vol. 10, pp 787-802

Leja, J., 1982, *Surface Chemistry of froth flotation*, Plenum Press, New York

Liddell, K.S., McRae, L.B. and Dunne, R.C., 1986, "Process routes for beneficiation of noble metals from Merensky and UG2 ores, Mintek Review, no. 4, pp 33-34

Liu, Q., Laskowski, J.S., 1999, "On the adsorption mechanism of carboxymethyl cellulose," Polymers in Mineral Processing, J. S. Laskowski., ed. 38th Annual Conference of Metallurgists of SIM, Quebec, Canada, pp 357-372

Loewenstein, W., 1954, "Aluminium avoidance principle by feldspars", Blackie and Son, Glasgow

Machatschki, R., 1928, *Feldspar Structures*

MacKenzie, J.M.W. E and M.J. 1980, Safil Int. Conf. Filtr. Sepn. Proc. 1980

Mailula, T.D., 2004 " An investigation into chemical factors that affect the behaviour of gangue minerals in the flotation of PGM ores," MSc Theses, Faculty of Engineering and the Built Environment, University of Cape Town, Cape Town, South Africa

Malysiak, V. Coetzer, L. P., Gerson, A., O'Connor, C. T., Raston, J. and Bradshaw, D., 2002, "Pentlandite-Feldspar Interaction and its Effect on Separation", International Journal of Mineral Processing, Vol. 66, Issue 1-4, pp 89-106

Malysiak, V., Shackleton, N.J., and Vaux de D., 2003, "Effect of water quality on pentlandite-pyroxene floatability with an emphasis on calcium ions", Proceedings of the 22nd International Mineral Processing Congress (IMPC) Cape Town, South Africa

Malysiak, V., 2003, "Pentlandite-pyroxene and pentlandite-feldspar interactions and their effect on separation by flotation", PhD Theses, Faculty of Engineering and the Built Environment, University of Cape Town, Cape Town, South Africa

Morris, G.E., 1996, "The adsorption characteristics of polymeric depressants as the talc-water interface", PhD Theses (Applied Technology), Faculty of Applied Science and Technology, University of South Australia,

Nagaraj, D.R., and Brinen, J., 1996,"SIMS and XPS study of the adsorption of sulphide collectors on pyroxene": a case for inadvertent metal ion activation,

Colloids and Surfaces, A: Physicochemical and Engineering Aspects 116, pp 241-249

Owada, S. and Harada, T., 1985, "Grindability and magnetic properties of chromites", J.Min.Metall.Inst.Japan, Vol.101, pp 781

Palmer, B.R., Fuerstenau, M.C. and Aplan, F.F., 1975, "Mechanisms involved in the flotation of oxides and silicates with anionic collectors", Transactions AIME, Vol. 258, pp 261-263

Parolis, L.A.S., Groenmeyer, G.V. and Harris, P.J., 2003, *Equilibrium adsorption studies of polysaccharides on talc*:"The effect of molecular weight, charge and the influence of metal cations", Paper accepted for presentation at SME, Denver

Rao, S.R., 1974, "Surface forces in flotation", Minerals Sci. Engineering, Vol. 6, no. 1

Rath, R.K., Subramanian, S. and Laskowski J.S., 1997, "Adsorption of dextrin and guar gum onto talc, a comparative study," Langumir, 13, 6260-6266

Savassi, O.N. Alexander, D.J. Franzidis, J.P. and Manlapig, E.V., 1998, "An empirical model for entrainment in industrial flotation plants", Mineral Engineering, Vol. 11, no. 3, pp. 243-256

Samoilov, H., 1965,"Structure of Aqueous Electrolyte Solutions", Consultants bureau, New York

Sobieraj, S. and Laskowski, J., 1973, "Flotation of chromite: 1-early research and recent trends; 2-flotation of chromite and surface properties od spinel minerals, Transactions Inst. Mining and Metallurgy, Vol. 82, pp C207-C213

Steenberg, E., Harris, P.J., 1984, "Adsorption of carboxymethyl cellulose, guar gum and starch, onto talc, sulphides, oxides and salt-type minerals," South African Journal of Chemistry, Vol. 37, pp 85-90

Shackleton, N.J., 2003, "The role of complexing agents in the flotation of pentlandite-pyroxene mixtures", MSc Thesis, Faculty of Engineering and the Built Environment, University of Cape Town, Cape Town, South Africa

Shortridge, P., Harris, P., Bradshaw, D., 1999, "The influence of ions on the effectiveness of polysaccharide depressants in the flotation of talc", Polymers in Mineral Processing, ed. J.S. Laskowski., Proceedings of the 3rd UBC-McGill Bi-Annual International Symposium on Fundamentals in Mineral Processing, Quebec City, pp 155-170

Smith, P.G. and Warren, L.J., 1989, "Entrainment of particles into flotation froths', in *Frothing in Flotation*, Gordon and Breach, New York, 123-145

Subrahmanyam, T.M. and Forsseberg, E., 1988, "Froth stability, particle entrainment and drainage in flotation", a review, Int. J. Miner. Process. 46: pp 21-34

Taggart, A.F., 1945, *Handbook of mineral dressing*. Wiley, New York

Wesseldijk, Q.I., 1998, "The behaviour of chromite in the flotation of UG-2 ores", MSc Thesis, Faculty of Engineering and the Built Environment, University of Cape Town, Cape Town, South Africa

Whistler R.L., 1973, in *Industrial Gums*, - "Polysaccharides and their derivatives", Second Edition, Academic Press, New York

Wood, T., 1996, "The platinum group metals in South Africa", in: http://www.bullion.org.za/publications/platinum.htm, ed. T. Wood, Chamber of Mines South Africa

APPENDIX 1: XRF AND XRD Analysis of Talc, Chromite, Quartz, Pyroxene and Feldspar

Printed by Eval on 07-May-2004 11:03:53
Sample :Talc
Sample measured on 26-Mar-2004 16:56:58

Na	Mg	Al	Si	P	S	Cl
0.1 KCps	93.0 KCps	0.4 KCps	81.1 KCps	0.8 KCps	0.4 KCps	0.5 KCps
0.0669 %	15.8 %	0.0591 %	13.6 %	0.0682 %	0.0210 %	0.0297 %

K	Ca	Sc	Ti	V	Cr	Mn
0.2 KCps	3.3 KCps	0.3 KCps	0.4 KCps	0.2 KCps	4.5 KCps	3.9 KCps
0.00394 %	0.0906 %	0.00193 %	0.00827 %	0.00556 %	0.0760 %	0.0507 %

Fe	Co	Ni	Cu	Ga	Ge	As
350.8 KCps	2.9 KCps	6.1 KCps	0.3 KCps	1.8 KCps	2.1 KCps	3.4 KCps
8.70 %	0.0204 %	0.336 %	0.00743 %	0.00786 %	0.00750 %	0.0560 %

Se	Br	Rb	Sr	Y	Zr	Nb
3.1 KCps	3.6 KCps	4.7 KCps	5.5 KCps	6.1 KCps	6.8 KCps	7.7 KCps
0.00674 %	0.00860 %	0.00945 %	0.0131 %	0.0166 %	0.0144 %	0.0156 %

Mo	Ru	Rh	Pd	Ag	Cd	In
9.3 KCps	0.2 KCps	0.2 KCps	0.3 KCps	0.3 KCps	0.4 KCps	0.6 KCps
0.0207 %	0.0215 %	0.0133 %	0.0181 %	0.0182 %	0.0228 %	0.0327 %

Sn	Sb	Te	I	Cs	Ba	La
12.2 KCps	12.3 KCps	12.1 KCps	11.9 KCps	0.3 KCps	0.4 KCps	0.4 KCps
0.190 %	0.267 %	0.279 %	0.387 %	0.0119 %	0.0227 %	0.0240 %

Ce	Pr	Nd	Sm	Eu	Gd	Tb
0.2 KCps	0.3 KCps	0.3 KCps	0.3 KCps	0.4 KCps	0.5 KCps	1.2 KCps
0.00423 %	0.0121 %	0.0211 %	0.0185 %	0.0155 %	0.0173 %	0.00123 %

Ho	Yb	Hf	Ta	W	Re	Ir
0.9 KCps	1.7 KCps	0.9 KCps	1.3 KCps	1.5 KCps	2.2 KCps	1.7 KCps
0.0143 %	0.0277 %	0.0516 %	0.0231 %	0.0117 %	0.00772 %	0.0156 %

Pt	Au	Tl	Pb	Bi	Th	U
1.9 KCps	2.1 KCps	2.4 KCps	4.2 KCps	2.8 KCps	4.4 KCps	4.9 KCps
0.0228 %	0.0168 %	0.0162 %	0.0380 %	0.0202 %	0.0113 %	0.0390 %

Sum
40.80 %

Printed by Eval on 07-May-2004 11:02:50
Sample :Chromite
Sample measured on 26-Mar-2004 15:35:35

Na	Mg	Al	Si	P	S	Cl
0.1 KCps	15.3 KCps	19.9 KCps	4.0 KCps	0.9 KCps	0.3 KCps	0.5 KCps
0.121 %	5.63 %	5.93 %	0.792 %	0.0924 %	0.0220 %	0.0387 %

K	Ca	Sc	Ti	V	Cr	Mn
0.3 KCps	1.8 KCps	0.3 KCps	11.3 KCps	4.2 KCps	810.0 KCps	10.7 KCps
0.00954 %	0.0677 %	0.00561 %	0.291 %	0.180 %	38.5 %	0.158 %

Fe	Co	Ni	Cu	Zn	Ga	Ge
434.0 KCps	2.2 KCps	0.6 KCps	0.1 KCps	3.4 KCps	0.8 KCps	0.6 KCps
20.9 %	0.0732 %	0.112 %	0.0102 %	0.0573 %	0.0137 %	0.00803 %

As	Se	Br	Rb	Sr	Y	Zr
1.0 KCps	0.9 KCps	1.0 KCps	1.3 KCps	1.5 KCps	1.6 KCps	1.8 KCps
0.0557 %	0.00681 %	0.00859 %	0.00915 %	0.0127 %	0.0159 %	0.0136 %

Nb	Mo	Ru	Rh	Pd	Ag	Cd
2.0 KCps	2.3 KCps	0.0 KCps	0.1 KCps	0.1 KCps	0.1 KCps	0.1 KCps
0.0142 %	0.0178 %	0.0161 %	0.0182 %	0.0137 %	0.0145 %	0.0163 %

In	Sn	Sb	Te	I	Cs	Ba
0.1 KCps	2.9 KCps	3.0 KCps	3.0 KCps	3.0 KCps	0.3 KCps	0.5 KCps
0.0196 %	0.115 %	0.155 %	0.157 %	0.209 %	0.0295 %	0.0478 %

La	Ce	Pr	Nd	Sm	Eu	Gd
0.6 KCps	0.2 KCps	0.3 KCps	0.9 KCps	0.8 KCps	2.5 KCps	0.4 KCps
0.0633 %	0.0156 %	0.0290 %	0.123 %	0.0783 %	0.0127 %	0.0588 %

Tb	Dy	Ho	Er	Yb	Hf	Ta
0.9 KCps	1.6 KCps	0.5 KCps	2.0 KCps	0.4 KCps	0.3 KCps	0.4 KCps
0.0486 %	0.0498 %	0.0275 %	-0.180 %	0.0314 %	0.0568 %	0.0233 %

W	Re	Ir	Pt	Au	Tl	Pb
0.4 KCps	0.6 KCps	0.5 KCps	0.6 KCps	0.6 KCps	0.7 KCps	1.2 KCps
0.00487 %	0.00892 %	0.0170 %	0.0245 %	0.0210 %	0.0161 %	0.0386 %

Bi	Th	U	Sum
0.8 KCps	1.2 KCps	1.4 KCps	
0.0209 %	0.0108 %	0.0386 %	74.65 %

Printed by Eval on 07-May-2004 11:04:28
Sample :Pyroxene
Sample measured on 26-Mar-2004 17:37:44

Na	Mg	Al	Si	P	S	Cl
0.2 KCps	52.9 KCps	4.6 KCps	109.5 KCps	0.8 KCps	0.4 KCps	0.4 KCps
0.122 %	11.0 %	0.739 %	18.7 %	0.0812 %	0.0258 %	0.0341 %

K	Ca	Sc	Ti	V	Cr	Mn
0.7 KCps	37.7 KCps	0.3 KCps	3.3 KCps	0.6 KCps	15.6 KCps	9.7 KCps
0.0225 %	1.27 %	0.00428 %	0.0765 %	0.0152 %	0.324 %	0.163 %

Fe	Co	Ni	Cu	Zn	Ga	Ge
622.0 KCps	3.2 KCps	1.2 KCps	0.2 KCps	2.1 KCps	1.1 KCps	1.3 KCps
15.9 %	0.0307 %	0.0943 %	0.00833 %	0.00502 %	0.00768 %	0.00708 %

As	Se	Br	Rb	Sr	Y	Zr
2.0 KCps	1.8 KCps	2.1 KCps	2.7 KCps	3.1 KCps	3.4 KCps	3.9 KCps
0.0484 %	0.00604 %	0.00729 %	0.00793 %	0.0113 %	0.0141 %	0.0126 %

Nb	Mo	Ru	Rh	Pd	Ag	Cd
4.1 KCps	4.9 KCps	0.1 KCps	0.2 KCps	0.2 KCps	0.2 KCps	0.2 KCps
0.0124 %	0.0157 %	0.0163 %	0.0128 %	0.0139 %	0.0141 %	0.0168 %

In	Sn	Sb	Te	I	Cs	Ba
0.3 KCps	6.9 KCps	7.2 KCps	7.3 KCps	7.4 KCps	0.2 KCps	0.3 KCps
0.0230 %	0.133 %	0.189 %	0.202 %	0.290 %	0.0130 %	0.0226 %

La	Ce	Pr	Nd	Sm	Eu	Gd
0.3 KCps	0.2 KCps	0.2 KCps	0.3 KCps	0.3 KCps	0.4 KCps	0.5 KCps
0.0246 %	0.00625 %	0.0122 %	0.0238 %	0.0211 %	0.0190 %	0.0225 %

Ho	Er	Yb	Hf	Ta	W	Re
0.9 KCps	2.9 KCps	0.8 KCps	0.5 KCps	0.8 KCps	0.8 KCps	1.3 KCps
0.0193 %	-0.117 %	0.0301 %	0.0480 %	0.0222 %	0.00612 %	0.00700 %

Ir	Pt	Au	Tl	Pb	Bi	Th
1.0 KCps	1.2 KCps	1.2 KCps	1.4 KCps	2.4 KCps	1.7 KCps	2.5 KCps
0.0148 %	0.0211 %	0.0167 %	0.0148 %	0.0318 %	0.0183 %	0.00852 %

U	Sum
2.8 KCps	
0.0329 %	50.05 %

Printed by Eval on 07-May-2004 11:03:12
Sample :Feldspar
Sample measured on 26-Mar-2004 16:16:23

Na	Mg	Al	Si	P	S	Cl
1.4 KCps	8.8 KCps	58.5 KCps	105.6 KCps	1.2 KCps	1.3 KCps	0.5 KCps
0.499 %	0.663 %	8.11 %	15.4 %	0.0815 %	0.0544 %	0.0287 %

K	Ca	Sc	Ti	V	Cr	Mn
4.2 KCps	161.3 KCps	0.2 KCps	0.7 KCps	0.2 KCps	1.2 KCps	0.8 KCps
0.114 %	9.87 %	0.00404 %	0.0199 %	0.00551 %	0.0289 %	0.0122 %

Fe	Co	Ni	Cu	Ga	Ge	As
40.1 KCps	0.7 KCps	0.2 KCps	0.3 KCps	1.7 KCps	1.7 KCps	2.7 KCps
0.431 %	0.00597 %	0.000440 %	0.00650 %	0.00577 %	0.00430 %	0.0296 %

Se	Br	Rb	Sr	Y	Zr	Nb
2.4 KCps	2.8 KCps	3.7 KCps	23.0 KCps	4.7 KCps	9.2 KCps	5.6 KCps
0.00375 %	0.00446 %	0.00512 %	0.0404 %	0.00905 %	0.00931 %	0.00838 %

Mo	Ru	Rh	Pd	Ag	Cd	In
6.7 KCps	0.1 KCps	0.2 KCps	0.2 KCps	0.2 KCps	0.3 KCps	0.4 KCps
0.0109 %	0.0117 %	0.00832 %	0.0107 %	0.0109 %	0.0137 %	0.0202 %

Sn	Sb	Te	I	Cs	Ba	La
9.1 KCps	9.3 KCps	9.3 KCps	9.2 KCps	0.2 KCps	0.3 KCps	0.2 KCps
0.120 %	0.172 %	0.184 %	0.266 %	0.0126 %	0.0289 %	0.0197 %

Ce	Pr	Nd	Sm	Eu	Gd	Tb
0.2 KCps	0.1 KCps	0.2 KCps	0.2 KCps	0.2 KCps	0.3 KCps	0.4 KCps
0.00175 %	0.00824 %	0.0162 %	0.0132 %	0.0119 %	0.0117 %	0.0147 %

Dy	Ho	Yb	Hf	Ta	W	Re
0.5 KCps	0.5 KCps	0.7 KCps	0.6 KCps	0.9 KCps	1.0 KCps	1.8 KCps
0.0116 %	0.00817 %	0.0159 %	0.0259 %	0.0109 %	0.00225 %	0.00479 %

Ir	Pt	Au	Tl	Pb	Bi	Th
1.4 KCps	1.5 KCps	1.6 KCps	2.0 KCps	3.2 KCps	2.2 KCps	3.4 KCps
0.00894 %	0.0127 %	0.0112 %	0.00877 %	0.0201 %	0.0113 %	0.00540 %

U	Sum
3.8 KCps	
0.0209 %	36.56 %

X'Pert Graphics & Identify
Graph: talc

terry
2003/02/20 10:53

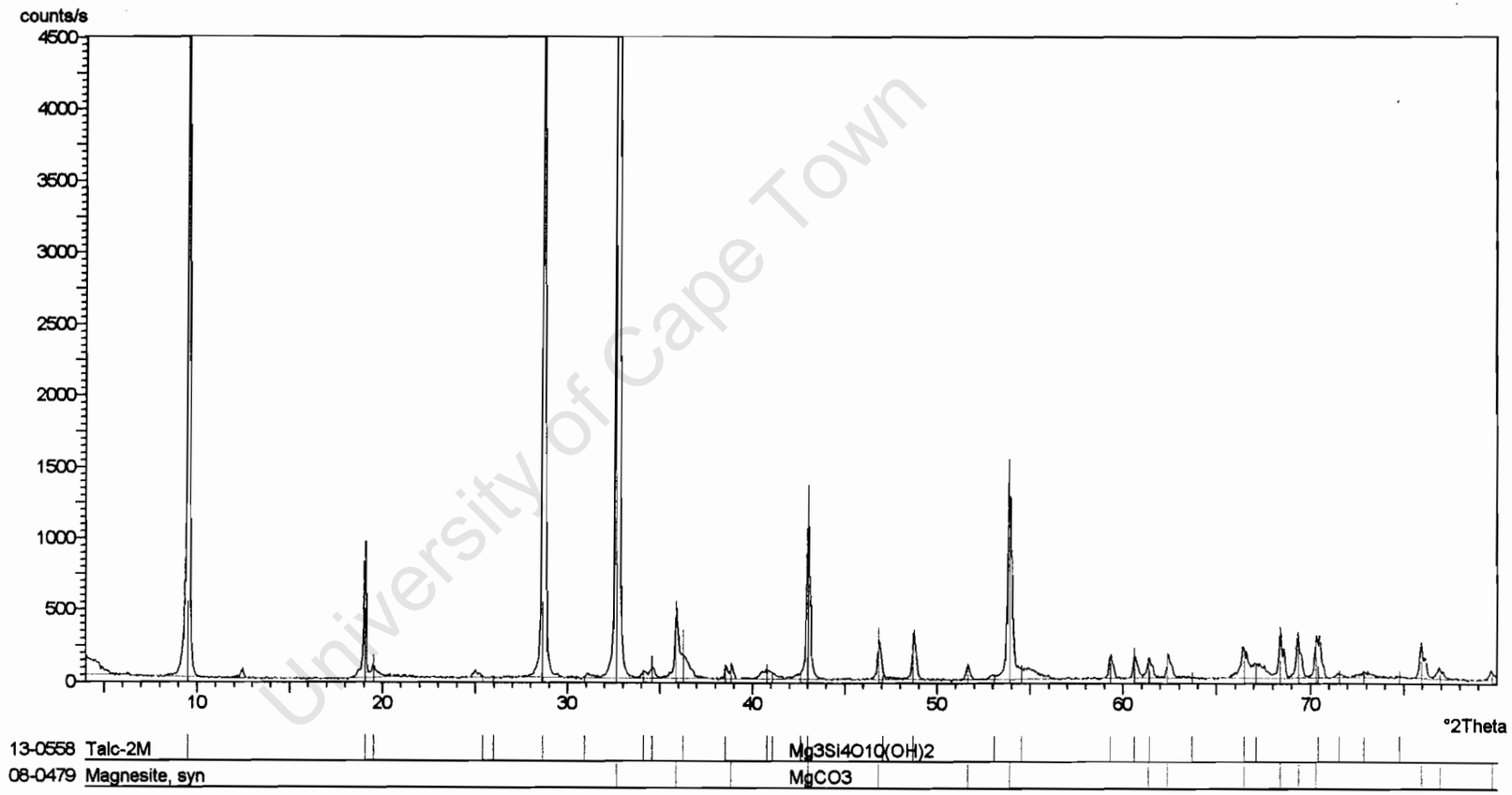

Philips Analytical

X'Pert Graphics & Identify
Graph: chromite

terry
2003/02/20 11:40

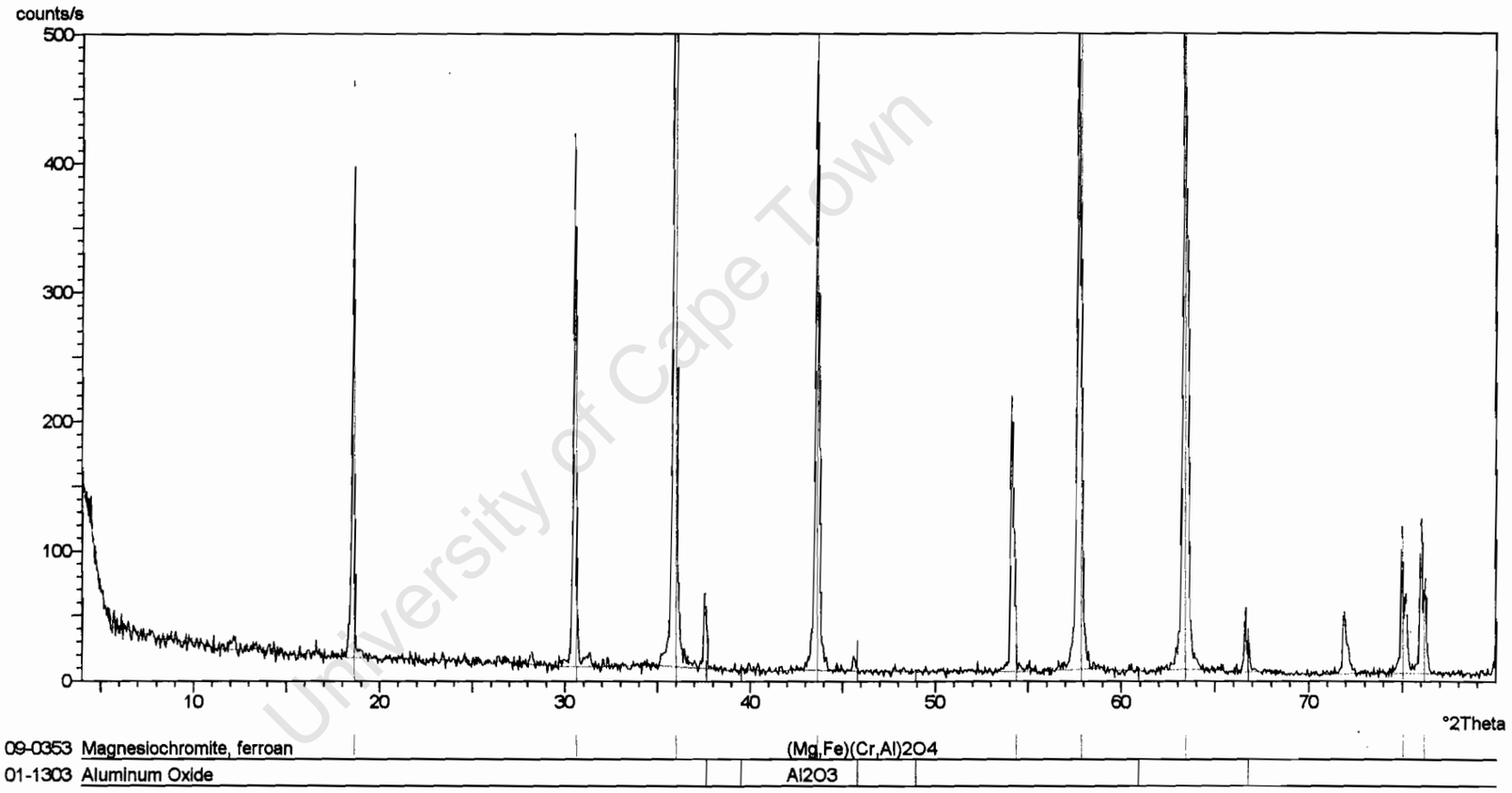

Philips Analytical

X'Pert Graphics & Identify
Graph: P

terry
2002/11/20 12:19

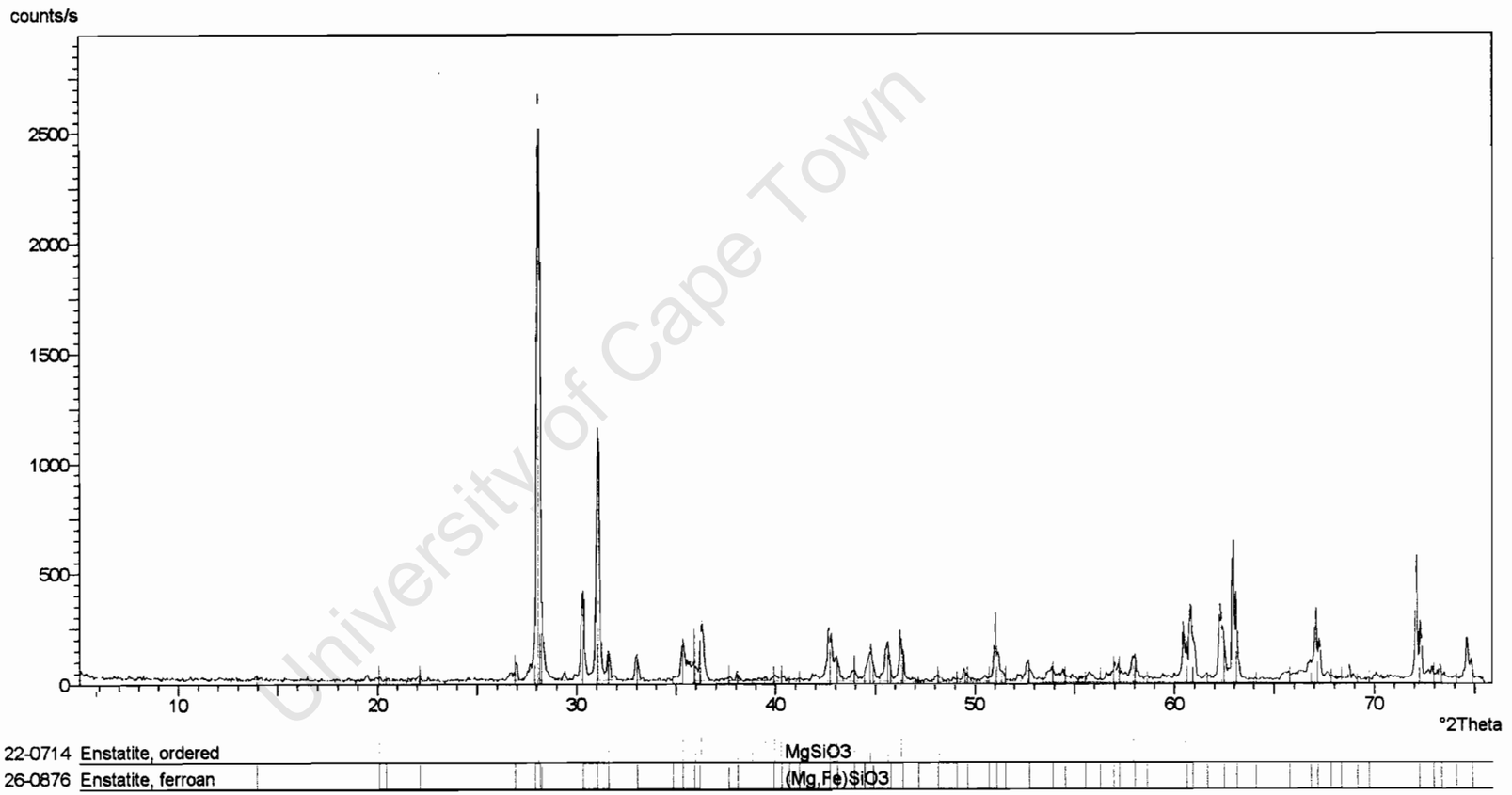

Philips Analytical

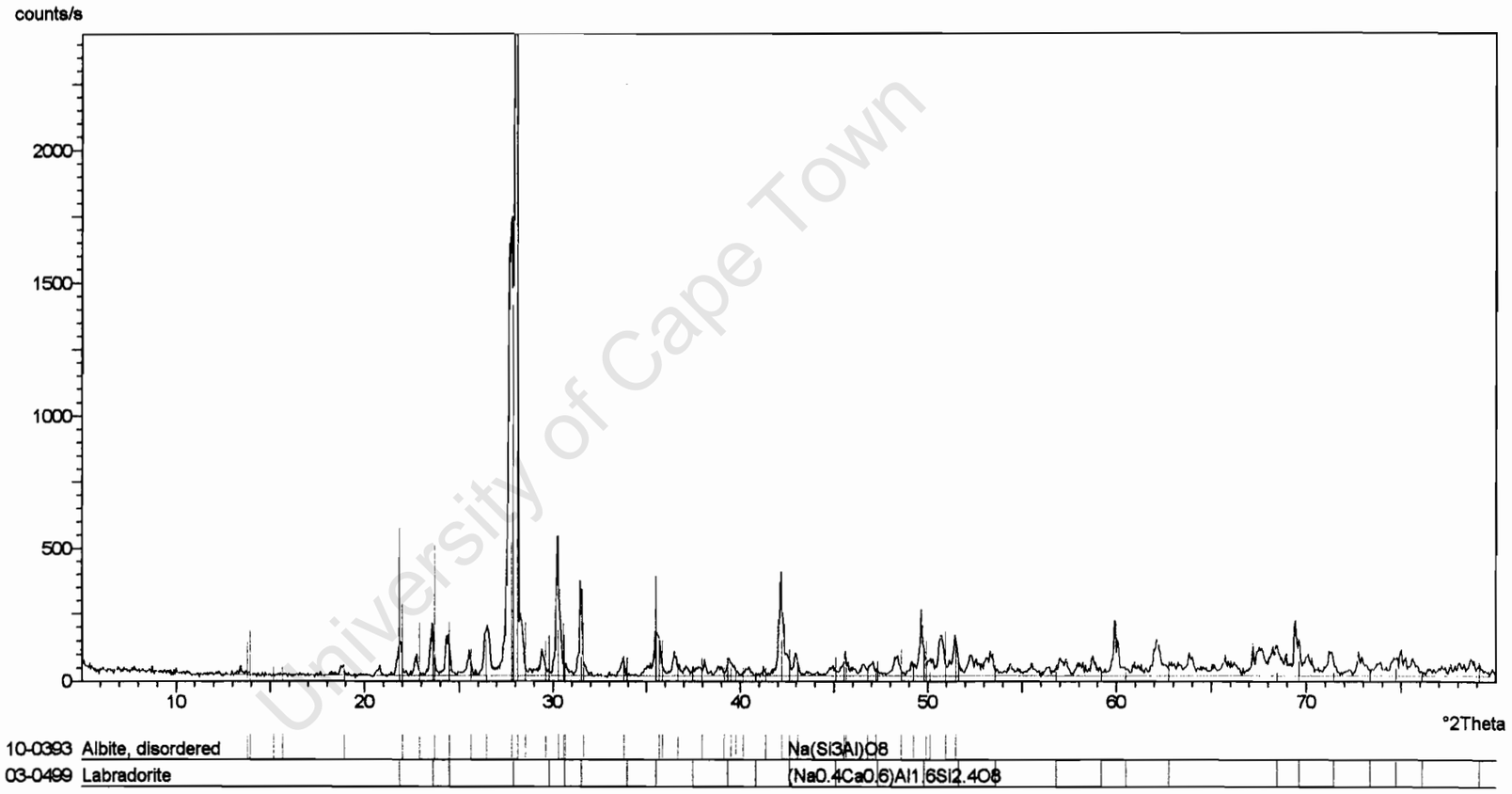

X'Pert Graphics & Identify
Graph: quartz

terry
2003/02/20 10:50

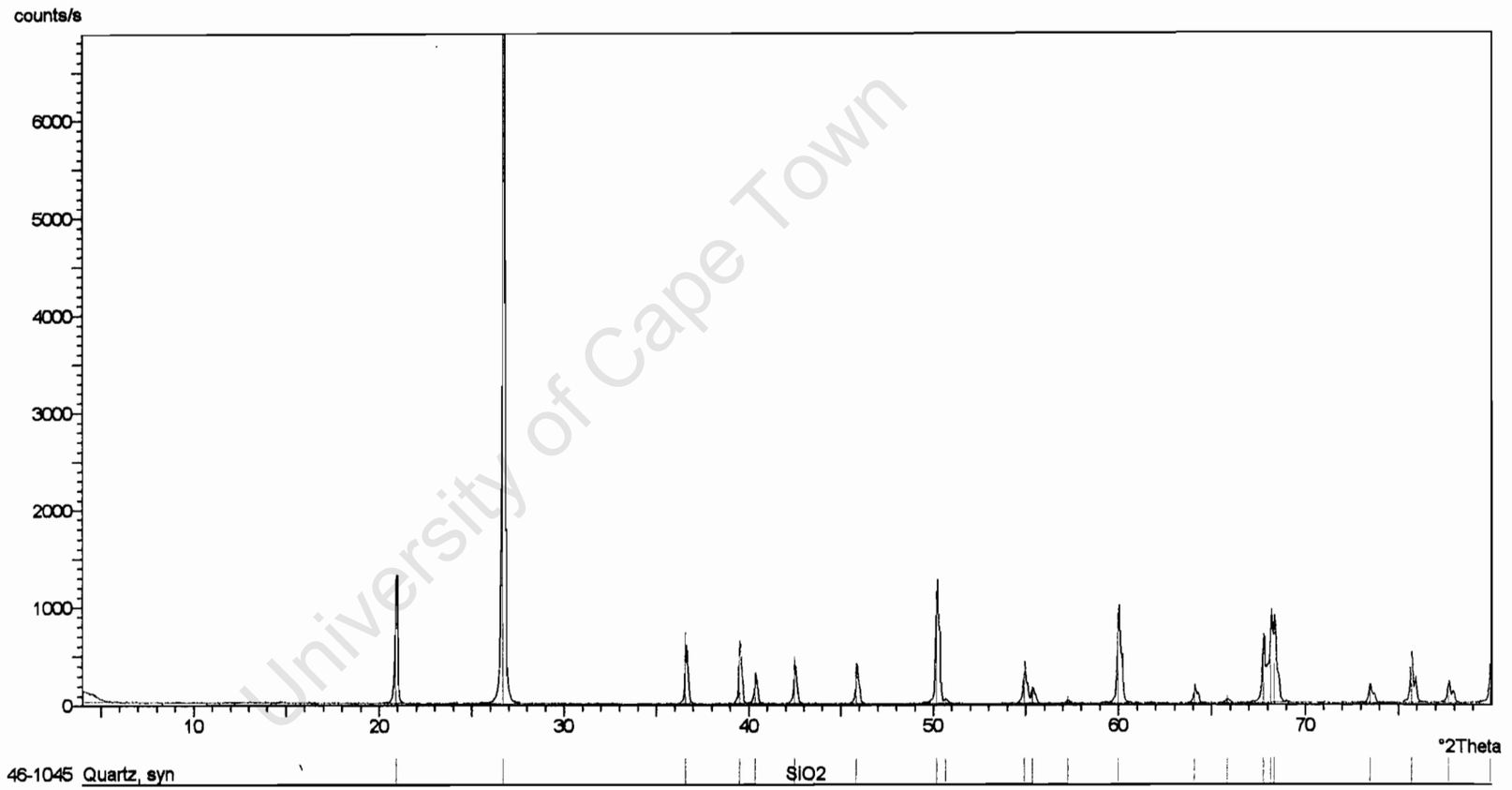

Philips Analytical

APPENDIX 2: SUMMARY OF ZETA POTENTIAL DETERMINATIONS DATA

Results of quartz in presence of KNO_3 10^{-3} M as a standard concentration

pH	Zeta Potential	Reading 1	Reading 2	Reading 3	Reading 4	Reading 5	Std Dev
	mV	mV	mV	mV	mV	mV	mV
10	-44.4	-47.9	-43.5	-45.1	-43.3	-42.4	1.3
8.8	-46.9	-48.4	-47.8	-48.2	-44.1	-45.8	1.2
7.65	-46.7	-46.1	-46.4	-48.2	-46.1	-46.8	0.8
6.93	-46.9	-47.2	-44.7	-48.0	-47.9	-46.6	1.1
6	-41.8	-44.4	-41.3	-41.0	-40.4	-42.1	1.1
5.03	-38.2	-37.1	-39.8	-35.7	-38.7	-39.7	1.21
4.1	-34	-36.2	-33.7	-33.4	-33.5	-33.1	0.9
3	-21.5	-21.5	-22.2	-22.0	-21.8	-21.8	0.5

Results of chromite in presence of KNO_3 10^{-3} M as a standard concentration

pH	Zeta Potential	Reading 1	Reading 2	Reading 3	Reading 4	Reading 5	Std Dev
	mV	mV	mV	mV	mV	mV	mV
9.95	-23.3	-24.0	-22.1	-22.8	-22.3	-25.2	1.3
8.95	-25.1	-21.5	-24.7	-24.0	-27.5	-27.6	2.6
8.1	-26.6	-25.6	-28.8	-26.9	-27.2	-25.5	1.3
6.92	-25.7	-26.5	-26.5	-24.7	-25.9	-25.1	0.8
6.08	-9.8	-7.5	-8.8	-10.0	-14.0	-8.6	2.5
4.93	-2.2	-1.8	-1.1	-0.6	-6.1	-1.1	2.2
4	9.3	3.0	2.6	2.3	6.3	4.7	3.0
3	21	26.3	19.9	18.0	22.1	18.6	3.4

Results of talc, pyroxene and feldspar in presence of KNO_3 10^{-3} M as a standard concentration

pH	Zeta Potential	pH	Zeta Potential	pH	Zeta Potential
	mV		mV		mV
9.96	-34.2	10.01	-32.7	9.98	-43.4
9.23	-32.1	8.94	-33.8	9	-42.0
8.24	-29.7	8.01	-31.5	8.08	-40.2
7.25	-28.7	7.1	-29.7	7.11	-37.9
6.1	-24.1	6.12	-27.9	6.09	-33.5
5.06	-22.7	5.1	-25.1	5.11	-29.8
4.23	-16.2	4.12	-18	4.19	-20.6
3.06	-0.6	30.8	-11.7	3.11	-12.8

Results of chromite in presence of KNO_3 10^{-2} M as a concentration

pH	Zeta Potential	Reading 1	Reading 2	Reading 3	Reading 4	Reading 5	Std Dev
	mV	mV	mV	mV	mV	mV	mV
9.95	-31.3	-30.4	-32.2	-31.6	-32.5	-29.6	1.2
8.95	-30.3	-28.1	-30.5	-31.5	-31.6	-29.7	1.5
8.1	-27.5	-27.5	-26.7	-26.0	-28.3	-29.2	1.3
6.92	-18.2	-18.7	-17.3	-18.2	-17.9	-18.6	0.6
6.08	-9.9	-10.3	-10.6	-9.4	-10.1	-9.2	0.6
4.93	-7.4	-5.1	-7.9	-9.3	-7.8	-6.9	1.5
4	2.2	3.4	1.6	2.8	1.8	1.4	0.8
3	6.4	8.4	5.6	6.0	7.2	5.0	1.4

Results of pyroxene in presence of KNO_3 10^{-2} M as a concentration

pH	Zeta Potential	Reading 1	Reading 2	Reading 3	Reading 4	Reading 5	Std Dev
	mV	mV	mV	mV	mV	mV	mV
10	-36.2	-35.8	-35.3	-35.5	-36.5	-38.0	1.1
9.08	-36.2	-36.3	-36.2	-36.5	-35.7	-36.4	0.3
8.04	-36.5	-36.2	-36.0	-35.5	-36.9	-38.0	0.3
7.09	-33.2	-32.5	-32.3	-34.2	-33.5	-33.2	0.7
5.93	-31.0	-31.0	-30.1	-30.2	-31.5	-32.5	1.0
5.05	-28.5	-27.9	-28.9	-27.4	-28.9	-29.2	0.8
4.1	-20.1	-20.0	-20.0	-19.9	-20.3	-20.3	0.2
3.07	-12.9	-12.8	-12.5	-13.1	-12.9	-13.4	0.3

Results of feldspar in presence of KNO_3 10^{-2} M as a concentration

pH	Zeta Potential	Reading 1	Reading 2	Reading 3	Reading 4	Reading 5	Std Dev
	mV	mV	mV	mV	mV	mV	mV
9.99	-26.6	-24.4	-28.2	-27.2	-	-	2.0
9.07	-22.8	-20.2	-23.9	-20.8	-25.4	-23.8	2.2
8.03	-22.1	-21.5	-21.5	-22.5	-22.7	-22.4	0.6
7.05	-16.5	-15.5	-16.2	-17.6	-16.4	-17.1	0.8
6.01	-14.1	-13.5	-14.4	-13.9	-14.8	-14.0	0.7
5.01	-13.3	-12.5	-14.4	-12.9	-13.7	-13.2	0.7
4.07	-9.3	-7.7	-9.4	-9.5	-9.7	-10.2	1.0
3.05	-2.0	-1.2	-1.4	-2.5	-2.2	-2.9	0.7

Results of talc in presence of KNO_3 10^{-2} M as a concentration

pH	Zeta Potential
	mV
9.96	-17.4
9.03	-14.8
7.84	-13.5

7.08	-12.5
6.02	-10.9
4.95	-4.7
4.09	-1.9
3.05	1.8

Results of quartz in presence of $CuSO_4$ 10^{-4} M as a concentration

pH	Zeta Potential	Reading 1	Reading 2	Reading 3	Reading 4	Reading 5	Std Dev
	mV	mV	mV	mV	mV	mV	mV
3.33	-15.8	-16.1	-15.0	-16.2	-	-	0.7
4.23	-19.1	-17.7	-20.3	-20.9	-18.5	-18.2	1.4
5.17	-12.4	-11.4	-11.7	-11.4	-11.8	-15.7	1.9
6.2	2.5	5.1	1.1	2.6	2.0	1.7	1.6
7.11	8.3	11.3	6.8	9.3	7.8	6.0	2.1
8.09	7.5	9.4	8.6	3.8	9.0	6.9	2.3
9.1	0.5	-5.8	2.4	4.9	-0.8	1.7	4.0
9.95	-17.1	-18.6	-9.7	-20.0	-19.7	-17.5	4.3

Results of chromite in presence of $CuSO_4$ 10^{-4} M as a concentration

pH	Zeta Potential	Reading 1	Reading 2	Reading 3	Reading 4	Reading 5	Std Dev
	mV	mV	mV	mV	mV	mV	mV
3.26	6.1	7.0	5.5	6.8	5.	5.6	0.8
4.20	2.7	5.5	4.1	5.4	1.0	-2.4	3.4
5.15	-1.9	-3.9	-4.5	1.5	1.0	-3.3	2.9
6.09	8.3	10.7	7.3	4.7	8.3	10.7	2.5
7.15	11.0	8.7	8.9	12.8	10.8	13.8	2.3
8.5	-3.0	-3.6	4.0	2.4	2.9	0.5	3.5
9.17	-10.3	-14.3	-5.7	-11.6	-10.3	-9.6	3.1
10.03	-22.9	-27.4	-21.3	-22.4	-25.4	-17.9	3.7

Results of talc, pyroxene and feldspar in presence of $CuSO_4$ 10^{-4} M as a concentration

pH	Zeta Potential	pH	Zeta Potential	pH	Zeta Potential
	mV		mV		mV
3.25	-10.7	3.17	-12.0	3.25	-14.8
3.9	-11.4	4.04	-1.0	3.9	-14.3
5.11	-17.1	5.15	0.1	5.02	-8.7
6.1	-17.9	6.18	-6.5	6.09	-9.2
7.24	4.4	7.05	3.5	7.09	0.9
8.3	0.1	8.28	-5.6	8.14	-4.3
9.25	-8.0	9.14	-17.6	9.3	-9.6
10.04	-17.2	9.99	-22.0	10.02	-21.0

Results of quartz in presence of $Ca(NO_3)_2$ 10^{-3} I.S.

pH	Zeta Potential	Reading 1	Reading 2	Reading 3	Reading 4	Reading 5	Std Dev
	mV	mV	mV	mV	mV	mV	mV
9.99	-20.7	-21.3	-20.9	-20.8	-19.6	-20.8	0.6
8.99	-23.3	-22.7	-23.8	-22.1	-23.5	-24.4	0.9
7.7	-21.3	-22.7	-21.7	-19.9	-20.6	-21.7	1.1
6.9	-23.6	-23.5	-23.9	-24.3	-23.5	-22.5	0.7
5.97	-21.1	-20.5	-22.5	-22.1	-20.8	-21.1	0.9
4.95	-21.5	-21.8	-21.8	-20.7	-22.5	-20.4	0.9
4.01	-21.4	-21.2	-23.0	-21.0	-20.9	-21.0	0.9
3.02	-17.0	-13.9	-17.2	-17.6	-18.9	-17.6	1.9

Results of feldspar in presence of $Ca(NO_3)_2$ 10^{-3} I.S.

pH	Zeta Potential	Reading 1	Reading 2	Reading 3	Reading 4	Reading 5	Std Dev
	mV	mV	mV	mV	mV	mV	mV
9.99	-17.3	-15.9	-18.1	-17.6	-17.3	-17.9	0.9
9.05	-17.8	-16.5	-17.7	-18.0	-18.4	-18.1	0.7
8	-17.5	-17.6	-17.3	-17.2	-17.5	-18.0	0.3
6.9	-16.2	-15.5	-16.2	-16.5	-16.5	-16.5	0.4
6.01	-16.7	-15.9	-15.9	17.2	-16.9	-17.6	0.8
4.97	-14.8	-14.7	-15.7	-14.6	-14.7	-14.3	0.5
4.07	-14.1	-13.8	-13.7	-14.0	-13.9	-15.0	0.5
3.07	-9.8	-9.4	-9.7	-9.6	-10.2	-9.9	0.3

Results of chromite in presence of $Ca(NO_3)_2$ 10^{-3} I.S.

pH	Zeta Potential	Reading 1	Reading 2	Reading 3	Reading 4	Reading 5	Std Dev
	mV	mV	mV	mV	mV	mV	mV
9.95	-17.7	-17.7	-18.1	-17.6	-18.0	-17.1	0.4
9.05	-16.0	-15.0	-14.1	-16.2	-17.3	-17.7	-16.0
8.05	-15.7	-15.1	-16.0	-14.2	-16.5	-16.6	1.0
6.9	-7.0	-6.5	-7.0	-5.4	-5.9	-10.2	1.9
6.03	-4.5	-5.7	-4.8	-1.9	-5.7	-4.4	1.5
5.02	-2.0	-3.0	-1.4	-2.8	-1.7	-1.0	0.9
4	5.7	5.3	7.6	5.6	5.5	4.6	1.1
3.05	10.4	11.4	9.7	9.5	9.7	10.1	0.8

Results of pyroxene in presence of $Ca(NO_3)_2$ 10^{-3} I.S.

pH	Zeta Potential	Reading 1	Reading 2	Reading 3	Reading 4	Reading 5	Std Dev
	mV	mV	mV	mV	mV	mV	mV
10.01	-17.9	-17.5	-17.8	-17.9	-18.4	-17.9	0.3
9.13	-18.3	-17.5	-19.1	-18.4	-19.0	-17.4	0.8
8.07	-18.0	-17.9	-18.1	-16.8	-18.3	-18.8	0.8

7.17	-17.4	-17.3	-17.0	-18.4	-17.0	-17.2	0.6
6.03	-17.2	-17.0	-16.9	-17.2	-17.5	-17.6	0.3
5.03	-16.6	-16.9	-16.7	-16.9	-15.9	-16.6	0.4
4.09	-15.3	-15.1	-15.3	-15.3	-15.6	-15.4	0.2
3.03	-9.6	-9.8	-9.0	-9.3	-10.1	-10.0	0.5

Results of talc in presence of $Ca(NO_3)_2$ 10^{-3} I.S.

pH	Zeta Potential
	mV
9.97	-28.5
9.06	-27.6
7.80	-26.7
7.02	-26.6
6.05	-26.3
5.00	-24.4
4.06	-19.6
3.05	-11.7

Results of pyroxene in presence of $Ca(NO_3)_2$ 10^{-2} I.S.

pH	Zeta Potential	Reading 1	Reading 2	Reading 3	Reading 4	Reading 5	Std Dev
	mV	mV	mV	mV	mV	mV	mV
9.96	-12.5	-12.2	-12.6	-12.2	-12.5	-12.8	0.3
9.12	-12.3	-12.0	-11.7	-13.3	-12.4	12.1	0.6
7.9	-12.7	-11.7	-13.6	-11.8	-13.1	-12.9	0.7
7.01	-12.7	-12.3	-12.5	-12.7	-12.9	-12.9	0.3
5.97	-10.8	-10.5	-11.3	-10.9	-11.1	-10.2	0.4
4.9	-8.2	-8.5	-8.6	-8.1	-8.2	-7.7	0.4
4.11	-4.6	-4.6	-4.2	-4.4	-5.9	-4.1	0.7
3.06	1.8	2.4	1.5	2.2	0.9	2.0	0.6

Results of talc, chromite and feldspar in presence of $Ca(NO_3)_2$ 10^{-2} I.S.

pH	Zeta Potential	pH	Zeta Potential	pH	Zeta Potential
	mV		mV		mV
9.97	-15.6	9.97	-13.2	9.97	-10.2
9.02	-16.0	8.95	-13.0	9.1	-11.6
8.02	-16.7	7.9	-13.6	7.9	-10.6
6.98	-15.7	6.93	-3.7	6.95	-8.7
6.02	-14.8	5.9	-3.2	5.91	-8.9
4.90	-12.1	4.9	-0.5	5.08	-6.9
4.09	-6.1	4.01	3.9	4.05	-7.5
3.08	4.0	3.14	10.4	3.12	4.4

Results of quartz in presence of KNO_3 10^{-3} M and guar gum (APX4M: 10ppm)

pH	Zeta Potential	Reading 1	Reading 2	Reading 3	Reading 4	Reading 5	Std Dev
	mV	mV	mV	mV	mV	mV	mV
9.99	-27.9	-30.9	-27.7	-26.7	-27.3	-27.1	1.7
8.99	-26.5	-28.9	-25.9	-26.2	-24.7	-26.9	1.6
7.93	-22.1	-22.4	-22.4	-22.6	-24.5	-18.8	2.1
6.9	-17.6	-19.8	-19.2	-16.8	-16.2	-16.0	1.8
6.03	-16.3	-16.0	-16.9	-17.7	-16.0	-14.9	1.0
4.99	-12.3	-11.2	-12.4	-12.9	-12.1	-12.7	0.7
4.02	-7.9	-7.0	-4.6	-10.1	-9.2	-8.9	2.2
3.01	-7.0	-6.4	-7.7	-7.1	-6.8	-6.8	0.5

Results of chromite and talc in presence of KNO_3 10^{-3} M and guar gum (APX4M: 10ppm)

pH	Zeta Potential	pH	Zeta Potential
	mV		mV
9.99	-15.8	10.02	-28.9
9.05	-17.0	9.05	-28.2
7.93	-14.6	7.93	-24.8
7.05	-10.6	7.05	-23.2
5.71	-6.1	5.71	-19.9
5.01	-7.1	5.01	-14.7
4.02	-4.5	4.02	-7.0
3.09	-3.1	3.09	-2.8

Results of pyroxene and feldspar in presence of KNO_3 10^{-3} M and guar gum (APX4M: 10ppm)

pH	Zeta Potential	pH	Zeta Potential
	mV		mV
9.98	-21.5	10.05	-35.9
9.17	-20.3	9.05	-36.7
8.05	-17.6	8.13	-33.6
7.07	-15.3	7.15	-29.7
6.15	-12.1	6.14	-25.3
5.2	-7.8	5.15	-18.8
4.2	-4.0	4.13	-8.0
3.2	-1.6	3.2	-2.4

Results of quartz in presence of KNO_3 10^{-3} M and CMC (FF30: 10ppm)

pH	Zeta Potential	Reading 1	Reading 2	Reading 3	Reading 4	Reading 5	Std Dev
	mV	mV	mV	mV	mV	mV	mV
9.99	-7.13	-74.5	-70.9	-73.2	-67.5	-7.05	2.7
9.07	-70.7	-68.7	-69.1	-72.1	-72.3	-71.2	1.7
7.95	-73.4	-76.6	-70.1	-74.7	-72.3	-73.3	2.4
7.15	-69.4	-66.8	-70.0	-71.2	-69.1	-70.0	1.6
6.05	-64.5	-64.9	65.6	-64.6	-63.9	-63.6	0.8
5	-55.1	-55.9	-52.8	-54.0	-55.7	-56.9	1.6
4.05	-42.4	-42.8	-42.6	-40.9	-43.8	-42.0	1.1
3.01	-31.3	-31.9	-30.9	-31.5	-30.5	-31.6	0.6

Results of chromite and talc in presence of KNO_3 10^{-3} M and CMC (FF30: 10ppm)

pH	Zeta Potential	pH	Zeta Potential
	mV		mV
9.99	-23.3	10.02	-56.7
9.03	-25.1	9.15	-55.1
8.09	-26.6	8.23	-53.1
6.99	-25.7	7.22	-50.7
5.7	-9.8	6.24	-47.7
4.9	-2.2	5.21	-40.9
4.0	4.7	4.17	-32.7
3.06	21	3.24	-24.3

Results of pyroxene and feldspar in presence of KNO_3 10^{-3} M and CMC (FF30: 10ppm)

pH	Zeta Potential	pH	Zeta Potential
	mV		mV
9.99	-58.5	10.02	-54.5
9.13	-60.5	9.12	-58.1
8.12	-60.0	8.2	-56.9
7.08	-57.2	7.19	-55.8
6.13	-53.9	6.2	-55.3
5.12	-45.6	5.17	-44.6
4.15	-31.9	4.17	-32.5
3.17	-18.4	3.17	-19.3

APPENDIX 3: SUMMARY OF ADSORPTION DATA

Adsorption results of all five minerals in presence of $Ca(NO_3)_2$ 10^{-2} I.S. and guar gum (APX4M)

2g SAMPLE		
BET	m^2/g	TOTAL AREA
PYROXENE	3.0995	6.199
FELDSPAR	3.4948	6.9896
TALC	2.0826	4.1652
CHROMITE	2.1393	4.2786
QUARTZ	2.8177	5.6354

PYROXENE

START CONCENTRATION	EQ. CONCENTRATION	av Amt ads/area
	0	0
50.74	14.45	0.58
99.71	61.95	0.63

FELDSPAR

START CONCENTRATION	EQ. CONCENTRATION	av Amt ads/area
	0	0
50.74	13.92	0.53
99.71	60.00	0.58

TALC

START CONCENTRATION	EQ. CONCENTRATION	av Amt ads/area
	0	0
50.74	17.91	0.78
99.71	55.39	1.09

CHROMITE

START CONCENTRATION	EQ. CONCENTRATION	av Amt ads/area
	0	0
50.74	17.91	0.63
99.71	55.39	0.60

QUARTZ

START CONCENTRATION	EQ. CONCENTRATION	av Amt ads/area
	0	0
50.74	54.47	-0.07

99.71	99.48	0.04

Adsorption results of all five minerals in presence of $Ca(NO_3)_2$ 10^{-2} I.S. and CMC (FF30)

2g SAMPLE		
BET	m^2/g	TOTAL AREA
PYROXENE	3.0995	6.199
FELDSPAR	3.4948	6.9896
TALC	2.0826	4.1652
CHROMITE	2.1393	4.2786
QUARTZ	2.8177	5.6354

PYROXENE

START CONCENTRATION	EQ. CONCENTRATION	av Amt ads/area
	0	0
51.93	28.18	0.41
10.38	81.13	0.38

FELDSPAR

START CONCENTRATION	EQ. CONCENTRATION	av Amt ads/area
	0	0
51.93	26.01	0.37
10.38	77.10	0.40

TALC

START CONCENTRATION	EQ. CONCENTRATION	av Amt ads/area
	0	0
51.93	13.30	0.93
10.38	64.01	0.97

CHROMITE

START CONCENTRATION	EQ. CONCENTRATION	av Amt ads/area
	0	0
51.93	24.34	0.63
10.38	77.65	0.60

QUARTZ

START CONCENTRATION	EQ. CONCENTRATION	av Amt ads/area

51.93 10.38	0 41.08 102.82	0 0.20 0.03

APPENDIX 4: SUMMARY OF THE MICROFLOTATION DATA

Microflotation results for talc(1), pyroxene(2), feldspar(3), quartz(4), chromite(5):

Run	I.S. and concentration of reagents	pH	Total mass (g)	Total mass (g)	Recovery (%)	Mean recovery (%)	Std Dev
1.1	10^{-2} $Ca(NO_3)_2$	9	2.15	1.5	18.60		
				5	41.86		
				10	63.25	20.44	2.13
2.1	10^{-2} $Ca(NO_3)_2$	9	2.17	1.5	21.66	38.50	3.87
				5	37.33	59.57	4.24
				10	58.52		
3.1	10^{-2} $Ca(NO_3)_2$	9	2.2	1.5	21.07		
				5	36.32		
				10	56.95		
1.1	10^{-2} $Ca(NO_3)_2$ 50mg/l FF30	9	2.04	1.5	0.98		
				5	2.94	0.98	0
				10	5.39	2.69	0.35
2.1	10^{-2} $Ca(NO_3)_2$ 50mg/l FF30	9	2.04	1.5	0.98	4.65	1.04
				5	2.45		
				10	3.92		
1.1	10^{-2} $Ca(NO_3)_2$ 100mg/l FF30	9	1.95	1.5	1.54		
				5	3.07	1.99	0.64
				10	5.12	4.23	1.63
2.1	10^{-2} $Ca(NO_3)_2$ 100mg/l FF30	9	2.04	1.5	2.45	6.97	2.61
				5	5.39		
				10	8.82		
1.1	10^{-2} $Ca(NO_3)_2$ 50mg/l APX4M	9	1.98	1.5	1.51		
				5	3.03	1.51	0
				10	4.54	3.28	0.36
2.1	10^{-2} $Ca(NO_3)_2$ 50mg/l APX4M	9	1.98	1.5	1.51	5.30	1.07
				5	3.53		
				10	6.06		
1.1	10^{-2} $Ca(NO_3)_2$ 100mg/l APX4M	9	1.97	1.5	1.52		
				5	3.55		
				10	4.57	1.74	0.31
2.1	10^{-2} $Ca(NO_3)_2$ 100mg/l APX4M	9	2.04	1.5	1.96	4.23	0.95
				5	4.90	6.20	2.31
				10	7.84		

1.1	10^{-2} $Ca(NO_3)_2$ 10^{-4} M $CuSO_4$ 10^{-4} M SIBX	9	2.07	1.5 5 10	9.17 24.64 40.09	9.66 25.36 41.78	0.68 1.02 2.39
2.1	10^{-2} $Ca(NO_3)_2$ 10^{-4} M $CuSO_4$ 10^{-4} M SIBX	9	2.07	1.5 5 10	10.14 26.08 43.47		

Run	I.S. and concentration of reagents	pH	Total mass (g)	Total mass (g)	Recovery (%)	Mean recovery (%)	Std Dev
1.1	10^{-2} $Ca(NO_3)_2$ 10^{-4} M $CuSO_4$ 10^{-4} M SIBX 50mg/l APX4M	9	2.09	1.5 5 10	3.82 7.65 12.44	2.66 6.56 10.94	1.65 1.54 2.11
2.1	10^{-2} $Ca(NO_3)_2$ 10^{-4} M $CuSO_4$ 10^{-4} M SIBX 50mg/l APX4M	9	2.01	1.5 5 10	1.49 5.47 9.45		
1.1	10^{-2} $Ca(NO_3)_2$ 10^{-4} M $CuSO_4$ 10^{-4} M SIBX 100mg/l APX4M	9	2.06	1.5 5 10	5.82 12.13 17.47	4.87 10.23 14.37	1.35 2.69 4.38
2.1	10^{-2} $Ca(NO_3)_2$ 10^{-4} M $CuSO_4$ 10^{-4} M SIBX 100mg/l APX4M	9	2.04	1.5 5 10	3.92 8.33 11.27		
1.1	10^{-2} $Ca(NO_3)_2$ 10^{-4} M $CuSO_4$ 10^{-4} M SIBX 50mg/l FF30	9	2.07	1.5 5 10	10.14 28.02 44.92	10.49 28.54 46.60	0.49 0.74 2.36
2.1	10^{-2} $Ca(NO_3)_2$ 10^{-4} M $CuSO_4$ 10^{-4} M SIBX 50mg/l FF30	9	2.03	1.5 5 10	10.83 29.06 48.27		
1.1	10^{-2} $Ca(NO_3)_2$ 10^{-4} M $CuSO_4$ 10^{-4} M SIBX 100mg/l FF30	9	2.17	1.5 5 10	18.60 41.86 63.25	20.13 39.59 60.89	2.16 3.20 3.34
2.1	10^{-2} $Ca(NO_3)_2$ 10^{-4} M $CuSO_4$ 10^{-4} M SIBX 100mg/l FF30	9	2.15	1.5 5 10	20.13 39.59 60.89		
1.2	10-2 Ca(NO3)2	9	2.14	1.5 5 10	1.87 2.33 3.27	1.62 2.54 3.47	0.34 0.29 0.28
2.2	10-2 Ca(NO3)2	9	2.18	1.5 5 10	1.37 2.75 3.67		
1.2	10^{-2} $Ca(NO_3)_2$ 10^{-4} M $CuSO_4$ 10^{-4} M SIBX	9	2.15	1.5 5 10	16.23 42.58 66.98	16.35	0.11

2.2	10^{-2} $Ca(NO_3)_2$ 10^{-4} M $CuSO_4$ 10^{-4} M SIBX	9	2.13	1.5 5 10	16.43 43.66 63.55	43.12 65.42	0.76 2.26
1.2	10^{-2} $Ca(NO_3)_2$ 10^{-4} M $CuSO_4$ 10^{-4} M SIBX 50mg/l APX4M	9	2.15	1.5 5 10	9.76 24.18 30.23	11.59 26.44 35.25	2.58 3.19 7.1

Run	I.S. and concentration of reagents	pH	Total mass (g)	Total mass (g)	Recovery (%)	Mean recovery (%)	Std Dev
1.2	10^{-2} $Ca(NO_3)_2$ 10^{-4} M $CuSO_4$ 10^{-4} M SIBX 100mg/l APX4M	9	2.12	1.5 5 10	9 16.58 20.85	9.85 16.89	1.19 0.44
2.2	10^{-2} $Ca(NO_3)_2$ 10^{-4} M $CuSO_4$ 10^{-4} M SIBX 100mg/l APX4M	9	2.15	1.5 5 10	10.69 17.21 21.39	21.12	0.38
1.2	10^{-2} $Ca(NO_3)_2$ 10^{-4} M $CuSO_4$ 10^{-4} M SIBX 50mg/l FF30	9	2.15	1.5 5 10	18.14 39.07 57.67	16.67 37.27 54.87	2.07 2.53 3.96
2.2	10^{-2} $Ca(NO_3)_2$ 10^{-4} M $CuSO_4$ 10^{-4} M SIBX 50mg/l FF30	9	2.17	1.5 5 10	15.20 35.48 52.07		
1.2	10^{-2} $Ca(NO_3)_2$ 10^{-4} M $CuSO_4$ 10^{-4} M SIBX 100mg/l FF30	9	2.12	1.5 5 10	8.02 23.58 33.49	8.47 21.88 30.83	0.64 2.40 3.76
2.2	10^{-2} $Ca(NO_3)_2$ 10^{-4} M $CuSO_4$ 10^{-4} M SIBX 100mg/l FF30	9	2.13	1.5 5 10	8.92 20.18 28.17		
1.3	10-2 Ca(NO3)2	9	2.15	1.5 5 10	0.93 1.86 2.79	0.91 1.83 2.52	0.02 0.04 0.38
2.3	10-2 Ca(NO3)2	9	2.22	1.5 5 10	0.9 1.8 2.25		
1.3	10^{-2} $Ca(NO_3)_2$ 10^{-4} M $CuSO_4$ 10^{-4} M SIBX	9	2.03	1.5 5 10	2.36 52.21 73.40	24.14 53.40 74.86	0.70 1.67 2.07
2.3	10^{-2} $Ca(NO_3)_2$ 10^{-4} M $CuSO_4$ 10^{-4} M SIBX	9	2.07	1.5 5 10	24.64 54.58 76.33		
1.3	10^{-2} $Ca(NO_3)_2$ 10^{-4} M $CuSO_4$ 10^{-4} M SIBX 50mg/l APX4M	9	2.06	1.5 5 10	8.25 19.42 25.73	8.43	0.254

2.3	10^{-2} $Ca(NO_3)_2$ 10^{-4} M $CuSO_4$ 10^{-4} M SIBX 50mg/l APX4M	9	2.09	1.5 5 10	8.61 17.70 23.44	18.56 24.58	1.21 1.61
1.3	10^{-2} $Ca(NO_3)_2$ 10^{-4} M $CuSO_4$ 10^{-4} M SIBX 100mg/l APX4M	9	2.02	1.5 5 10	5.94 13.36 21.28	5.23 12.96 20.19	1.0 0.57 1.55

Run	I.S. and concentration of reagents	pH	Total mass (g)	Total mass (g)	Recovery (%)	Mean recovery (%)	Std Dev
1.3	10^{-2} $Ca(NO_3)_2$ 10^{-4} M $CuSO_4$ 10^{-4} M SIBX 50mg/l FF30	9	2.05	1.5 5 10	13.47 37.07 18.04	15.63 42.31 64.07	3.51 7.40 8.52
2.3	10^{-2} $Ca(NO_3)_2$ 10^{-4} M $CuSO_4$ 10^{-4} M SIBX 50mg/l FF30	9	2.04	1.5 5 10	18.13 47.55 70.09		
1.3	10^{-2} $Ca(NO_3)_2$ 10^{-4} M $CuSO_4$ 10^{-4} M SIBX 100mg/l FF30	9	2.08	1.5 5 10	10.57 31.73 47.59	10.93 31.63 46.56	0.53 0.14 1.61
2.3	10^{-2} $Ca(NO_3)_2$ 10^{-4} M $CuSO_4$ 10^{-4} M SIBX 100mg/l FF30	9	2.03	1.5 5 10	11.33 31.53 45.32		
1.4	10-2 Ca(NO3)2	9	2.13	1.5 5 10	2.82 7.51 11.74	3.25 8.13 12.55	0.61 0.88 1.15
2.4	10-2 Ca(NO3)2	9	2.17	1.5 5 10	3.68 8.75 13.36		
1.4	10^{-2} $Ca(NO_3)_2$ 10^{-4} M $CuSO_4$ 10^{-4} M SIBX	9	2.11	1.5 5 10	21.33 48.34 65.40	18.26 45.14 61.73	4.33 4.53 5.18
2.4	10^{-2} $Ca(NO_3)_2$ 10^{-4} M $CuSO_4$ 10^{-4} M SIBX	9	2.17	1.5 5 10	15.21 41.93 58.06		
1.4	10^{-2} $Ca(NO_3)_2$ 10^{-4} M $CuSO_4$ 10^{-4} M SIBX 50mg/l APX4M	9	2.12	1.5 5 10	13.68 28.77 35.85	12.14 26.36 34.28	2.17 3.40 2.21
2.4	10^{-2} $Ca(NO_3)_2$ 10^{-4} M $CuSO_4$ 10^{-4} M SIBX 50mg/l APX4M	9	2.17	1.5 5 10	10.60 23.96 32.72		
1.4	10^{-2} $Ca(NO_3)_2$ 10^{-4} M $CuSO_4$ 10^{-4} M SIBX 100mg/l APX4M	9	2.08	1.5 5 10	15.86 32.21 40.86	14.94	1.31

2.4	10^{-2} $Ca(NO_3)_2$ 10^{-4} M $CuSO_4$ 10^{-4} M SIBX 100mg/l APX4M	9	2.07	1.5 5 10	14.01 27.53 34.78	29.87 37.82	3.30 4.30
1.4	10^{-2} $Ca(NO_3)_2$ 10^{-4} M $CuSO_4$ 10^{-4} M SIBX 50mg/l FF30	9	1.95	1.5 5 10	41.54 78.46 90.77	40.37 77.46 89.99	1.64 1.41 1.10
2.4	10^{-2} $Ca(NO_3)_2$ 10^{-4} M $CuSO_4$ 10^{-4} M SIBX 50mg/l FF30	9	2.04	1.5 5 10	39.21 76.47 89.21		
Run	**I.S. and concentration of reagents**	**pH**	**Total mass (g)**	**Total mass (g)**	**Recovery (%)**	**Mean recovery (%)**	**Std Dev**
1.4	10^{-2} $Ca(NO_3)_2$ 10^{-4} M $CuSO_4$ 10^{-4} M SIBX 100mg/l FF30	9	2.1	1.5 5 10	33.81 70 80.95	36.31 70.57 82.27	3.53 0.81 1.86
2.4	10^{-2} $Ca(NO_3)_2$ 10^{-4} M $CuSO_4$ 10^{-4} M SIBX 100mg/l FF30	9	2.01	1.5 5 10	38.81 71.14 83.58		
1.5	10-2 Ca(NO3)2	9	2.05	1.5 5 10	10.73 18.05 22.44	8.93 15.93 20.74	2.54 2.99 2.39
2.5	10-2 Ca(NO3)2	9	2.1	1.5 5 10	7.14 13.81 19.0		
1.5	10^{-2} $Ca(NO_3)_2$ 10^{-4} M $CuSO_4$ 10^{-4} M SIBX	9	2.07	1.5 5 10	32.36 56.04 68.11	31.21 54.1 65.74	1.64 2.77 3.35
2.5	10^{-2} $Ca(NO_3)_2$ 10^{-4} M $CuSO_4$ 10^{-4} M SIBX	9	2.13	1.5 5 10	30.47 52.11 63.38		
1.5	10^{-2} $Ca(NO_3)_2$ 10^{-4} M $CuSO_4$ 10^{-4} M SIBX 50mg/l APX4M	9	2.17	1.5 5 10	13.36 24.88 33.64	12.61 25.0 33.41	1.07 0.16 0.32
2.5	10^{-2} $Ca(NO_3)_2$ 10^{-4} M $CuSO_4$ 10^{-4} M SIBX 50mg/l APX4M	9	2.11	1.5 5 10	11.85 25.12 33.17		
1.5	10^{-2} $Ca(NO_3)_2$ 10^{-4} M $CuSO_4$ 10^{-4} M SIBX 100mg/l APX4M	9	2.08	1.5 5 10	13.94 25.48 31.25	13.44 23.93 29.06	0.71 2.18 3.10
2.5	10^{-2} $Ca(NO_3)_2$ 10^{-4} M $CuSO_4$ 10^{-4} M SIBX 100mg/l APX4M	9	2.01	1.5 5 10	12.93 22.34 26.86		
1.5	10^{-2} $Ca(NO_3)_2$ 10^{-4} M $CuSO_4$ 10^{-4} M SIBX 50mg/l FF30	9	2.09	1.5 5 10	13.39 29.18 35.88	12.88	0.72

2.5	10^{-2} $Ca(NO_3)_2$ 10^{-4} M $CuSO_4$ 10^{-4} M SIBX 50mg/l FF30	9	2.1	1.5 5 10	12.38 30.95 41.43	30.07 38.65	1.25 3.91
1.5	10^{-2} $Ca(NO_3)_2$ 10^{-4} M $CuSO_4$ 10^{-4} M SIBX 100mg/l FF30	9	2.05	1.5 5 10	6.34 19.02 24.39	7.49 18.65 24.93	1.63 0.53 0.77
2.5	10^{-2} $Ca(NO_3)_2$ 10^{-4} M $CuSO_4$ 10^{-4} M SIBX 100mg/l FF30	9	2.08	1.5 5 10	8.65 18.27 25.48		